Defining the residues governing the mitotic destruction of *Drosophila* cyclin A

Inaugural-Dissertation

zur

Erlangung des Doktorgrades
der Mathematisch-Naturwissenschaftlichen Fakultät
der Universität zu Köln

vorgelegt von
Vimal Ramachandran
aus Indien

Köln 2007

Berichterstatter: PD Dr. Frank Sprenger

Prof. Dr. Maria Leptin

Tag der mündlichen Prüfung: 02. Juli 2007

Index

Abstract

Mitotic destruction of cyclin A has remained enigmatic ever since it was discovered. Regulation of cyclin A proteolysis appears to be different from that of other mitotic cyclins in diverse species. Despite being substrates of the same destruction machinery - the E3 ligase called Anaphase Promoting Complex/Cyclosome (APC/C) - the proteolysis of cyclin A concludes before that of the B-type cyclins and other crucial substrates like securin. Moreover cyclin B and securin, but not cyclin A, gets stabilized upon activation of the spindle assembly checkpoint, which is a surveillance mechanism that inhibits the APC/C. Somehow, APC/C activity towards cyclin A escapes checkpoint control. Defining the cyclin A destruction signals is paramount for solving this riddle. Unfortunately, in spite of years of research, the cyclin A degradation signal remains ill-defined and poorly characterized. A single and simple destruction box (D-box) motif is responsible for cyclin B turnover. But the cyclin A degradation signal is much more complex. In *Drosophila* cyclin A (CycA), a putative D-box and another element called the KEN box have been implicated; but eliminating these do not cause stability. In order to characterize the elusive CycA destruction signals, an extensive analysis was carried out in this study. It was found that both the N- and C-terminal regions are involved in turnover, which implies a synergistic action by multiple parts of the molecule. A KEN box, a D-box and an aspartic acid at position 70 are required at the N-terminus and they make additive contributions to degradation when the checkpoint is active or inactive. From the C-terminal region, the cyclin box contributes. Single point mutations in these four elements totally abolish mitotic destruction. Very importantly, it was observed that the cyclin box mediates the spindle checkpoint bypass. The normal function of the cyclin box is to mediate Cdk1 binding, and previous studies had claimed that this interaction is essential for timely destruction. But it was found here that the cyclin box provides a function different from Cdk1 binding for turnover; most likely it presents an interaction motif for the APC/C. Furthermore, eight potential ubiquitin acceptor lysine residues surrounding the N-terminal signals were found to be preferentially used for proteolysis. Combining mutations in these lysines and the N-terminal signals caused full stability leading to mitotic arrest phenotypes. But,

mutating the lysines alone only prolonged the duration of mitosis. Thus, presumably, lysines elsewhere on the protein are used when the preferred ones are absent. This apparent shift in ubiquitination is mediated by the N-terminal signals. In conclusion, this study defines the CycA destruction signals and gives an explanation for how checkpoint destruction can be accomplished.

1. Introduction

1.1 The cell cycle

"When a cell arises there must be a previous cell, just as animals can only arise from animals and plants from plants"

The German pathologist Rudolf Virchow put forth this cell doctrine in 1858, reflecting on the continuity of life (Alberts et al., 2002).

The only way to make more cells is by the division of those that already exist. Repeated rounds of cell growth and division are what generates and sustains all living organisms from unicellular bacteria to complex multicellular mammals. The cell cycle can be essentially defined as an orderly sequence of events by which a cell duplicates its contents and then divides into two. The most basic function of the cell cycle is to accurately replicate the DNA as well as other organelles and macromolecules, and then distribute the copies into genetically identical daughter cells with skillful precision. Despite variations, every cell cycle comprises a minimum set of universal processes to satisfy this basic function.

1.2 The eukaryotic cell cycle

The eukaryotic cell cycle is traditionally divided into four sequential phases - G1, S, G2 and M (Fig: 1). Synthesis of RNA and protein occur during G1 (first gap) phase, while preparation for DNA synthesis and chromosome replication occur during S (synthesis) phase. This is followed by a second gap phase or G2 phase, where the cell monitors its environment and ensures that the conditions are suitable for commitment to division. If conditions are favorable, the cell proceeds into M-phase, which is comprised of two dramatic events - the division of the nucleus, referred to as mitosis and the splitting of the cell into two, referred to as cytokinesis. There are times when a cell quits the cell cycle and stops dividing. This phase is called the G0 (Gap0) phase and it may either be a temporary

resting period or more permanent. An example of the latter case is the neuron, which stops dividing after it has reached an end stage of development.
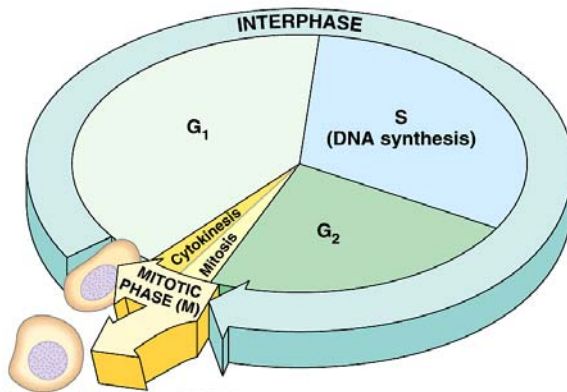
Figure: 1 The classical eukaryotic cell cycle
A 360º representation depicting the four phases of the archetypical eukaryotic cell cycle. G1, S and G2 constitute interphase, the period of growth and DNA synthesis. This alternates with the mitotic (M) phase during which both nuclear division (mitosis) and cytoplasmic division (cytokinesis) occur. Adapted from (Simmons, 2006).

Mitosis is a complex process which distributes the duplicated chromosomes equally into a pair of daughter nuclei. The events of mitosis are further divided into five phases - prophase, prometaphase, metaphase, anaphase and telophase (Fig: 2). Prophase begins at the onset of chromosome condensation. Centrosome separation and initiation of spindle assembly occur in mid to late prophase. Prometaphase begins with nuclear envelope breakdown and continues until sister chromatids are captured by the spindle and transported to its central region. Metaphase is the period during which the sisters are aligned at the spindle equator forming a so-called metaphase plate. Anaphase witnesses the most dramatic event in mitosis, when the cohesion between sister chromatids is abruptly dissolved, pulling them apart to the opposite spindle poles. The stage of initial sister separation is called early anaphase or anaphase A (AnaA). Later, the spindle poles themselves move farther apart from each other, completing the segregation of sister chromatids. This period is designated as late anaphase or anaphase B (AnaB). Telophase is the last mitotic stage, when the segregated chromosomes and other nuclear components are repackaged into identical daughter nuclei followed by spindle disassembly, bringing mitosis to an end. The daughter cells resulting from mitosis have the same DNA compliment as their parent cell.
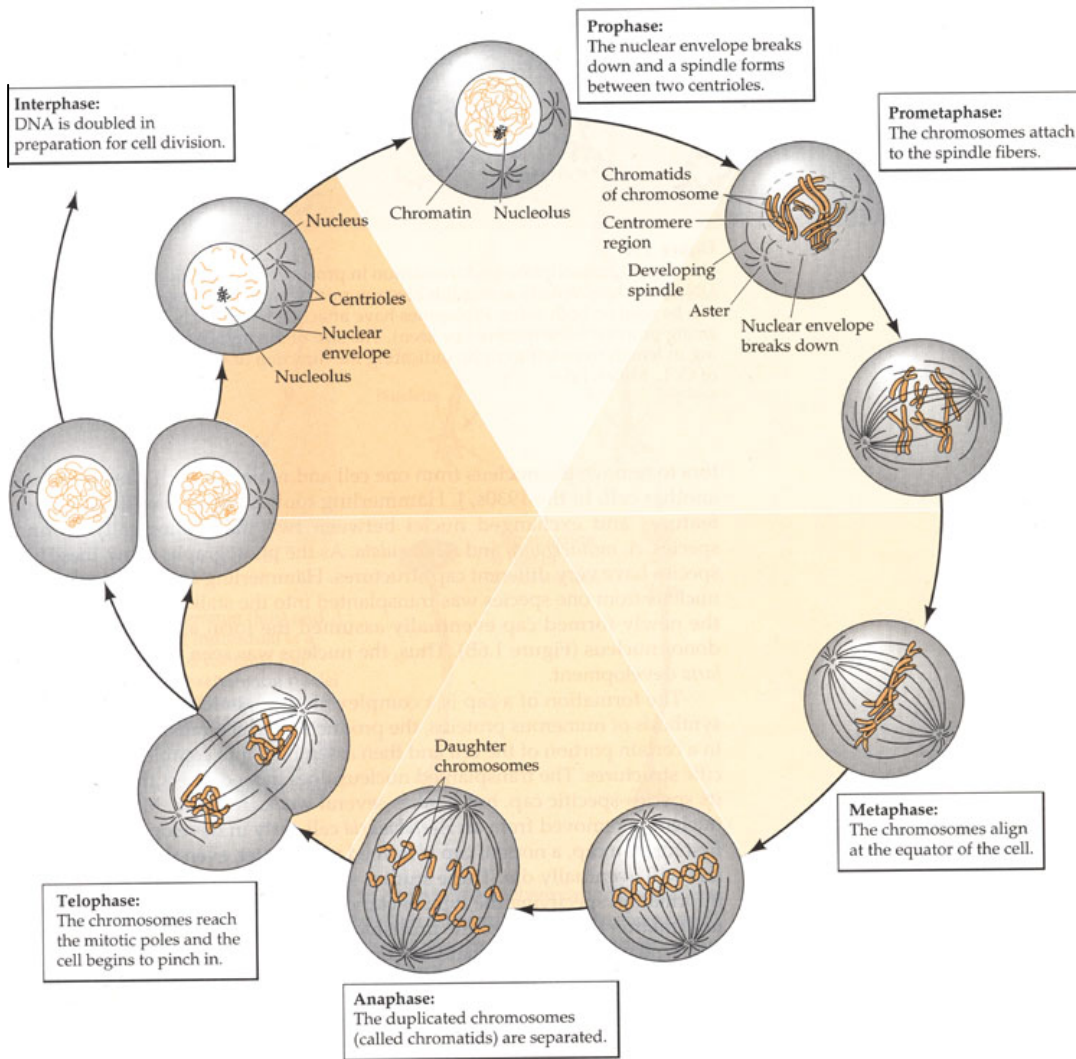
Figure: 2 The different stages of mitosis
Prophase is the stage of chromosome condensation. Nuclear envelope breakdown is completed in prometaphase. Chromosome alignment occurs during metaphase and sister chromatid separation during anaphase. Telophase is the stage of nuclear restitution, chromosome decondensation and the onset of cytokinesis. Adapted from (Amundson, 2007).

G1, S and G2 constitute the period between the two M-phases and are collectively referred to as interphase. Interphase serves as a time period for the cell to not only replicate its genetic information, but also to synthesize proteins and grow in mass. If interphase lasted only long enough for DNA replication, the cell would not have time to double its mass before it divided and would

consequently get smaller and smaller with each division. Indeed, this is just what happens during the first few cleavage divisions in animal embryos, wherein G1 and G2 are drastically shortened so that the cells do not grow before they divide. This facilitates rapid subdivision of a giant egg cell into many daughter cells.

1.2.1 Meiosis - A special type of cell division

In nearly all eukaryotes, a divergent from of cell division occurs during gametogenesis which halves the DNA compliment in daughter cells and produces haploid gametes. This is called meiosis. During meiosis, a single round of DNA replication is followed by two cycles of chromosome segregation and cell division, termed meiosis I and meiosis II. In meiosis I, both chromatids of each homologous chromosome segregate together to opposite spindle poles, so that each of the resulting daughter cells contains one homologous chromosome with two chromatids. In meiosis II, which resembles mitosis, the sister chromatids segregate to opposite poles generating haploid gametes. Meiosis results in four haploid germ cells from one diploid parent cell.

1.2.2 Methods to study cell cycle stages

The different cell cycle stages can be observed and studied in various ways. Cells undergoing mitosis and cytokinesis can be distinguished by microscopy. Mitotic cells look typically rounded up under a microscope and cells undergoing cytokinesis can be caught in the act of division. Cells in different mitotic stages have characteristic chromosome morphology. They can be distinguished with DNA stains such as *Hoechst* or antibody probes against specific chromosome proteins like phosphorylated Histones. S-phase cells can be recognized with visualizable molecules that are incorporated into newly synthesized DNA, such as ^{3}H-thymidine or the artificial thymidine analogue, bromo-deoxyuridine (BrdU). By giving a pulse of the label and allowing cells to continue around the cell cycle for measured lengths of time, one can determine the duration of various stages as well as the proportion of cells in S-phase (labeling index) and M-phase (mitotic

index). The most efficient way to assess cell cycle stages is by flow cytometry or fluorescence activated cell sorting (FACS); wherein the DNA is labeled with a fluorescent dye so that the amount of fluorescence detected is directly proportional to the DNA content in each cell (Alberts et al., 2004). With this approach, the lengths of G1, S and G2+M phases can be determined by following a synchronized population of cells over time.

1.3 Cell cycle modifications during *Drosophila* development

The development of multicellular organisms requires coordination of cell proliferation and growth with patterning and differentiation. This is accomplished in part by subjecting the archetypical cell cycle of G1-S-G2-M phases to extrinsic cues, promoting division or cell cycle exit. Most organisms employ variant cell cycles apart from the archetypical cycle for specific developmental strategies. The cell cycle is malleable and flexible in that it adjusts and acclimatizes to the needs of a specific tissue or the developmental process of a particular organism. Marked variations from the classic eukaryotic cell cycle are seen in the fruit fly *Drosophila melanogaster* (Edgar et al., 1994) (Fig:3). During *Drosophila* embryogenesis, the first thirteen mitoses occur without cytokinesis, producing a syncytial multi-nucleate embryo with a shared cytoplasm. These syncytial cycles are characterized by the rapid oscillations between S phase and M phase without intervening gap phases, G1 and G2. The first ten of these divisions are fast, lasting approximately 10 minutes each, while the next three divisions are slightly slower (Edgar and Lehner, 1996). After the seventh division, about 75% of the nuclei migrate from the center of the embryo to the periphery and continue dividing syncytially until cell cycle 13. The nuclei remaining at the center exit the cell cycle and form yolk nuclei. Among the migrating nuclei, those that reach the posterior pole of the embryo undergo cellularization and form pole cells, from which the germ cells later originate. These syncytial cycles are driven by maternal reserves deposited during oogenesis, alleviating the need for zygotic transcription (Merrill et al., 1988). Interphase gradually lengthens during late syncytial cycles and a G2 phase is introduced during cell cycle 14, following the

initiation of zygotic transcription and the onset of cytokinesis. This process is termed as the midblastula transition (MBT) and it results in a cellular blastula (Edgar and O'Farrell, 1989; Edgar and O'Farrell, 1990). The next three divisions (14-16) are asynchronous and called postblastoderm cycles, wherein cells typically undergo mitosis in groups known as mitotic domains in response to patterning events (Foe, 1989). After mitosis 16, epidermal cells exit the cell cycle and enter a terminal G1 phase in which they remain until embryogenesis is completed. But cells constituting the nervous system continue to divide using S-G2-M cycles.
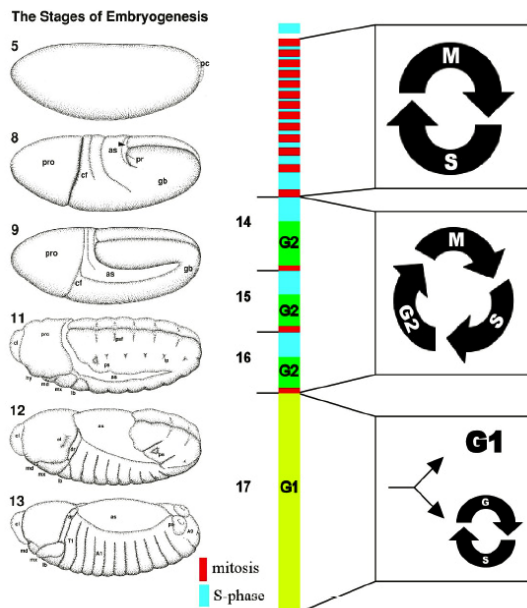
Figure: 3 Variations from the standard cell cycle in *Drosophila*
The first 13 divisions during *Drosophila* embryogenesis consist of just S and M phases. Following the midblastula transition, cycles 14, 15 and 16 incorporate a G2 phase also. After mitosis 16, most cells enter the first G1 in cycle 17 and remain quiescent thereafter. Few cells that give rise to larval tissues endoreplicate with alternating G1 and S phases. The numbers on the left indicate the stage of embryogenesis and those on the right indicate cell cycle stages. Adapted from (Zielke, 2006).

The end product of embryogenesis is a feeding larva. Cells that differentiate into larval tissues such as the gut, salivary gland and fat body, undergo a modified cell cycle comprising just S- and G-phases, devoid of mitosis (Smith and Orr-Weaver, 1991). These are called endoreplication cycles or endocycles which lead to an increase in ploidy or DNA content, coincident with a dramatic increase in cell size (Edgar and Orr-Weaver, 2001). However, groups of cells called imaginal discs, that later differentiate into adult structures; continue to divide in archetypical fashion. In the adult fly, a subset of tissues such as the ovarian nurse cells and follicle cells undergo endoreplication (Lilly and Duronio, 2005).

1.4 Cell cycle control

Events of the cell cycle are triggered by a regulatory network dubbed the cell cycle control system. This system ensures that the events are properly timed, follow a correct order and occur only once per cycle. It is responsive to various intracellular and extracellular signals, so that cell cycle progression can be halted when the cell either fails to complete an essential process or encounters unfavorable conditions.

1.4.1 Cyclin-Cdk

The central components of the control system are Cyclin dependent kinases (Cdk), which is a conserved family of proline-directed serine/threonine kinases. Cdk levels remain constant throughout the cell cycle. But they have no activity unless they associate with regulatory subunits called cyclins. True to their name; cyclins undergo a cycle of synthesis and degradation in each cycle. Therefore oscillations in cyclin-Cdk activity result from cyclical changes in cyclin levels. This results in cyclical changes in the phosphorylation of intracellular proteins that regulate cell cycle events.

There are four classes of cyclins in eukaryotic cells, based on the stage at which they function:

1. G1 cyclins - helps promote passage through the restriction point in late G1 (CycE-Cdk2 in *Drosophila*).

2. G1/S cyclins - commits the cell to DNA replication (CycD-Cdk4, CycD-Cdk6 in *Drosophila*).

3. S-phase cyclins - promotes initiation of DNA replication (CycA-Cdk1, CycE-Cdk2 in *Drosophila*).

4. M-phase cyclins - mediates events of mitosis (CycB-Cdk1, CycA-Cdk1 in *Drosophila*).

The best characterized cyclins are those required for the G2-M transition, which is mediated by a complex dubbed the Maturation Promoting Factor (MPF),

comprised of CycB and cdc2/Cdk1 (Lohka et al., 1988). *Drosophila* has three mitotic cyclins: cyclin A (CycA), cyclin B (CycB) and cyclin B3 (CycB3), whose activity facilitates entry into and progression through mitosis. All three associate with cdc2/Cdk1 (Edgar and Lehner, 1996).The mammalian/human A-type cyclin family consists of two members, cyclin A1 (CycA1) and cyclin A2 (CycA2). CycA2 is the somatic cyclin that promotes both G1/S and G2/M transitions. CycA1 is expressed in mice exclusively in the germline lineage, and expressed in humans at highest levels in the testis and certain myeloid leukemia cells (Yang et al., 1997). Human CycA2 associates with two Cdks - Cdk2 during S-phase and Cdk1 during mitosis. CycA is the most crucial of the *Drosophila* mitotic cyclins and a null mutation in *CycA* causes embryonic lethality due to the failure of epidermal cells to progress through mitosis 16 (Lehner and O'Farrell, 1989). The important function CycA performs is to inhibit the ubiquitin ligase APC/C^{Fzr} from ubiquitinating and degrading proteins required for mitotic entry (Reber et al., 2006). It is believed to do this together with Rca1, the homologue of vertebrate Emi1, which can also inhibit AP/C^{Fzr}. Overexpression of Rca1 can rescue the *CycA* null mutant phenotype (Dienemann and Sprenger, 2004).

Several additional mechanisms other than the rise and fall of cyclins contribute to the fine-tuning of Cdk activity. For example, phosphorylation of a threonine residue (T160) near the active site is required for full Cdk activation. T160 is located on the T-loop, a structural element that blocks binding of the substrate at the entrance of the active-site cleft. Upon phosphorylation by Cdk-activating kinases (CAKs), the T-loop flattens and is displaced from the active site, thereby facilitating substrate binding. In *Drosophila* and vertebrates, the major CAK is a trimeric complex containing a Cdk-related protein kinase known as Cdk7,its activating partner cyclin H, and a third subunit, Mat1. Cdk7 temperature-sensitive mutants are lethal in *Drosophila* (Fisher and Morgan, 1994; Larochelle et al., 1998). The budding yeast CAK is, however, a small monomeric kinase called Cak1 or Civ1, which bears only distant homology to Cdks (Thuret et al., 1996). Prior to mitosis, Cdk activity is also controlled by inhibitory phosphorylation at conserved threonine 14 and tyrosine 15 residues, mediated by the kinases Wee1 and Myt1 (Gould and Nurse, 1989; Morgan, 1995; Russell and Nurse, 1987).

During the onset of mitosis, this is reversed by the phosphatases of the Cdc25 family to facilitate mitotic entry (Nurse, 1990). *Drosophila* possesses two Cdc25 homologues - String and Twine. String governs the midblastula transition as well as all the succeeding mitotic divisions during development, whereas Twine functions in the germ line and promotes meiosis (Edgar and Datar, 1996; Edgar and O'Farrell, 1990; Edgar et al., 1994).

Cyclin-Cdk complexes are also regulated by the binding of Cdk inhibitor proteins (CKIs). The CKI proteins are classified into two families based on their primary amino acid structure and by their targets. The first family, the INK4 (Inhibitors of Cdk4) proteins are composed of four gene products that selectively inhibit Cdk4 and Cdk6. The four INK4 inhibitors (p16INK4a, p15INK4b, p18INK4c, and p19INK4d) do not bind to any of the other Cdks or to the cyclins. In contrast, the second family, Cip/Kip inhibitors (Cdk interacting protein/Kinase inhibitory protein) constitute three members - $p21^{Cip1}$, $p27^{Kip1}$, and $p57^{Kip2}$. These CKIs inhibit a wider range of Cdks. Unlike the INK4a family, the Cip/Kip proteins bind to both the cyclin and the Cdk subunit (Mainprize et al., 2001). During *Drosophila* embryogenesis, entry into the first G1 phase and the quiescence that follows requires the inactivation of both CycE-Cdk2 and CycA-Cdk1, since both can trigger progression into S-phase. CycE-Cdk2 is inactivated by Dacapo, which encodes the single *Drosophila* Cip/Kip type CKI (de Nooij et al., 1996; Lane et al., 1996).

1.4.2 Checkpoints in cell cycle regulation

Most cell types possess surveillance mechanisms to ensure the proper order and correct execution of cell cycle events. These are called checkpoint pathways and they consist of sensors which detect the completion of a process, aborting it if something malfunctions, thereby minimizing catastrophic genetic damage.

The G1 checkpoint prevents S-phase entry and DNA replication in response to DNA damage induced by genotoxic stress. Kinases including those of the ATM/ATR pathway phosphorylate and activate the tumor suppressor protein p53, which in turn stimulates the expression of $p21^{Cip1}$. $p21^{Cip1}$ expression suppresses

cyclin E- and cyclin A-associated Cdk2 activities, and thereby prevents G_1 to S phase progression. p53 also stimulates genes modulating intracellular redox status and apoptosis (Abraham, 2001).

The S-phase checkpoint senses intrinsic anomalies in DNA replication such as stalled forks, strand breaks or misincorporation of bases and orchestrates high-fidelity DNA repair through homologous recombination. This is mediated by the kinases Rad3/ATM and Chk1 (Mei-41 and Grapes, respectively, in *Drosophila*) (Lee and Orr-Weaver, 2003). The checkpoint response leads to the proteosome-mediated degradation of Cdc25A/String, and in turn, the failure to maintain activation of cyclin-Cdk2 complexes results in an inhibition of DNA synthesis. Inhibitory phosphorylation of Cdk1 by Wee1 kinase delays mitotic entry. *Drosophila* embryos from *mei-41* or *grp* females undergo unusually rapid syncytial mitoses, continue cleavage divisions after cycle 13, and fail to cellularize or perform the midblastula transition (Sibon et al., 1999; Sibon et al., 1997). *Drosophila* eye discs possess Mus304, an additional S-phase checkpoint component (Brodsky et al., 2000). A recent study also demonstrates that DNA damage-induced centrosome inactivation requires the *Drosphila* homologue of downstream Chk2 kinase - DmChk2 or Mnk (Takada et al., 2003).

The G2 checkpoint is the final gatekeeper that blocks the entry of DNA-damaged cells into mitosis. This pathway has two branches. One branch is governed primarily by ATR and gets activated when cells incur DNA damage before the completion of S-phase. The other branch is governed by ATM and it responds to DNA damage occurring in G2. ATR acts via Chk1 while ATM acts via Chk2, and both serve to phosphorylate Cdc25, that creates a binding site on it for a peptide called 14-3-3. This catalytically inhibits Cdc25, preventing activation of cyclin-Cdk complexes required for mitotic entry (O'Connell et al., 2000; Peng et al., 1997).

1.4.2.1 The spindle assembly checkpoint

The spindle assembly checkpoint monitors the attachment of kinetochores to the mitotic spindle and the generation of tension that results from the bipolar attachment of sister chromatids. The signal from even a single unattached

kinetochore is sensed by the checkpoint, which then arrests cells in metaphase until all chromosomes are precisely aligned (Musacchio and Salmon, 2007). The core spindle checkpoint proteins are Mad1, Mad2, BubR1 (Mad3 in yeast), Bub1, Bub3 and Mps1 (May and Hardwick, 2006). The Mad and Bub proteins were first identified in budding yeast by genetic screens for mutants that failed to arrest in mitosis when the spindle was destroyed (Taylor et al., 2004). These proteins are conserved in all eukaryotes. Loss-of-function mutations in *Drosophila bub1* result in lethality and severe mitotic abnormalities, consistent with premature anaphase entry observed in *bub1* larval neuroblasts (Basu et al., 1999). Several other checkpoint components such as Rod, Zw10 and CENP-E have since been identified in higher eukaryotes, but they have no yeast orthologues (Karess, 2005; Mao et al., 2003). Mad1 and Mad2 localize to unattached kinetochores, but not to attached kinetochores that lack tension. Bub1 and BubR1 localize to kinetochores lacking either tension or microtubule attachment. The protein kinase Aurora B, a component of the chromosomal passenger complex, is required to establish the checkpoint in response to lack of tension (Vagnarelli and Earnshaw, 2004).

The downstream target of the spindle checkpoint is the anaphase-promoting complex/cyclosome (APC/C) associated with its coactivator protein Cdc20 (or Fzy). APC/C^{Cdc20} promotes anaphase by targeting crucial substrates for proteasomal destruction, such as cyclin B and securin, which the checkpoint prevents. However, APC/C^{Cdc20} activity towards all substrates is not inhibited by the checkpoint and proteins such as cyclin A and Nek2A kinase continue to get ubiquitinated and degraded. The spindle checkpoint is established when Bub1 and Mad1 form a scaffold at the unattached kinetochore recruiting the more dynamic BubR1 and Mad2. Mad2 binds to Cdc20 and this interaction is essential for checkpoint-dependent inhibition of the APC/C (Hwang et al., 1998). In solution, Mad2 adopts an open conformation (O-Mad2), but on binding Mad1 or Cdc20, it changes to a closed conformation (C-Mad2) (De Antoni et al., 2005). In the currently favored model called the template model, the kinetochore bound Mad1/C-Mad2 complex acts as a template recruiting O-Mad2 and then

transferring it onto Cdc20 (Fig: 4). Thus, the unattached kinetochore generates a diffusible 'wait anaphase' signal (Yu, 2006).

But Mad2 alone does not appear to be the APC/C inhibitor. BubR1 can also bind Cdc20 and inhibit the APC/C independently of Mad2. Mad2 and Cdc20 found in a complex with BubR1 and Bub3 is called the Mitotic Checkpoint Complex (MCC). The MCC is a much more potent inhibitor of the APC/C than Mad2-Cdc20 alone (Sudakin et al., 2001).
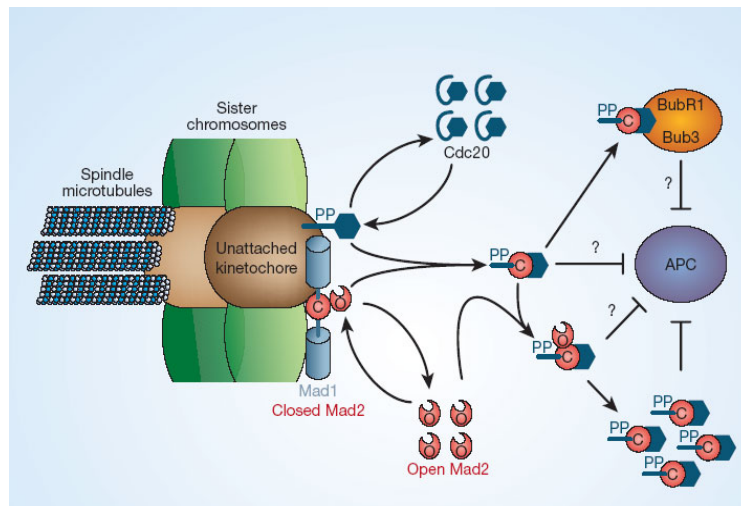
Figure: 4 The Template model for the spindle assembly checkpoint
Mad2 exists in two conformations, the unbound Open Mad2 (O) and the Mad1/Cdc20-bound Closed Mad2 (C). Mad1-C-Mad2 complexes occupying the unattached kinetochore recruit more O-Mad2, which then binds to activated Cdc20 present at the kinetochore (PP, phosphorylation). The resulting C-Mad2-Cdc20 complex inhibits the APC/C. It may also act as a template for the formation of more C-Mad2-Cdc20 complexes from the cytosolic O-Mad2 pool, thus amplifying the checkpoint signal. Further, it may act in conjunction with the BubR1-Bub3 complex to inhibit the APC/C. Adapted from (Hagan and Sorger, 2005).

Therefore, both Mad2 and BubR1 appear to act synergistically to fully inhibit APC/C^{Cdc20}. Consistent with this, recent data indicate that the spindle checkpoint in *Drosophila* S2 cells is Mad2-independent (Buffin et al., 2007), and that Mad2 is required only for delaying progression through prometaphase in order to provide enough time for the actual checkpoint proteins such as BubR1 and Bub1 to setup

the spindle checkpoint (Orr et al., 2007). The spindle checkpoint has also been found to destabilize Cdc20 in budding yeast (Pan and Chen, 2004), and therefore it has been proposed that the checkpoint also regulates Cdc20 protein levels, apart from inhibiting its activity towards certain substrates (Chen, 2007).

1.4.3 Proteolysis and the ubiquitin-mediated Proteasome system

The cell cycle is predominantly regulated by two types of post-translational protein modification - phosphorylation and ubiquitination. Ubiquitination is the covalent attachment of ubiquitin, a 76 amino acid 8 kDa polypeptide, to the lysine residues of substrates by the ubiquitination machinery. Although ubiquitination is known to mediate processes such as activating protein kinases, protein-protein interactions and marking proteins for endocytosis; proteolysis remains its most widely known function. The process of ubiquitination is mediated by at least three enzymes: an ubiquitin activating enzyme (E1), an ubiquitin conjugating enzyme (E2) and an ubiquitin ligase (E3) (Fig: 5). ubiquitin is first bound to and activated by E1 in an ATP-dependent manner. This activated ubiquitin moiety is then transferred to E2, which catalyzes its attachment to substrates. But the repertoire of E2 enzymes is small and they have only limited substrate specificity. This is where the E3 enzymes assume importance. E3s mediate substrate recognition and recruitment, and function in concert with E2s to perform ubiquitination. This specificity allows ubiquitin modifications to be targeted to specific proteins in a temporally and spatially regulated manner. Substrates tagged with ubiquitin are consumed by the large, 2.5MDa multicatalytic 26S Proteasome (Fig: 6). The Proteasome is composed of two subcomplexes, a 20S core protease (20S CP) harboring the catalytic activity and a 19S regulatory particle (19S RP) (Glickman and Ciechanover, 2002). The core particle is a barrel-shaped structure with a large internal cavity and it is composed of four stacked rings - two identical outer α-rings and two identical inner β-rings. The catalytic sites are localized to the β-rings. One or both ends of the barrel are capped by the 19S RP. It performs two functions: (1) binding and recognition of ubiquitinated substrates and (2) open an orifice in the α-ring to allow entry of the substrate into the proteolytic chamber (Glickman and Ciechanover, 2002).

While there is only one E1 in eukaryotic cells (Uba1), there are 10-32 E2s. The E3s are far greater in number and they belong to two main subfamilies: HECT domain proteins and RING-finger proteins. HECT proteins have a 350 amino acid HECT domain at the C-terminus, which contains a conserved cysteine to which activated ubiquitin is transferred from the E2 enzyme. RING-finger E3s contain a RING-finger domain that binds two Zn cations, or the structurally related U-box domain, and they promote the transfer of ubiquitin without forming a covalent intermediate (Passmore and Barford, 2004).
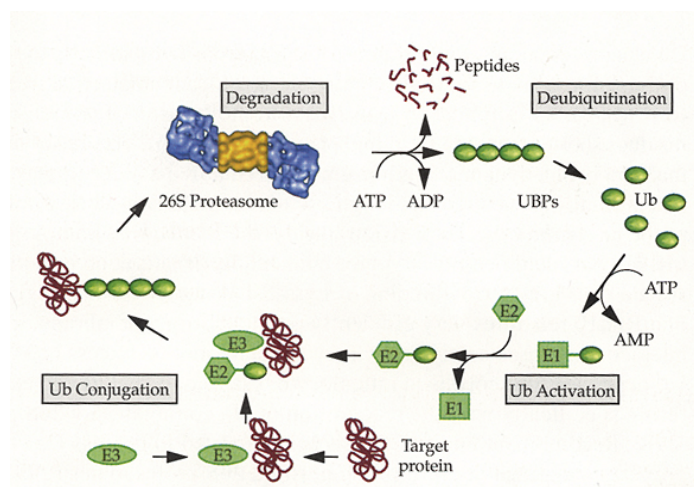
Figure: 5 The ubiquitin-Proteasome pathway
An enzyme cascade tags proteins with ubiquitin. First, the E1 enzyme activates the ubiquitin molecule by forming a thioester bond between a conserved cysteine at the enzyme active site and glycine 76 at the ubiquitin C-terminus. Next, the ubiquitin is transferred to an E2 enzyme, again through a thioester linkage. The E2 enzyme then conjugates the activated ubiquitin onto a lysine residue on the substrate, by forming an isopeptide bond in cooperation with an E3 enzyme. The substrate is recognized and recruited by the E3 enzyme. Monoubiquitinated substrates can be further ubiquitinated by linking additional ubiquitins to lysine 48 of the previous ubiquitin. The ubiquin-tagged substrates are degraded by the 26S Proteasome, releasing the ubiquitin chains. These chains are depolymerized by deubiquitinating enzymes or ubiquitin binding proteins (UBPs), releasing mono ubiquitin back into the cellular pool for reuse. Adapted from (Gordon, 2004).

The RING-finger E3 family is further composed of two distinct subgroups, single and multisubunit proteins. Mdm2, Ubr1/E3α and Parkin are examples for monomers or homodimers harboring both the RING-finger domain and the substrate-binding site in the same molecule. On the other hand, the SCF complex (Skp1-Cullin-F-box protein), the VBC complex (von-Hippel Lindau-

Elongins B and C) and the APC/C (Anaphase Promoting Complex/Cyclosome) are examples of multisubunit RING-finger containing E3 ligases (Glickman and Ciechanover, 2002; Passmore and Barford, 2004). Both the SCF and the APC/C are Cullin-based E3s involved in proteolysis of the core components of the cell cycle machinery.
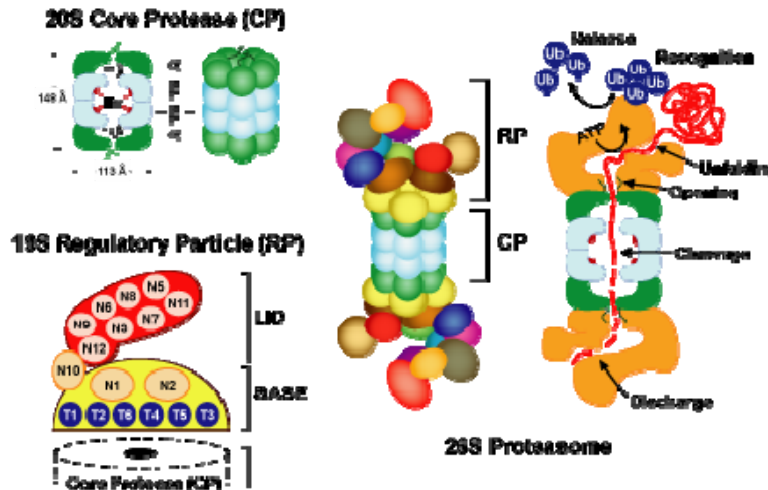
Figure: 6 The 26S Proteasome
The Proteasome is composed of a core protease and two regulatory complexes.The 20S core protease is a cylinder made up of four stacked heptameric rings, with the general structure α_{1-7} β_{1-7} β_{1-7} α_{1-7}. The active sites are on the inside of the cylinder and these can be reached via openings at either end. Access to both these openings is controlled by the 19S regulatory particle, which is composed of a lid and a base. The ubiquitinated substrate is recognized and unfolded by the 19S RP, facilitating entry into the proteolytic chamber. Adapted from (Gribskov, 2007).

The SCF complex consists of three invariable components - Rbx1 (RING-finger protein), Cul1 (scaffold protein) and Skp1 (adaptor protein) - as well as one variable component known as the F-box protein, that binds through its F-box motif to Skp1 and is responsible for substrate recognition. About seventy F-box proteins have been identified in humans and they fall into three categories - those with WD40 repeats (FBXW), leucine-rich repeats (FBXL) or other domains (FBXO). Skp22, Gbw7 and β-TrCP (β-transducin repeat-containing protein) are the major F-box proteins involved in cell cycle control (Nakayama and Nakayama, 2006). Recently it has been proposed that the APC/C inhibitor Rca1 may function as a G1-specific F-box protein, as part of an SCF complex in *Drosophila* (Zielke et al., 2006).

1.4.3.1 The Anaphase Promoting Complex/Cyclosome (APC/C)

The APC/C is structurally similar to the SCF, but is much larger at 1.5MDa and much more complex with thirteen subunits. It consists of invariable core components - Apc11 (RING-finger protein), Apc2 (scaffold protein) and at least eleven other components without defined roles. For ubiquitinating substrates, the APC/C needs to associate with either of two WD40 repeat-containing coactivator proteins - Cdc20 (Fizzy; Fzy in *Drosophila*) in early mitosis, and Cdh1/Hct1 (Fizzy-related; Fzr in *Drosophila*) in late mitosis and G1. Cdc20 and Cdh1 confer a certain degree of substrate specificity in much the same way the F-box proteins do in the SCF complex. APC/C^{Cdc20} performs the function that gives APC/C its name - promoting anaphase (Fig: 7). Additional meiosis-specific coactivators are present in *Drosophila* (eg: Cortex) and budding yeast (eg: Ama1) (Peters, 2006). The APC/C is known to collaborate with only two E2 enzymes - UbcH5 and UbcH10. UbcH5 is a highly promiscuous enzyme that can interact with several E3 ligases, but UbcH10 is known to support APC/C only. UbcH10 orthologues in *Drosophila* are essential for the initiation of anaphase, indicating that UbcH5 alone cannot support APC/C activity *in vivo* (Peters, 2006). The first structural insights into the APC/C was obtained by cryo-EM of complexes purified from human cells, *Xenopus laevis* egg extracts and budding yeast (Dube et al., 2005; Gieffers et al., 2001; Passmore et al., 2005b). 3D modeling showed that in all cases the APC/C is an asymmetric triangular complex (200 by 230 Å in size), composed of an outer wall and an internal cavity (Fig: 8). Cdh1 and the Cullin domain of the Apc2 subunit are located on the outside of the complex, making it plausible that ubiquitination reactions occur on the outside and not inside the cavity. An emerging view of the APC/C is that of a four-part enzyme composed of a structural arm (Apc1,Apc4,Apc5), a catalytic arm that houses the E2 binding sites (Apc2,Apc11,Doc1), a tetratricopeptide repeat (TPR) arm mediating the binding of activators (Cdc23,Cdc16,Cdc27,Cdc26,Swm1) and coactivators that help in the recognition of substrates (Cdc20,Cdh1,Cortex) (Thornton and Toczyski, 2006).
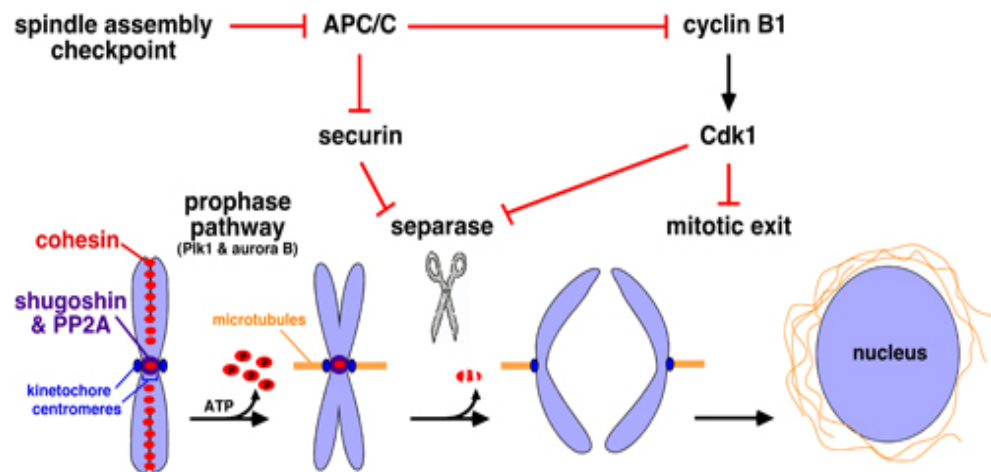
Figure: 7 APC/C mediates the progression through mitosis
Sister chromatids of replicated chromosomes are paired by the chromosomal cohesin complex, which is made up of four subunits - Smc1, Smc3, Scc1 and Scc3. Cohesin is removed from chromosomes during mitosis in two waves – those from the arms are displaced by the so-called prophase pathway involving Plk1 and Aurora B, which phosphorylate the Scc3 subunit. The centromeric cohesin is shielded by Shughoshin and protein phosphatase 2A (PP2A). Later in mitosis, this centromeric Cohesin can be cleaved by Separase, which is inhibited by Securin and cyclin B-Cdk1. Both inhibitors are targeted for proteolysis by the APC/C, once it is liberated from the spindle assembly checkpoint after bi-orientation of chromosomes at the metaphase plate. Thus APC/C mediates the cleavage of Cohesin by Separase to facilitate anaphase entry. The destruction of cyclin B-Cdk1 also accelerates mitotic exit. Adapted from (Stemmann, 2007).

How the APC/C-coactivator complex recognizes substrates is a mystery that remains unresolved despite being subjected to years of intense scrutiny. APC/C^{Cdc20} substrates possess a conserved nine-residue destruction element called the destruction box (D-box) with the consensus sequence RxxLxxxxN (Glotzer et al., 1991). APC/C^{Cdh1} substrates have another destruction motif called the KEN box (Pfleger and Kirschner, 2000). In general, D-boxes are recognized by both forms of the APC/C while KEN boxes are preferentially, but not exclusively, recognized by APC/C^{Cdh1}. Other destruction signals have also been identified in APC/C substrates; such as the A-box in Aurora A, O-box in ORC1 and the CRY box in Cdc20 (Araki et al., 2005; Littlepage and Ruderman, 2002; Reis et al., 2006). However, it is not clear whether these signals are recognized by the coactivators or by the APC/C core or both. Few substrates have been shown to bind to Cdc20 and Cdh1 in a D-box dependent manner, strengthening

the case for a substrate-specific adaptor role for the coactivators (Burton et al., 2005; Hilioti et al., 2001; Kraft et al., 2005).
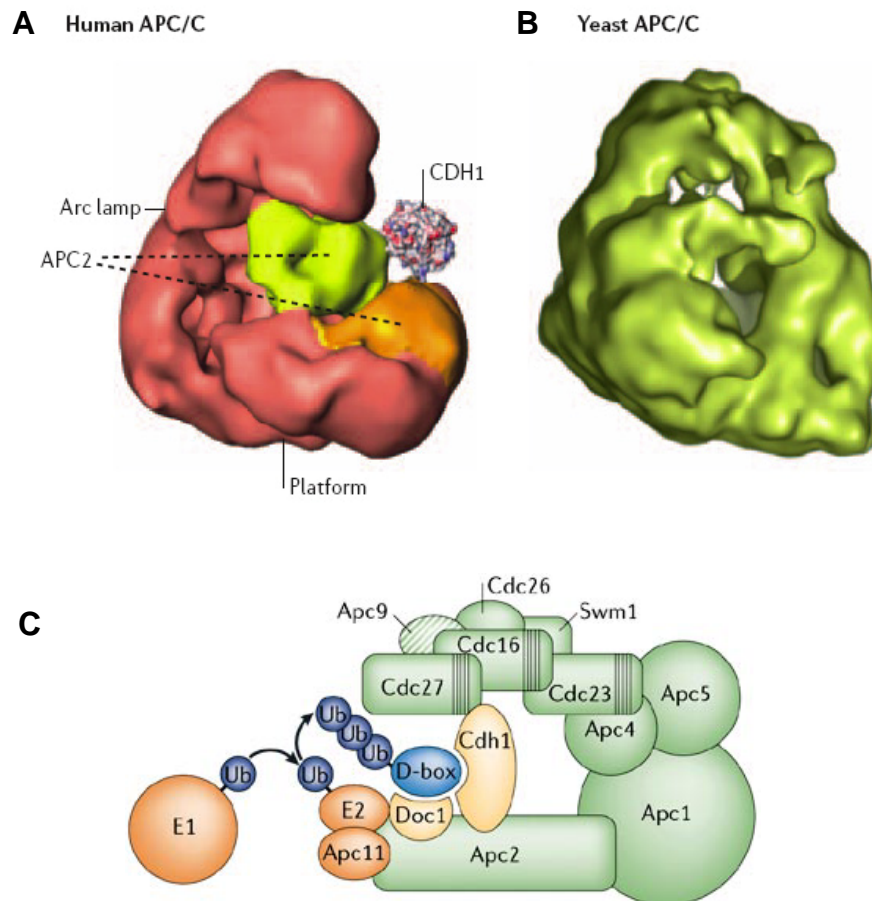
Figure: 8 APC/C architecture
The three dimensional structure of human APC/C (A) and budding yeast APC/C (B) obtained by cryo-EM and angular reconstitution. Both complexes are triangular in shape, have similar size and possess an internal cavity. Human APC/C has two large domains – platform and arc lamp, which are flexible with respect to their relative positions to each other. Candidate locations for the subunit Apc2 and the coactivator Cdh1 are shown. (C) Model for the ubiquitination of substrates by the APC/C. The subunits implicated in substrate recognition are shown in pale orange. TPR domains in certain subunits are indicated as vertical stripes. Apc9 is shown hatched since it has been detected only in budding yeast APC/C so far. Adapted from (Peters, 2006).

But recent demonstrations of the direct interaction of the APC/C with the cyclin B D-box and the mitotic kinase Nek2A independent of the coactivators, have challenged this idea (Hayes et al., 2006; Yamano et al., 2004). A stoichiometric role for coactivators in substrate recruitment is supported by the observation that

APC/C, coactivator and substrate form a ternary complex, and that the amount of substrate that binds to APC/C is directly proportional to the amount of coactivator associated with the APC/C (Eytan et al., 2006; Passmore and Barford, 2005).

1.5 Mitotic degradation of *Drosophila* cyclin A (CycA)

Ordered degradation of the mitotic cyclins; CycA, CycB and CycB3 is a hallmark of exit from mitosis in *Drosophila*. Induction of stable versions of each of the three mitotic cyclins arrests mitosis with different phenotypes. Stable CycA, depending on its levels, prolongs or blocks chromosome disjunction leading to a metaphase or anaphase arrest. Stable CycA also hampers the establishment of a quiescent G1 phase, after terminal mitosis 16 in the *Drosophila* embryonic epidermis and instead, triggers an extra division cycle. Stable CycB allows the transition to anaphase, but anaphase A chromosome movements are slowed, anaphase B spindle elongation does not occur, and the mono-oriented disjoined chromosomes begin to oscillate between the spindle poles. Stable CycB3 prevents normal spindle maturation and blocks major mitotic exit events such as chromosome decondensation. It is concluded that sequential degradation of distinct mitotic cyclins is required to transit specific steps of mitosis (Parry and O'Farrell, 2001). This sequential degradation is mediated by APC/C^{Fzy} in early M phase and by APC/C^{Fzr} during late M phase and G1 (Dawson et al., 1995; Sigrist et al., 1995; Sigrist and Lehner, 1997; Zachariae and Nasmyth, 1999). However, Fzr is not necessary for the completion of mitosis, but is necessary during G1 in *Drosophila* (Jacobs et al., 2002). Therefore Fzr may not be obligatory for completion of mitosis in metazoans and Fzy might be sufficient to do the job. But, Fzy cannot function in G1 probably because the APC/C is not phosphorylated in G1 and Fzy can only associate with phosphorylated APC/C. Thus, Fzr becomes crucial for APC/C function during G1.

Despite being targeted by the same destruction machinery, CycA turnover differs significantly from that of the B-type cyclins. Firstly, CycA disappears earlier than CycB and CycB3 (Lehner and O'Farrell, 1990). Secondly, when the spindle checkpoint is kept constantly active with microtubule poisons such as colchicine, both B-type cyclins are stabilized, but CycA is still degraded (Whitfield et al.,

1990). The destruction signal in CycB and CycB3 is essentially a single D-box; inactivating which, completely stabilize these proteins causing mitotic phenotypes (Jacobs et al., 2001) (Fig:9). But the CycA destruction signal is much more complex and poorly understood (Fig: 9). Cyclin A has D-boxes and KEN boxes (depending on the species), but inactivating those do not prevent proteolysis in *Drosophila* or vertebrates (den Elzen and Pines, 2001; Geley et al., 2001; Kaspar et al., 2001). Large deletions are required instead. In *Xenopus*, the cyclin B D-box can confer instability when grafted onto cyclin A1, but not vice versa (Klotzbucher et al., 1996). Initial analysis of the *Drosophila* CycA destruction signal had implicated the N-terminal first 170 amino acids in proteolysis (Sigrist et al., 1995).
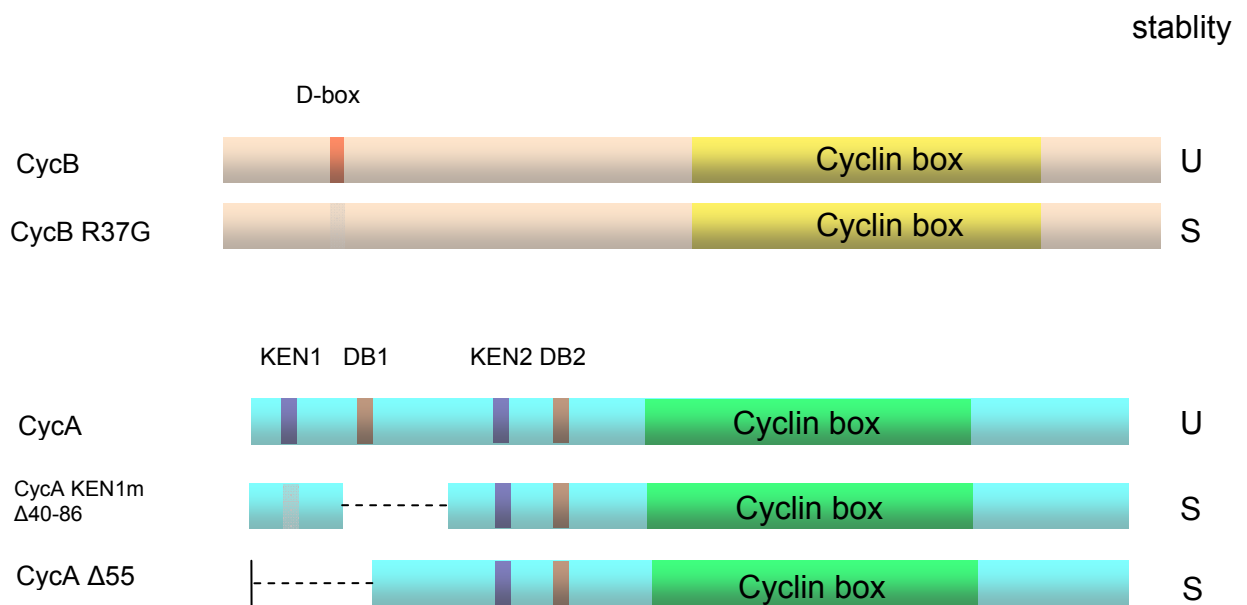
Figure: 9 The destrucution signals of *Drosophila* CycA and CycB
CycB is 530 residues long and its mitotic destruction is mediated by a single destruction box (D-box) at the N-terminus. A point mutation of the first D-box residue (R37G) renders the protein mitotically stable. CycA is 491 residues in length and shares homology with CycB in the region of the cyclin box, which mediates Cdk1 interaction. It has four potential destruction signals - two D-boxes (DB1 and DB2) and two KEN boxes (KEN1 and KEN2). Large N-terminal deletions which inactivate/remove KEN1, DB1 and surrounding residues are required to render CycA mitotically stable. U-unstable; S-stable.

There are four putative destruction signals in this region; two D-boxes and two KEN boxes (Fig: 9). Residues 46-54 constitute the first D-box (DB1; sequence RANFAVLNG), while the second D-box (DB2; sequence RSILGVIQS) extends from residues 160-168. The first KEN box (KEN1) starts at residue 13 and the second KEN box (KEN2) at residue 123. In DB1, the conserved L at position 4 is exchanged for F, a feature shared with the putative D-box in CycB3 (Sigrist et al., 1995). A point mutation in KEN1 along with a deletion removing DB1 and thirty-two residues downstream of it (K13A Δ40-86), stabilizes CycA (Kaspar et al., 2001). A deletion of the first 53-55 amino acids that removes KEN1, DB1 and the residues in between, also causes stability (Jacobs et al., 2001; Kaspar et al., 2001) (Fig:9). Thus, the first 86 residues encompassing KEN1, DB1 and surrounding regions seems to be essential for CycA destruction. However, these observations only throw up more questions; like which elements are being removed by these large deletions and how exactly do they influence stability? To make things more complicated, a CycA truncation having the entire N-terminal regulatory domain intact still does not undergo proper destruction (Kaspar et al., 2001).

2. Aim

Producing a mitotically stable form of CycA requires large N-terminal deletions, much unlike CycB, which can be stabilized by a single point mutation in its D-box motif. It is not clear what the deletions remove that result in stability. Even the roles played by the elements identified, KEN1 and DB1, are not properly defined. The fact that N-terminal deletions render CycA stable, implies that the destruction signals are located at the N-terminus. But, having the whole N-terminal region intact still does not ensure normal proteolysis, if the C-terminal half is lacking. Previous studies in other systems have claimed that the cyclin A C-terminal half is required to provide Cdk1 binding for cyclin A proteolysis. It is also not understood which elements mediate the unique degradation of CycA when the spindle checkpoint is active. Thus, our understanding of CycA turnover is incomplete and riddled with paradoxes.

The aim of this study in general was to properly define the elements responsible for CycA destruction during postblastoderm mitosis in the *Drosophila* embryo. In order to realize this goal, few sub-goals were set:

1. Identify what the large N-terminal deletions remove to cause stability.

2. Define the contributions of the two KEN boxes and the two D-boxes.

3. Characterize the elements mediating checkpoint proteolysis.

4. Figure out how the checkpoint bypass is achieved.

5. Verify claims by previous studies that interaction with Cdk1 is necessary for cyclin A proteolysis.

3. Results

3.1 Crystal structure of cyclin A: N-terminal half structure not available

Several crystal structures are available for cyclin A - that of bovine cyclin A3 (Brown et al., 1995), the human Cdk2-CycA2 complex (Jeffrey et al., 1995), the phosphorylated Cdk2-CycA2 complex (Russo et al., 1996b), and the phosphorylated complex bound to the p27^{Kip1} inhibitor (Russo et al., 1996a). But all structures lack the cyclin A N-terminal ~170 amino acids, which is not amenable to crystallization because of its floppy structure. This impairs the study of destruction signals which are located at the N-terminus. The conformation of the motifs governing destruction, their interactions with each other and the destruction machinery etc cannot be validated by structural data. But nevertheless, these structures do nicely bring out the mechanism of Cdk binding and activation, as well as the mode of cyclin-Cdk inhibition by CKIs.

The crystal structure of the truncated version of human CycA2 (homologous to *Drosophila* CycA), which lacks the N-terminal ~170 amino acids but has all the sequences required to form a minimal Cdk-binding interface; shows that CycA2 has a globular structure consisting of twelve α-helices (Jeffrey et al., 1995). Ten of these helices are arranged into two compact domains of five helices each (Fig: 10A). These domains are structural repeats with identical folds, which is surprising because they have very little sequence identity. The first domain consists of a right-handed three-helix bundle ($\alpha1, \alpha2, \alpha3$) along with two additional helices ($\alpha4$ and $\alpha5$). The corresponding helices of the second domain are named $\alpha1', \alpha2', \alpha3', \alpha4'$ and $\alpha5'$.

In addition to the ten helices in these two repeats, there is an N-terminal α-helix which packs against the second domain as an extension to it. There is also an extended α-helix at the C-terminus of the protein. The first domain corresponds to the cyclin box, which is approximately 100 residues long and forms the key element at the CycA2-Cdk2 interface (Morgan, 1997). The cyclin box is well

conserved in different cyclins (30-50% similarity among cyclins A, B, D1 and E) and it forms the binding site for the PSTAIRE helix, the T-loop and N-terminal β-sheet of Cdk2 (Fig: 10B&C).
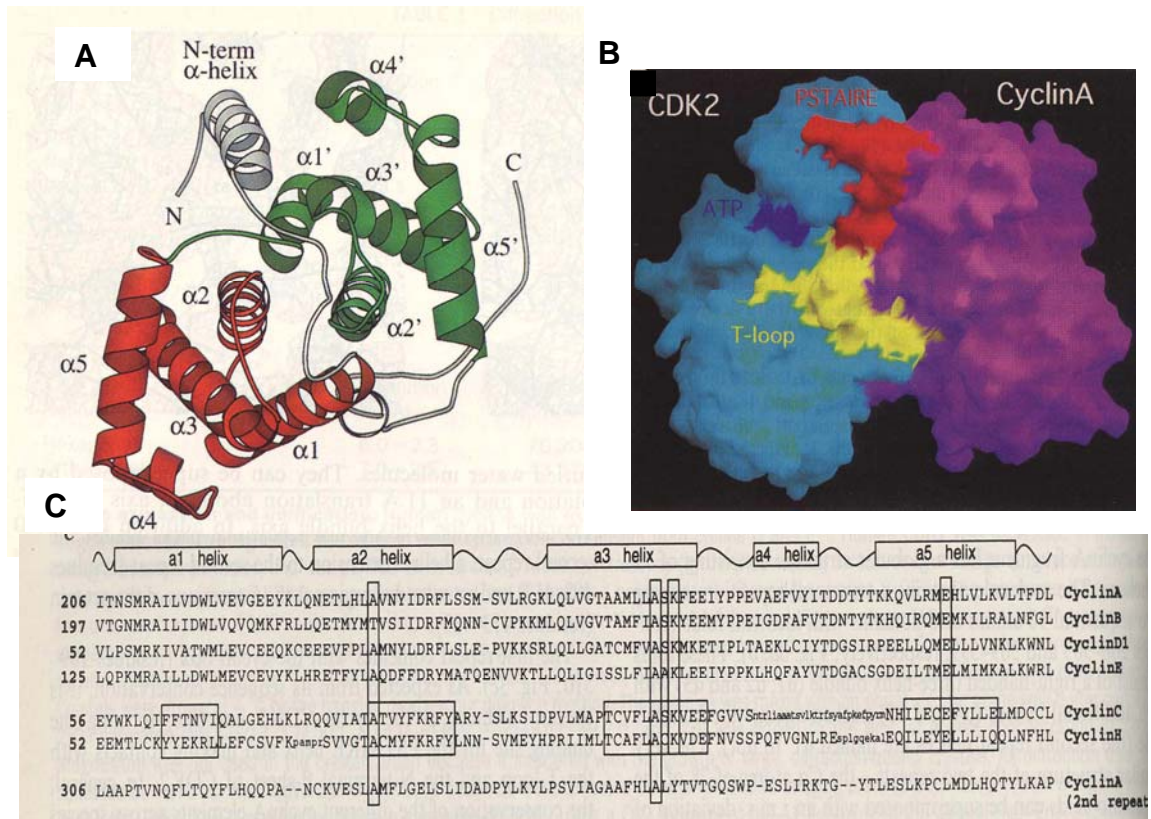
Figure: 10 The Structure of cyclin A
(A) The tertiary conformation of truncated human cyclin A2 (amino acids 173-432). The first domain and its five α-helices are shown in red, while the second domain with its five helices is shown in green. The N-and C-terminal helices are depicted in grey. (B) Surface representation of CycA2 (magenta) bound to Cdk2 (blue) indicating the intimate interface between the two proteins. (C) Alignment of the cyclin box (first domain) sequence of CycA2 with that of cyclins B, D, E, C and H. The corresponding secondary structures in CycA2 are shown on the top. Cyclins B, D and E show 40-50% similarity with CycA2 in this region; but cyclins C and H are more distantly related. The horizontal boxes around the sequences of cyclins C and H show hydrophobic residues that share homology with similar residues in other cyclins; and the lower case letters represent insertions. The vertical boxes indicate conserved alanine, lysine and glutamate residues. Lysines and glutamate are involved in interactions with Cdk2. Sequence from the second repeat of CycA2 show very little conservation with the sequence of the cyclin box. Adapted from (Jeffrey et al., 1995).

It has conserved lysines and glutamic acid residues for these purposes, which are absent, from the second domain that does not contact Cdk2 (Fig: 10C). CycA2-Cdk2 is a high-affinity complex and the binding interface exhibits an unusually large surface area (Fig: 10B). About 35% of this interface involves

interactions between Cdk2 and the poorly conserved N-terminal helix of CycA2. Several other helices in CycA2 contact both lobes of Cdk2 in the region adjacent to the active site cleft. Interestingly, CycA2 structure is unaffected by Cdk2 binding, indicating that cyclin A provides a rigid framework against which the pliable Cdk2 subunit is molded. But CycA2 binding has a major impact on the conformation of the Cdk2 active site. The most obvious change occurs in the T-loop which no longer occludes the substrate binding site, but lies almost flat at the entrance of the cleft (Morgan, 1997). Cyclin binding also exposes the Thr160 residue on the T-loop to the solvent, allowing its phosphorylation by CAK. Substantial changes also occur in the ATP-binding site - the small helix (L12) that disrupts the active site in the Cdk2 monomer is melted, allowing the PSTAIRE helix to move inward. These movements cause the reorientation of several key side chain residues (Asp145, Glu51, Lys33), leading to the precise positioning of the ATP phosphate for the phosphotransfer reaction.

The crystal structure of Cdk2-CycA2 with the p27[Kip1] inhibitor bound to it provided a breakthrough in the understanding of CKI inhibitory mechanisms. The structure includes a 69 amino acid N-terminal segment of p27 that contains both the cyclin and Cdk binding motifs (Russo et al., 1996a). The p27[Kip1] peptide is stretched across the top of the CycA2-Cdk2 complex in an extended conformation. The inhibitor employs a multifaceted approach to thoroughly disrupt the active site. At the N-terminus of p27[Kip1] is the cyclin-binding region, which interacts with a binding pocket on CycA2 without affecting its structure. At the C-terminus is the Cdk-binding region which interacts extensively with the upper lobe of the kinase.

3.2 Monitoring CycA destruction *in vivo*: A transient expression system

The postblastoderm cell cycles in the developing *Drosophila* embryonic epidermis (cycles 14-16) provide an ideal setup for following the mitotic expression and destruction of introduced constructs. The first 13 cycles are powered by maternal supplies and zygotic transcription is established only by cycle 14. In contrast to the rapid initial cycles lasting just 10-20 minutes each, the

zygotically controlled cycles 14-16 are long and drawn out with a lengthy interphase comprising G2. Division 14, which is the first of these zygotic divisions, is especially useful because the 14th mitosis occurs in a temporally and spatially regulated pattern in which groups of cells undergo a similar developmental fate and divide together as a domain. The chromosomes are well ordered during this stage and the nuclei are polarized relative to the embryo surface. The cells are also relatively large which facilitates microscopic observations. Interference from maternally derived gene products is absent and the expression of an introduced gene can be more efficiently followed. For these reasons, the 14th mitosis was chosen to analyze CycA proteolysis *in vivo*. Where indicated, constructs were tagged with an HA (hemagglutinin) tag at the N-terminus. RNA encoding the desired constructs were synthesized *in vitro* and injected close to the embryo periphery just prior to the onset of cellularization, so as to allow uptake into the newly forming cells. The injected RNA gets translated as cells progress through interphase 14 which can be detected by whole embryo Western blotting (Fig: 11).
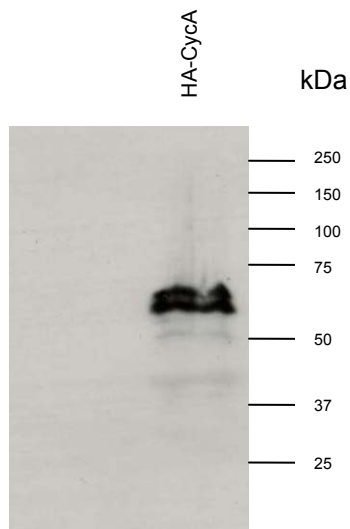
Figure: 11 HA-CycA is expressed *in vivo* from injected RNA
1h old wild type embryos were injected with RNA encoding HA-CycA and subjected to Western blotting with anti-HA antibody after incubation for a further 1h 30min. HA-CycA is 56.15 kDa in size and runs as multiple bands due to phosphorylation (discussed below).

For following HA-CycA destruction, embryos were fixed as cells passed through mitosis 14, stained with anti-HA antibody and analyzed by fluorescence microscopy. These cells also express endogenous CycA in addition to that from

the injected RNA; which leads to increased CycA expression. But elevated CycA levels do not interfere with the normal timing and pattern of degradation or cell cycle progression (Kaspar et al., 2001). Moreover, the turnover profile of HA-CycA produced from the injected transcript is identical to that of endogenous CycA (Kaspar et al., 2001). The mitotic turnover of HA-CycA is shown in figure 12A. Protein levels are highest in prophase and start to decline during prometaphase. Metaphase cells typically possess varying amounts of HA-CycA suggesting that destruction is an ongoing process during this stage. Endogenous CycA exhibits the same destruction profile (Su and Jaklevic, 2001). Owing to the high variation in metaphase signals, fluorescence intensities quantified from metaphase cells exhibit a high standard deviation (Fig: 12D). HA staining is reduced substantially by early anaphase (down to ~20%) indicating that proteolysis is more or less completed by this stage, and it remains essentially absent from succeeding anaphase and telophase stages. The same destruction pattern is observed when HA-CycA is expressed in *Drosophila* Schneider (S2) cells (Fig: 12C). In sharp contrast to this, cells from embryos injected with HA-tagged GFP show equal HA fluorescence levels in all mitotic stages (Fig: 12B). Quantification of fluorescence intensities from embryos injected with HA-CycA or HA-GFP show that while HA-GFP remains stable throughout all mitotic stages, HA-CycA levels dramatically fall early in mitosis (Fig: 12D). Therefore, the observed fall in HA-CycA levels occurs due to proteolysis and not as a consequence of inefficient antibody staining.

HA-CycA destruction can also be followed by directly injecting the protein into embryos. When bacterially expressed and purified GST-HA-CycA (GST fused to the N-terminus of HA-CycA) was tested in this manner, the construct appeared to remain stable throughout mitosis (data not shown). This might be due to the large GST moiety (28 kDa in size) interfering with the folding of HA-CycA and hindering access to the N-terminal destruction signals. Since the results obtained with protein injections were vague and ambiguous compared to RNA injections, this strategy wasn't employed for further experiments.
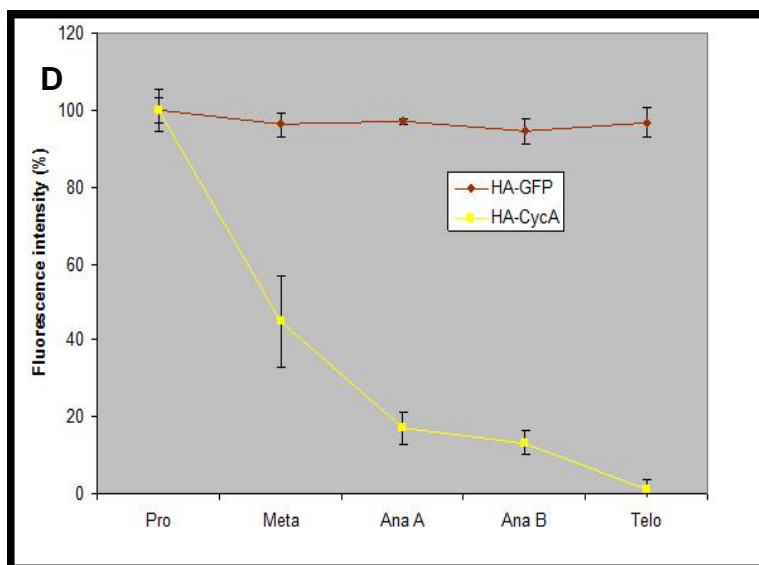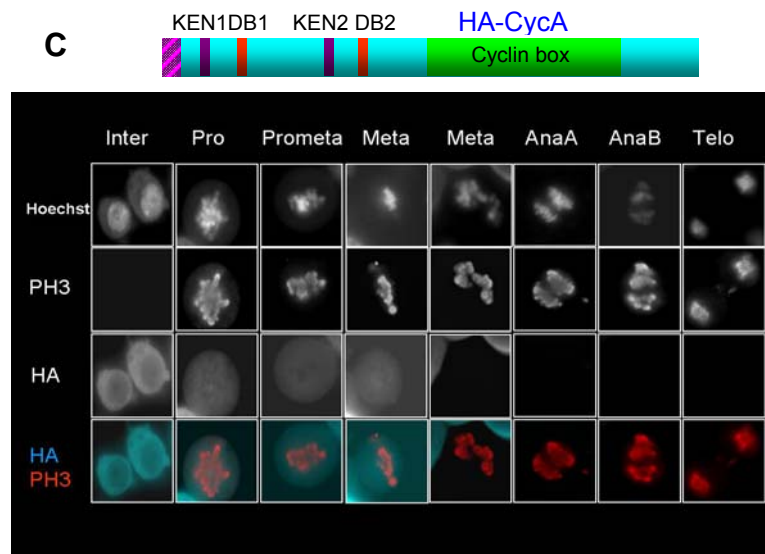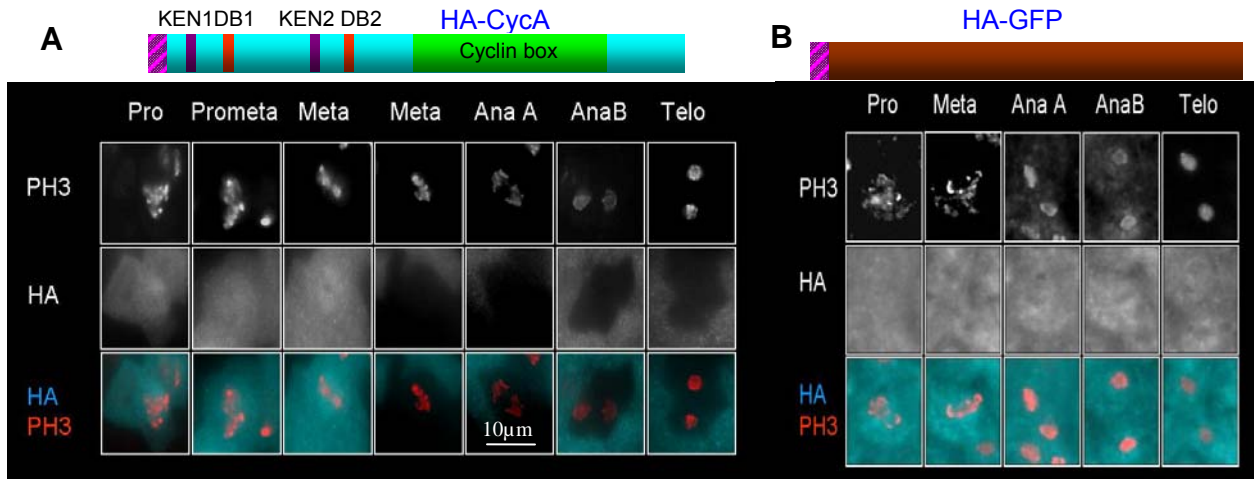
Figure: 12 Mitotic degradation of HA-CycA

Hoechst stains the DNA. HA corresponds to immunofluorescent detection of the HA-tagged protein translated *in vivo* from the injected RNA. Mitotic chromosomes were visualized with antibodies against phosphorylated Histone3, PH3.

(A) Cells undergoing mitosis from an embryo injected with HA-CycA. Metaphase cells with and without high HA fluorescence are typically seen, while succeeding mitotic stages have negligibly small signal intensities. (B) In an embryo injected with HA-GFP, cells progress through and exit from mitosis normally, although constant levels of HA fluorescence are visible in all mitotic stages. (C) S2 cells transfected with HA-CycA degrades the protein in much the same manner as embryos. During interphase, HA-CycA is cytoplasmic and is mostly absent from the nucleus marked by *Hoechst*. Metaphase cells having and lacking HA-signal are observed. (D) Quantification of HA fluorescence from cells progressing through mitosis 14 in embryos injected with HA-CycA (n=176 from 11 embryos) or HA-GFP (n=148 from 10 embryos). A high standard deviation is obtained for HA-CycA metaphase fluorescence which is due to variations in signal intensities ranging from high to none.

3.3 Cyclin destruction under the influence of the spindle checkpoint

Cyclin A is one among a unique set of proteins that are degraded by APC^{Cdc20} even when the spindle assembly checkpoint is operational. While substrates such as cyclin B and securin are stabilized; cyclin A, Nek2A and HOXC10 are unstable prior to metaphase, when the unattached sister chromatids keep the spindle checkpoint active (Gabellini et al., 2003; Geley et al., 2001; Hames et al., 2001b).
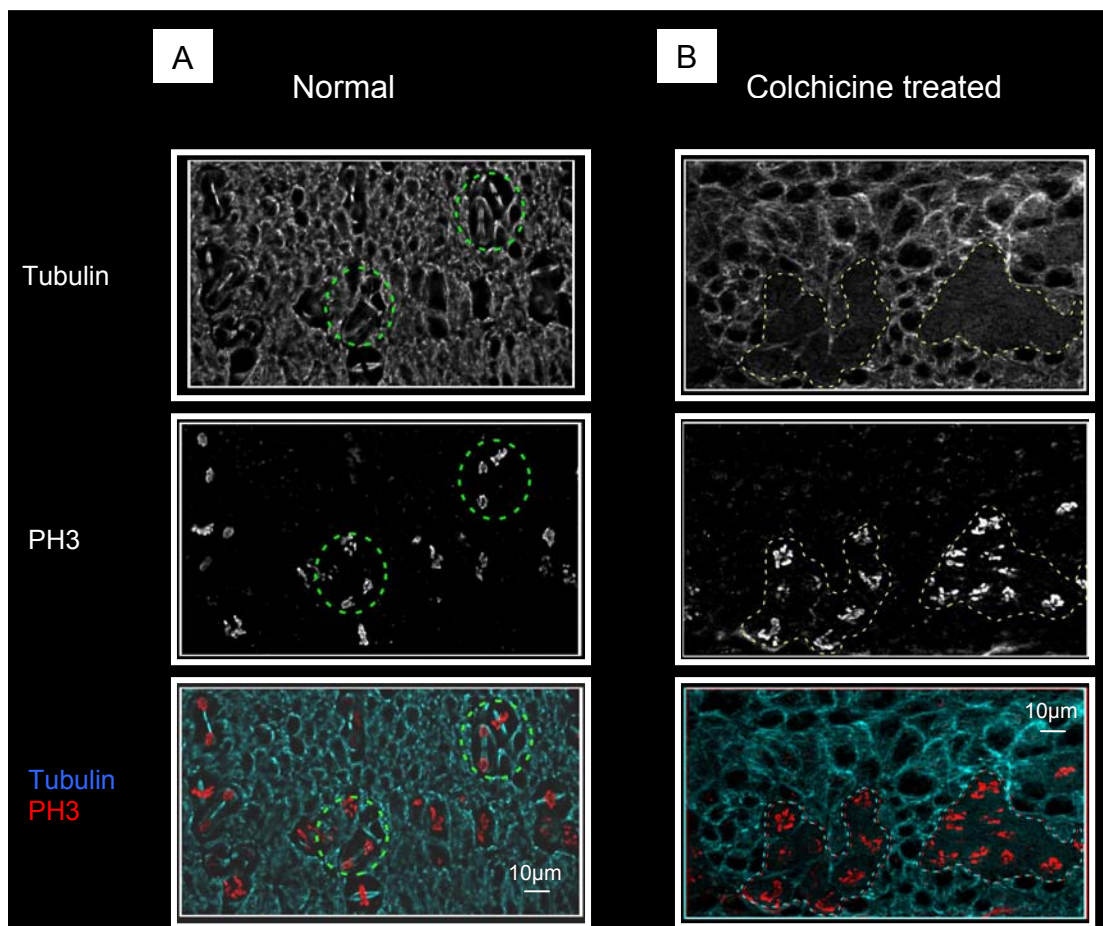
Figure: 13 Colchicine arrests mitotic cells in c-metaphase
(A) A portion of a normal embryo showing cells undergoing mitosis 14. Mitotic cells form normal looking spindle structures (Tubulin) with proper chromosome figures (PH3) ,indicated by green circles. Non-mitotic cells negative for PH3 are in interphase and show typical interphase spindle morphology. (B) A portion of an embryo of the same age treated with colchicine. Outlined regions show c-metaphase arrested cells with abnormally condensed chromosome figures (PH3) and a lack of corresponding mitotic spindle (Tubulin). But interphase cells exhibit normal tubulin structures.

36

To test whether the transient assay system employed in this study can reproduce the checkpoint behavior of cyclins, embryos injected with the relevant constructs were treated with the microtubule depolymerising drug colchicine prior to fixation. When immersed in colchicine-containing media, the drug penetrates into the embryo and disrupts dynamic microtubules that form the mitotic spindle. Interphase spindle, which is constituted of more static microtubules, is less susceptible to the action of the drug. Colchicine forms a tight complex with tubulin, inducing a conformational change in the protein and inhibiting microtubule growth substoichiometrically. It has been proposed that tubulin associated with colchicine does undergo polymerization; but this polymerization is different from normal and results in a polymer with an altered morphology (Andreu and Timasheff, 1982). This happens because the correct binding geometry between tubulin protomers is distorted by the binding of the drug (Andreu and Timasheff, 1982).

In the absence of microtubules, most features of the G2-M transition take place except for spindle formation. Consequently, chromosomes neither undergo prophase movements nor align properly on the metaphase plate. Anaphase movements are also disrupted. Instead, chromosomes continue condensing to produce disfigured structures and arrest in a metaphase-like state. This is referred to as a c-metaphase (Whitfield et al., 1990) (Fig: 13). The spindle checkpoint remains permanently switched on in such cells owing to the presence of unattached kinetochores. In the experimental setup used here, embryos were subjected to colchicine treatment for 90 min. This length of treatment results in the c-metaphase arrest of many, but not all, cells. Affected cells can be distinguished by the lack of mitotic tubulin structures and by the over-condensed chromosome morphology (Fig: 13). When embryos injected with HA-CycB were treated with colchicine, almost all c-metaphase arrested cells were found to retain the protein in high levels (Fig: 14A). Quantification of fluorescence intensities in these cells revealed that about 95% of them retained HA-CycB (Fig: 14C). By contrast, HA-CycB-injected embryos not subjected to colchicine treatment, readily degraded the protein by early anaphase (Fig: 15). It is

concluded that HA-CycB is stabilized by activation of the spindle checkpoint resulting from colchicine treatment.
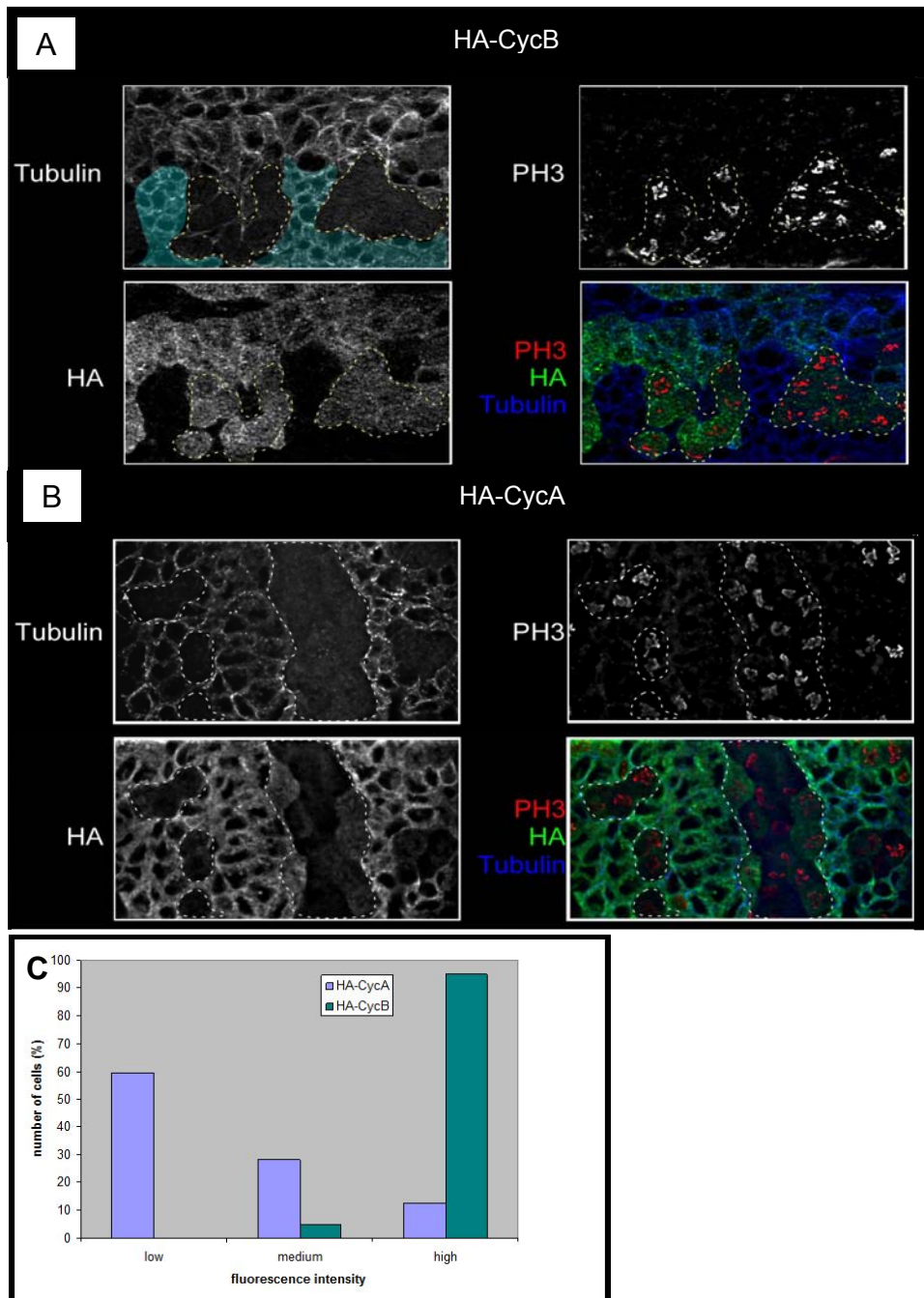
Figure: 14 Cyclin A is unstable when the spindle checkpoint is active
(A) Outlined regions show cells arrested in metaphase of mitosis14 with disrupted spindle (Tubulin) and abnormal chromosomes (PH3), retaining high levels of HA-CycB fluorescence. The blue-shaded region in the tubulin stain indicates interphase cells which have already passed through mitosis 14 before colchicine arrest and hence have degraded HA-CycB. These cells are relatively smaller. (B) Most c-metaphase arrested cells (outlined regions) from an HA-CycA injected embryo show little or no HA signal. (C) Quantification of the number of colchicine-arrested cells retaining high, medium or low fluorescence (see Materials and Methods) in embryos expressing HA-CycB (n=92 from 9 embryos) or HA-CycA (n=114 from 10 embryos).

Next, the behavior of HA-CycA was tested under the same conditions. In this case, the majority of c-metaphase arrested cells harbored little or no protein after being subjected to colchicine treatment for the same duration (Fig: 14B). Quantification of HA signal intensities showed that just 13% of the cells analyzed retained significant amounts of HA-CycA (Fig: 14C). About 60% of the cells had little or no amounts of the protein, while ~27% cells had medium amounts. Thus, HA-CycA is unstable even when the spindle checkpoint is kept active. These observations are in perfect agreement with the checkpoint degradation of endogenous CycA in the embryo as well as that of CycA and CycB in larval brains (Leismann et al., 2000; Whitfield et al., 1990). Hence, the transient expression system employed in this sudy can efficiently reproduce the proteolytic behavior of cyclins under the influence of the spindle checkpoint.
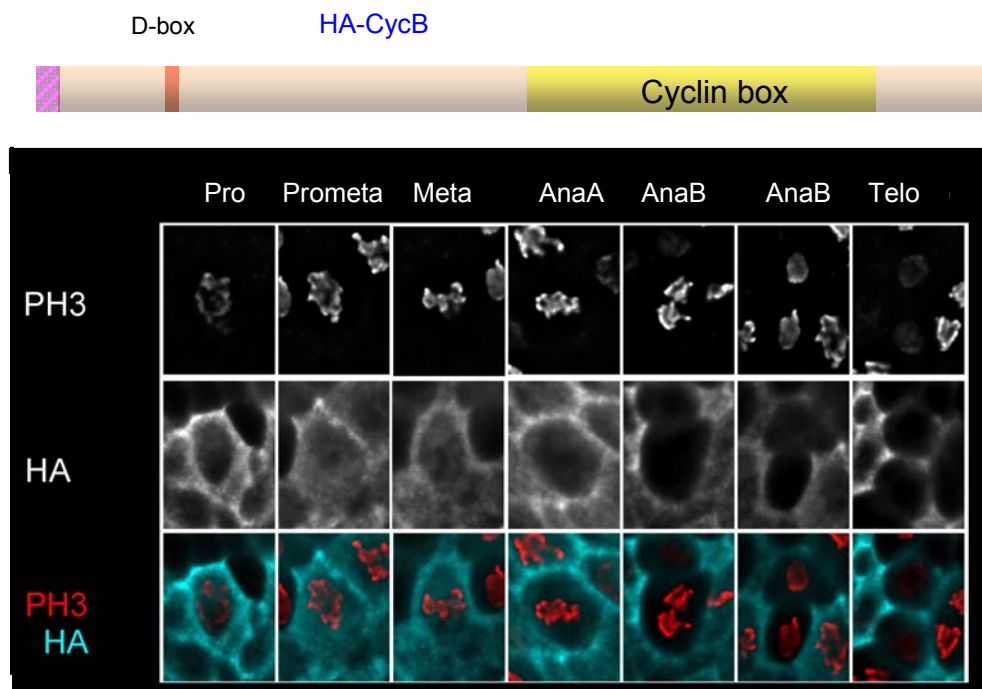
Figure: 15 HA-CycB is turned over during anaphase in an unperturbed mitosis
Cells from an embryo injected with HA-CycB are shown ordered according to mitotic stage. Constant HA signal intensities are observed until metaphase, but levels fall by early anaphase and remains absent from subsequent stages. This anaphase degradation is similar to that observed for endogenous cyclin B in *Drosophila* as well as in vertebrate systems.

3.4 N-terminal signals have additive effects in CycA destruction

Previous deletion and mutagenic analyses had implicated the N-terminal half in CycA proteolysis (Kaspar et al., 2001). Among the putative destruction signals present in that region, the first KEN box (KEN1) and the first D-box (DB1) were found to be the motifs that were involved.
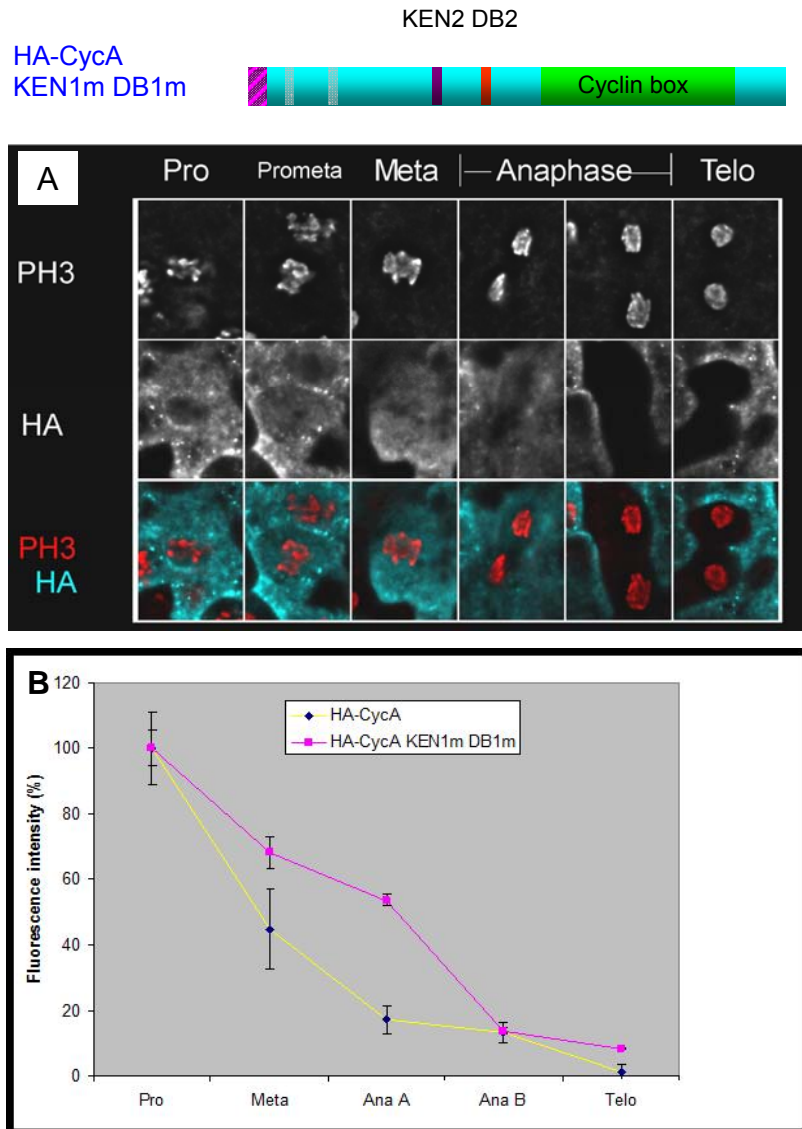
Figure: 16 Mutating KEN1 and DB1 delays proteolysis
(A) Cells representing mitotic stages from an embryo injected with HA-CycA having point mutations in KEN1 (K13A) and DB1 (R46G) are shown. Fluorescence levels persist till early anaphase and disappear only later in anaphase. (B) Quantification of data from embryos injected with this construct is shown plotted with that for wild-type HA-CycA. Higher HA fluorescence of the double mutant is present in metaphase and anaphase A, indicating inefficient turnover.

However, eliminating either or both of them did not stabilize the protein although it did impair proteolysis to some extent. Eliminating both KEN1 and DB1 delayed turnover more than eliminating any one of them. This hinted at an additive contribution of these elements towards proteolysis. To study the role of these elements in further detail, the construct with point mutations in both KEN1 (K13A) and DB1 (R46G) was re-analyzed, this time quantifying the fluorescence in M14 cells and collecting statistical data of its turnover profile (Fig: 16). These point mutations at conserved positions have been previously shown to inactivate the respective elements as effectively as their deletions (Kaspar et al., 2001). Unlike wild-type HA-CycA, the double mutant is no longer turned over by metaphase, instead, it persists till early anaphase in significant amounts (53% of the prophase value) and disappears only late in anaphase (n=52). Apparently, efficient proteolysis of this construct occurred only after the checkpoint was turned off in anaphase. Moreover, in contrast to wild-type HA-CycA, this construct does not show varying metaphase signal intensities and therefore does not have a high metaphase standard deviation (Fig: 16B). Thus KEN1 and DB1 contribute to CycA destruction; but additional elements must be present since inactivation of KEN1 and DB1 does not cause full stability.

Indeed, the minimum deletion required to stabilize CycA is one that removes 47 residues around DB1, along with a point mutation in KEN1 (HA-CycA KEN1m Δ40-86) (Kaspar et al., 2001). The Δ40-86 deletion removes DB1, six residues upstream of it and 32 residues downstream of it. In an attempt to narrow down on the elusive motif(s) being removed by that deletion, an equivalent construct was made wherein the KEN1 mutation was retained, but DB1 was point-mutated instead of being deleted, and the 32 residues downstream of it was deleted (HA-CycA KEN1m DB1m Δ55-86). The 6 residues upstream of DB1 that are removed by the Δ40-86 deletion were not considered important, because shorter deletions involving those residues had not produced similar effects (Kaspar et al., 2001). Figure 17 shows the destruction profile of the equivalent construct. Surprisingly, it was not mitotically stable like the KEN1m Δ40-86 mutant. However, proteolysis was considerably compromised and the protein remained stable well into late anaphase stages. Quantification of fluorescence data showed that the additional

deletion of the DB1 downstream region (DDR) impaired destruction more severely than inactivating just KEN1 and DB1 alone (Fig: 17B). Degradation seemed to be more compromised during metaphase and anaphase A. These results stress on the fact that there are multiple N-terminal signals on CycA, which cooperate to effect timely mitotic destruction.
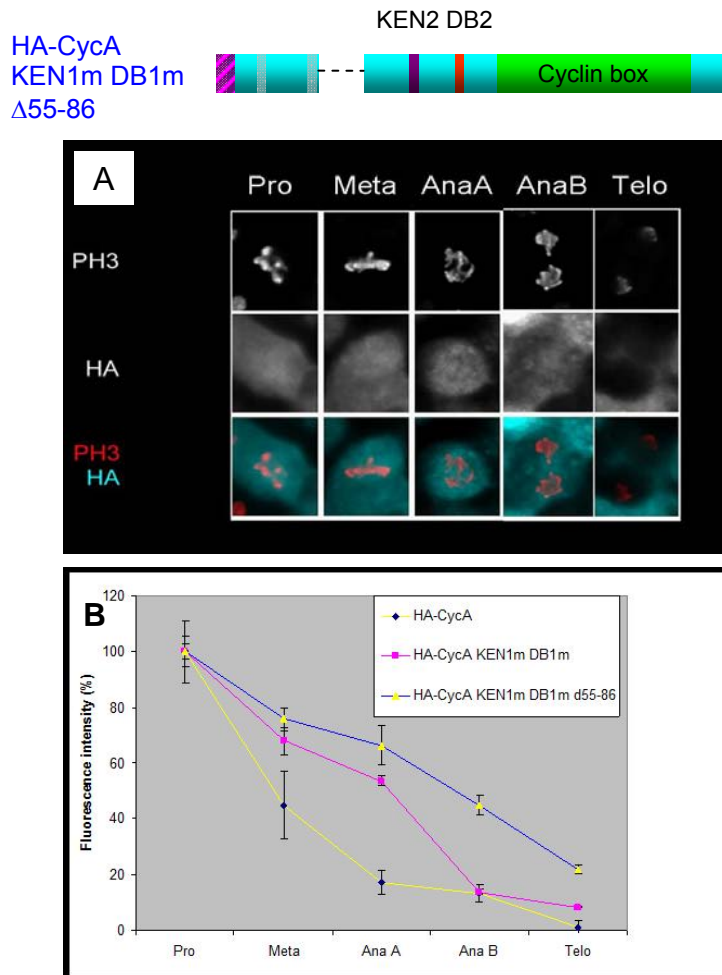
Figure: 17 The region downstream of DB1 contributes to CycA proteolysis
(A) An embryo injected with HA-CycA lacking KEN1, DB1 and 32 residues downstream of DB1 shows M14 cells with high HA signal intensities in early anaphase (AnaA) and persisting well into late anaphase stages (AnaB). Telophase cells have low levels. (B) Quantification of data from embryos expressing this construct is shown plotted with that of HA-CycA and HA-CycA lacking KEN1 and DB1. An increased stability is obvious when the DB1 downstream region is additionally deleted.

Figures 16 and 17 show that the elimination of N-terminal signals prolongs HA-CycA destruction until anaphase, which is when the spindle checkpoint is turned off and the APC/C switches coactivators from Fzy to Fzr. This suggests that the

above alterations in HA-CycA make it an inefficient substrate of the checkpoint-controlled APC/C^{Fzy}. In order to analyze the role of the N-terminal signals specifically in checkpoint destruction, HA-CycA versions lacking one or more of those elements were generated, and their turnover was followed in c-metaphase arrested cells.
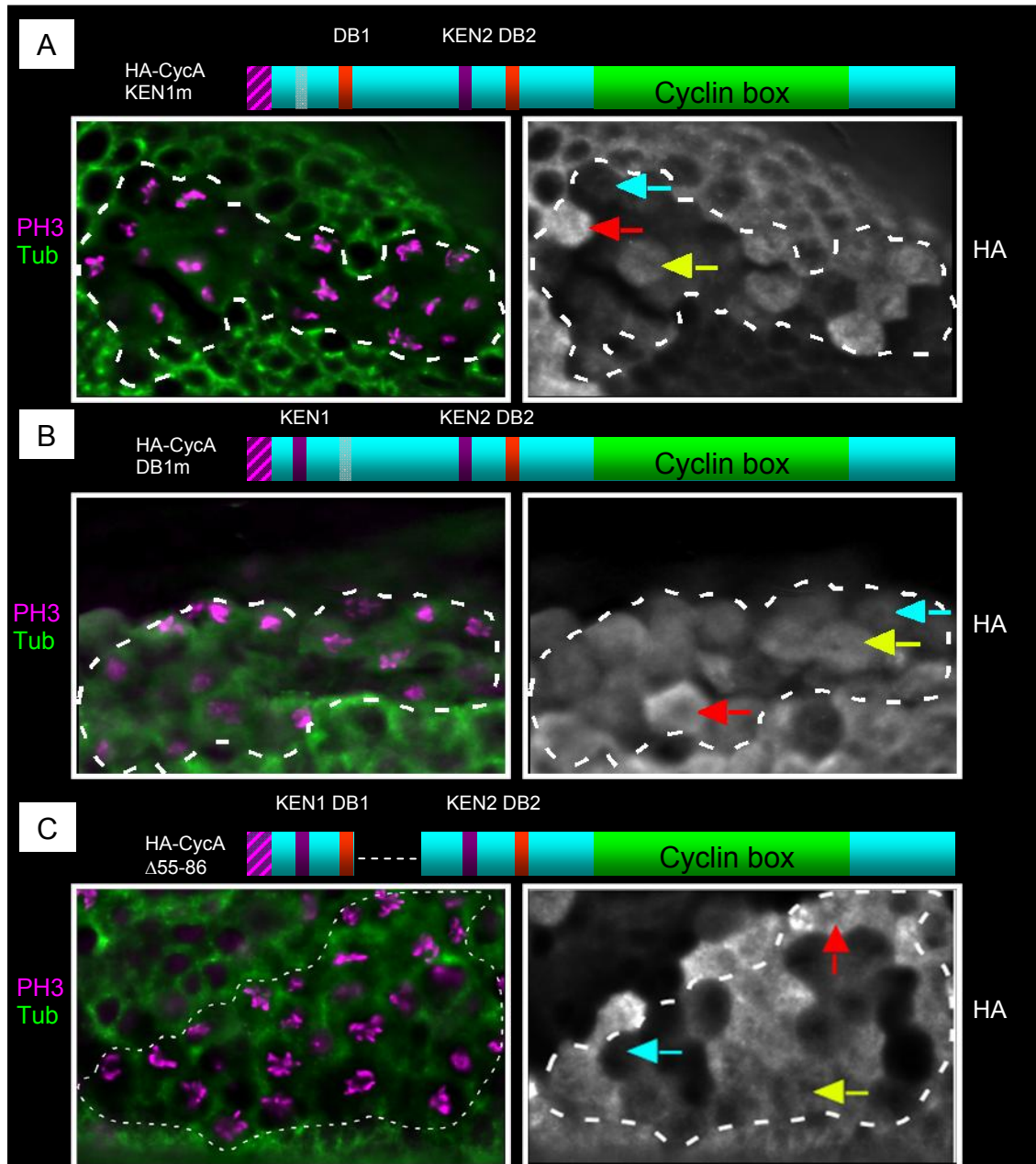
Figure: 18 Single element knockouts cause partial stability under checkpoint conditions
Destruction of HA-CycA with point mutations in KEN1 (K13A) (A), DB1 (R46G) (B) or the deletion Δ55-86 (C), in c-metaphase arrested cells from embryos of the same age are shown (outlined regions). In each case, intermediate stability was obtained with cells having high (red arrows), medium (yellow) or low (blue) levels of the protein.
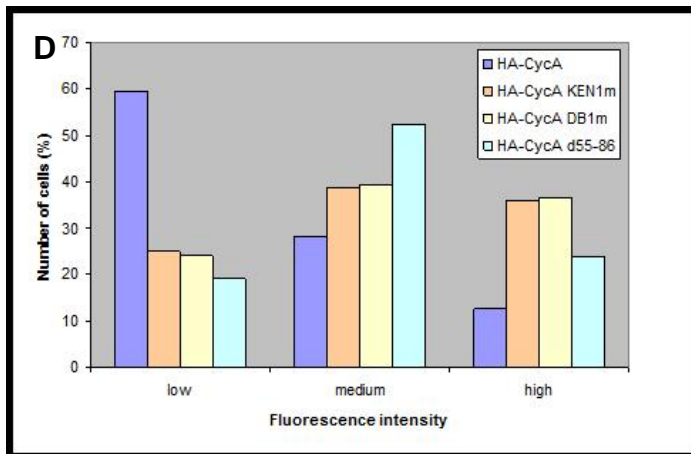
Figure: 18(D) Quantification of HA fluorescence from embryos injected with the constructs in (A), (B) and (C). Constructs lacking KEN1, DB1 or residues 55-86 is retained in high and medium levels by more number cells than for wild-type HA-CycA, which is retained in low levels by most cells (see Materials and Methods).

As above, point mutations K13A and R46G were used to knock-out KEN1 and DB1 respectively, and the DB1 downstream region was eliminated by the Δ55-86 deletion. Individual elimination of these elements have no significant effect on CycA destruction during an unperturbed mitosis (Kaspar et al., 2001); but under constant checkpoint conditions, each knock-out partially stabilized the protein (Fig: 18). In each case, cells expressing the protein were grouped into three classes based on the level of HA fluorescence they had – low, medium and high (Fig: 18D). Cells from the same mitotic domains were examined in all cases so that the cells would have spent roughly the same time in mitosis. For HA-CycA, most cells had low signals (~60%), indicating an efficient turn over. But for each of the individual knock-outs, most cells retained HA signals in high or medium levels, indicating inefficient turn over. When either KEN1 or DB1 was inactivated, close to 40% of the cells retained high HA signals and when residues 55-86 were deleted ~25% cells harbored high levels, as opposed to just 13% for wild-type HA-CycA (Fig: 18D).

Next, simultaneous knock-outs of any two motifs were analyzed. All three double knock-out combinations; namely KEN1m-DB1m, KEN1m-Δ55-86 and Δ40-86 (ΔDB1 Δ55-86) rendered HA-CycA completely stable in colchicine arrested epidermal cells (Fig: 19). In each case, nearly all cells retained high and constant amounts of HA fluorescence.
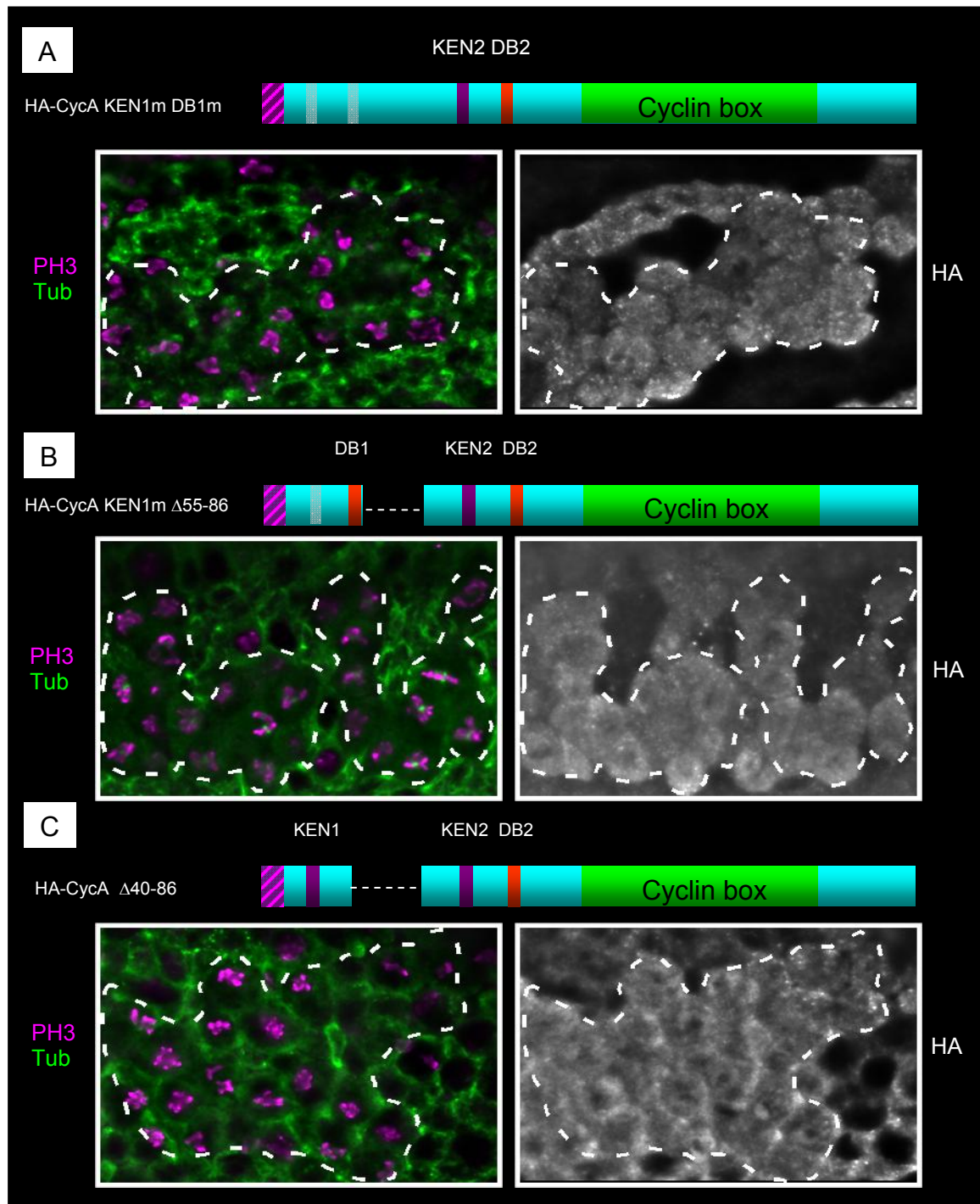
Figure: 19 Double element knock-outs abolish checkpoint degradation of CycA
Eliminating any two N-terminal signals; KEN1m DB1m (A), KEN1m ∆55-86 (B) and ∆40-86 (C) cause high HA fluorescence levels to remain constant in virtually all c-metaphase arrested cells (outlined regions).

The stability achieved with all three double knock-outs was comparable to that of CycB (data not shown). Cumulatively, these results confirm that the N-terminal motifs make additive contributions to CycA proteolysis both in an unperturbed mitosis as well as under conditions where the spindle checkpoint is permanently switched on. Inactivation of these elements have more profound effects for checkpoint degradation, as proven by the observation that single knock-outs cause partial checkpoint stability, while double knock-outs cause complete stability. On the other hand, in an unperturbed mitosis, single knock-outs have little effect while double knock-outs only delay proteolysis. But this delayed proteolysis occurs efficiently only after the checkpoint is switched off in anaphase. Thus checkpoint destruction entails more stringent requirements than what is required for checkpoint-independent proteolysis.

3.5 Aspartate 70, a residue in the region downstream of DB1 is important for CycA proteolysis

The role of the DB1 downstream region in CycA proteolysis is clear from the above results. Similar results have been obtained with human CycA2 as well, wherein a deletion of residues 40-72 that removes the D-box and residues immediately downstream of it, is the minimum deletion required to achieve mitotic stability (Geley et al., 2001). This stretch is referred to as the "extended D-box". In order to define the DB1 downstream stretch in *Drosophila* CycA, a multiple sequence alignment of A2 type cyclins from different species was performed and homologies were searched downstream of DB1 (Fig: 20A). Some residues with a high degree of conservation were revealed in the alignment, such as those between positions 77-80 and the basic amino acid at position 60. To identify whether these or other residues in this region participate in proteolysis, an alanine scan was carried out from position 55 to 86 (Matzkies, 2004). Each residue was individually mutated to alanine or to serine in cases where the wild-type sequence had alanine. Every substitution was made in the background of point mutations that knocked-out KEN1 and DB1 (K13A and R46G respectively). Thirty-two such triple mutants were analyzed in total (Matzkies, 2004).
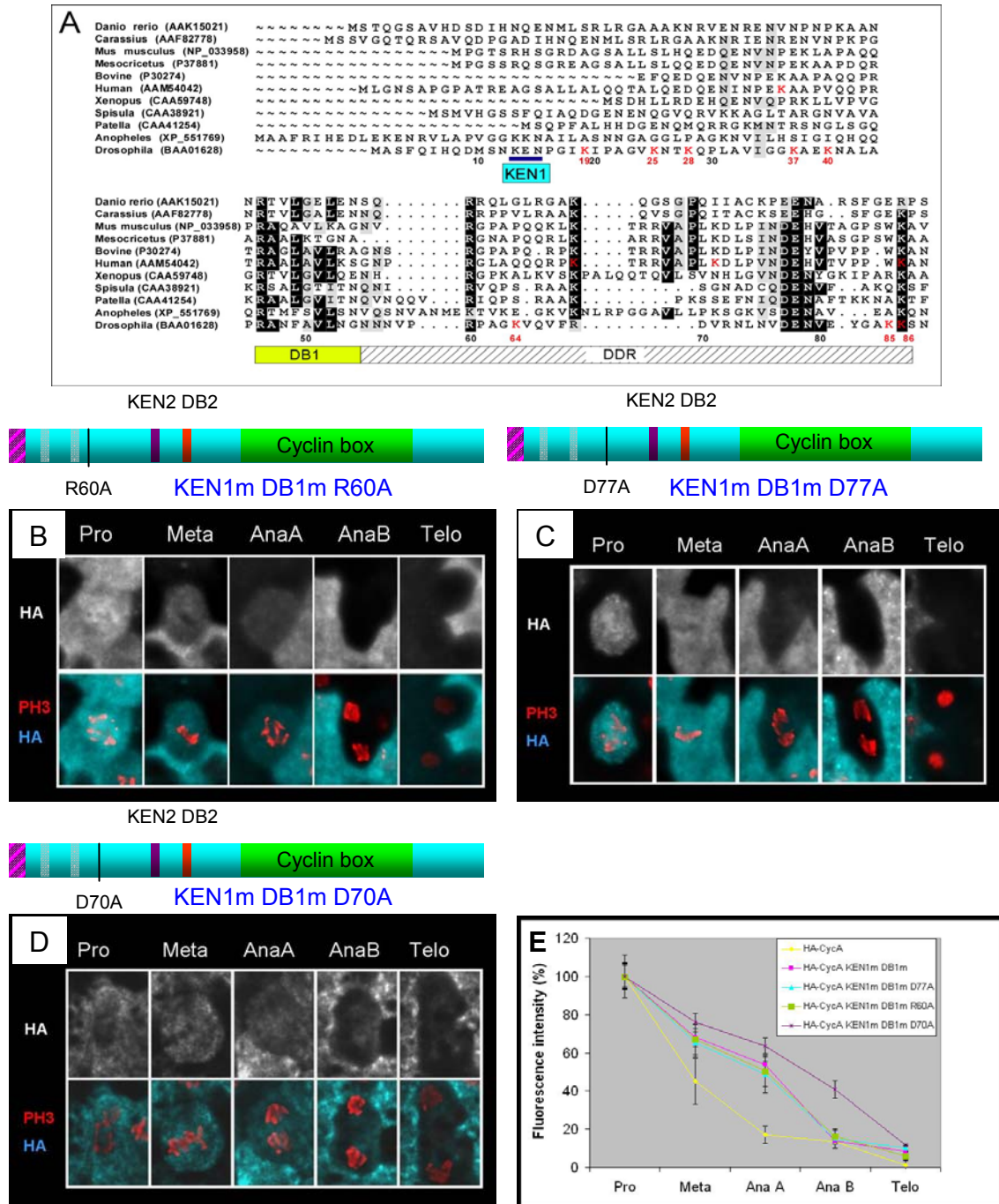
Figure: 20 Alanine substituiton of aspartate 70 (D70) interferes with turnover
(A) The first 88 amino acids of *Drosophila* CycA are shown aligned with the corresponding region of cyclin A from a variety of species. Residues with significant homology are highlighted in black and those with lesser homology in grey. Lysines in CycA and human CycA2 are marked in red. Numbers at the bottom correspond to CycA residues (black) or CycA lysines (red). DDR stands for DB1 downstream region. (B) – (D) Mitotic destruction of the indicated mutant constructs. Substituting D70, but not R60 or D77, to alanine, along with substitutions in KEN1 and DB1 renders the protein more stable than mutations in KEN1 and DB1 alone. (E) Quantification of data from embryos expressing the constructs in (B)-(D) shows the increased stability achieved on additionally mutating D70.

Surprisingly, thirty-one of the thirty-two constructs were not any further stable than HA-CycA lacking just KEN1 and DB1. Even mutations in the conserved residues like R60 or D77 did not have an effect (Matzkies, 2004). The destruction profiles of a few of these constructs were re-examined, this time quantifying the fuorescence data. The mitotic destruction of HA-CycA lacking KEN1, DB1, R60 and that lacking KEN1, DB1, D77 are shown in figure 20. In both cases, proteolysis is delayed until the completion of metaphase, but proceeds once the cells are in anaphase. This delayed turnover was not different from HA-CycA lacking just KEN1 and DB1 alone. Quantification of fluorescence signals revealed that the destruction profiles of all three constructs are more or less identical (Fig: 20E). Therefore, the additional substitutions do not have an effect. However, one of the thirty-two substitutions analyzed gave more stability than the background knock-outs. This was the alanine replacement of aspartic acid at position 70 (D70A) (Matzkies, 2004). Rexamination of its destruction showed that significant protein levels remained throughout mitosis (Fig: 20C). Fluorescence levels above 40% were measured in late anaphase as opposed to just 20% for the background knock-outs (Fig: 20E). Protein levels persisted as late as the beginning of telophase and got lowered only as telophase progressed. It is intriguing that while even the conserved residues do not have an effect, the non-conserved D70 does. Hence, D70 is probably a *Drosophila*-specific CycA destruction motif. Human CycA2 may have residue(s) which are similarly important in its extended D-box.

However, knocking out KEN1, DB1 and D70 (triple mutant) still does not fully stabilize the protein, unlike the KEN1m Δ40-86 construct. This is perplexing because the alanine scan from position 55-86 did not reveal any residue or motif other than D70 (Matzkies, 2004). To make sure that no residual D-box activity remains in the triple mutant, an additional conserved residue in DB1 was mutated (L52G). But this extra substitution did not stabilize the triple mutant any further (Fig: 21).
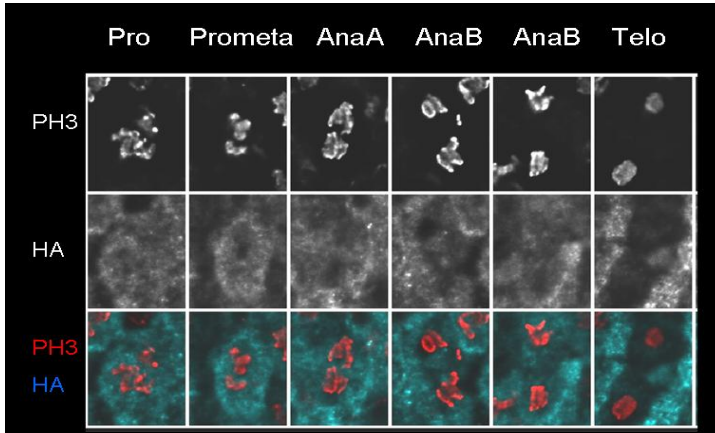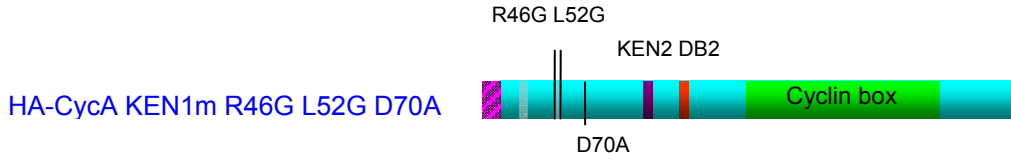
Figure: 21 An extra mutation in DB1 does not increase stability
An extra mutation (L52G) was introduced into the first D-box of HA-CycA which already had the R46G mutation, along with K13A (KEN1m) and D70A. But this did not stabilize the protein any further than the latter three mutations and the protein still disappeared by late anaphase/telophase.

The next obvious question to ask was whether D70 is the only contributing residue from position 55-86. To this end, the destruction profile of the D70A mutant (HA-CycA KEN1m DB1m D70A) was compared with the destruction profile of the Δ55-86 deletion (HA-CycA KEN1m DB1m Δ55-86).
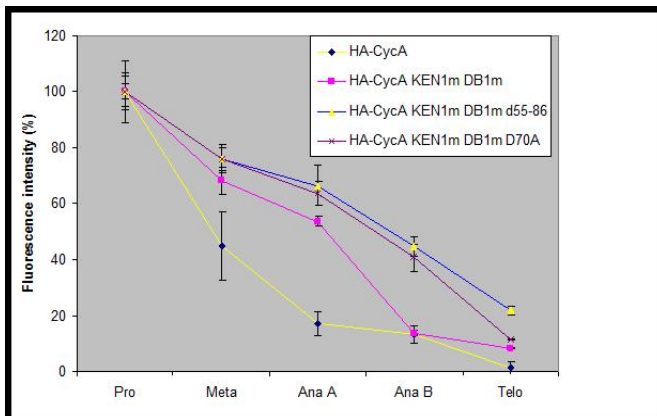
Figure:22 The D70A substitution is not as stabilizing as the Δ55-86 deletion
Quantification of HA fluorescence intensities in M14 cells from embryos injected with the indicated constructs. In anaphase and telophase, the construct with the Δ55-86 deletion is present at levels higher than the construct with the D70A substitution,

As shown in figure 22, both constructs follow similar destruction patterns during mitotis 14; but nonetheless, the deletion is slightly more stable than the aspartic acid substitution. This throws up two scenarios; either the deletion leads to gross conformational changes that make destruction more inefficient, or the deletion

removes something more than just D70. The second scenario is supported by a previous observation that CycA KEN1m Δ40-70 is not completely stable like CycA KEN1m Δ40-86 (Kaspar et al., 2001). Both constructs have D70, DB1 and KEN1 eliminated; but still one is degraded while the other is stable. It is unlikely that the difference comes down to the conformation of the two constructs, because the distortion caused by the Δ40-70 deletion should not be very different from that caused by the Δ40-86 deletion, if at all a structural distortion happens, given that the CycA N-terminus has a floppy structure.

3.6 Eliminating N-terminal signals along with surrounding lysines stabilize CycA

As mentioned above, it was intriguing that KEN1m DB1m D70A was not stable like KEN1m Δ40-86, although no residue other than aspartate 70 seemed to be contributing from the region downstream of DB1. The Δ40-86 deletion also removes six residues upstream of DB1. But these do not seem to be making the difference, because as mentioned above, a Δ40-70 deletion, which also removes those six residues, does not cause similar stability. This stretch, as well as the entire N-terminus, is rich in lysine residues. Lysines serve as the ubiquitin acceptor sites on proteins that are targeted for destruction through ubiquitination. Cyclin ubiquitnation has been generally assumed to occur randomly and non-selectively on lysines spread all over the protein. This notion was fuelled by the discovery that ubiquitination occurs non-selectively on *Arbacia* cyclin B (King et al., 1996). However, in the case of *Drosophila* CycA, it was tempting to speculate that lysines removed by the Δ40-86 deletion and other large N-terminal deletions, play an important part in proteolysis. There are eight lysines in the first 86 amino acids, apart from the K of KEN1 (Fig: 20A). Four of these lie between positions 40 and 86. These four lysines had been individually replaced by alanine in the alanine scan discussed above and those substitutions were found to have no mentionable effect (Matzkies, 2004). However, it was still possible that there is a cumulative effect of some kind. To test this, five lysines in this region were mutated to arginine (5K mutant). Four of these five lysines (Lys40, Lys64, Lys85

and Lys86) are the ones removed by the Δ40-86 deletion, while the fifth one (Lys37) was mutated because it was possible that the deletion affects ubiquitination of this lysine owing to its proximity. The 5K mutant underwent normal proteolysis and was turned over pretty much like wild-type HA-CycA (data not shown). However, when this was combined with point mutations in KEN1 and DB1, a dramatic effect was observed (Fig: 23). This construct was much more stable than the KEN1-DB1 double mutant. HA signals were visible until late anaphase. But it didn't prevent mitotic exit as it eventually got destroyed by telophase.
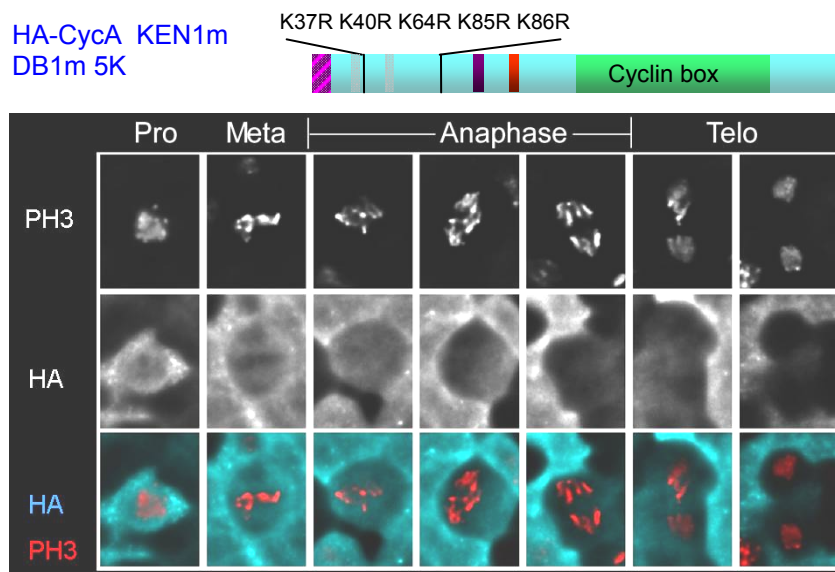
Figure: 23 Mitotic destruction of KEN1m DB1m 5K mutant
Replacing five lysines between positions 37 and 86 in the KEN1m DB1m background considerably stabilizes HA-CycA. HA signals persist well into late anaphase stages and disappear only by telophase.

When D70 was also additionally mutated in this construct (KEN1m DB1m D70A 5K), CycA became essentially stable in mitosis (Fig: 24B). ~95% and ~90% of the protein remained in metaphase and anaphase respectively. In all cells, mitosis 14 was arrested at the late anaphase stage and chromosomes segregated abnormally. Few anaphase cells had reduced amounts of the protein, but even in those cells, enough HA-CycA remained to produce an anaphase arrest.

In short, the stability of KEN1m Δ40-86 could be mimicked by replacing the lysines removed or affected by the Δ40-86 deletion. Next, a construct was made

with all eight lysines contained in the first 86 residues changed to arginine (8K mutant). Like the 5K mutant; this too did not dramatically alter the destruction profile (Fig: 24A). However, an unusual enrichment of over-condensed metaphase figures was observed in embryos injected with this construct. Such over-condensed metaphase figures have been previously observed with stable deletion constructs of CycA and it was associated with compromised CycA degradation and a prolongation of metaphase length (Jacobs et al., 2001). Strikingly, when KEN1 and DB1 were knocked out in the 8K mutant, CycA was again essentially stabilized (Fig: 24C). Like with the previous stable construct, this too produced mitotic arrest phenotypes with abnormal anaphase figures, although few anaphases had reduced protein levels. But, interestingly, when D70 was also substituted, this construct (KEN1m DB1m D70A 8K) became completely stable in mitosis (Fig: 24D). More than 90% of the protein accumulated in anaphase and importantly, there were no anaphases with reduced protein levels, unlike what was observed with the other two stable constructs; indicating that this construct gives maximum stability.

To check whether the chromosome missegregation observed with the stable constructs is due to persistent CycA-Cdk1 activity, the fully stable construct was made non-functional with a point mutation in the cyclin box (F329R; see below). This totally revoked the anaphase arrest and cells underwent normal mitotic exit, although HA-CycA levels still remained stable (Fig: 24E). It is concluded that the chromosome missegregation phenotype is a fallout of stabilized CycA-associated Cdk1 activity.

In order to characterize the effects of the stable constructs in detail, mitotic progression was followed in real time in living GFP-His2AvD embryos (Clarkson and Saint, 1999) expressing the degradation-compromised HA-CycA constructs (Fig: 25). Cells from non-injected control embryos, and those injected with wild-type HA-CycA formed normal metaphase plates and proceeded normally through anaphase and telophase. Metaphase durations were the same for control embryos and embryos injected with HA-CycA, reasserting previous observations that increased CycA levels do not affect mitotic timing or progression (Kaspar et al., 2001).

K19R K25R K28R K37R
K40R K64R K85R K86R   **8K**

K37R K40R K64R K85R K86R

Cyclin box

Cyclin box

KEN1m DB1m 5K

D70A

A — Meta Meta Meta Ana Telo
HA
HA PH3
HA PH3

B — Meta AnaA aa aa aa
HA
HA PH3

K19R K25R K28R K37R
K40R K64R K85R K86R   **KEN1m DB1m 8K**

Cyclin box

K19R K25R K28R K37R
K40R K64R K85R K86R

Cyclin box

KEN1m DB1m D70A 8K

D70A

C — Meta Ana aa aa aa
HA
HA PH3

D — Meta Meta aa aa aa
HA
HA PH3

K19R K25R K28R K37R
K40R K64R K85R K86R

KEN1m DB1m D70A 8K F329R

Cyclin box

D70A   F329R

E — Meta Ana Ana Ana Telo
HA
HA PH3

Figure: 24 Simultaneous knock-outs of N-terminal destruction signals and lysines stabilize CycA.

m=metaphase, cm=over-condensed metaphase, a=anaphase, aa=abnormal anaphase, t=telophase.

Mitotic destruction of the indicated constructs is shown. Degradation is compromised for the constructs in (B) - (D), which cause anaphase arrest. (E) A point mutation in the cyclin box (F329R) that converts the stable construct in (D) into one that cannot activate Cdk1, fully revokes the anaphase arrest although protein levels still remain constant.
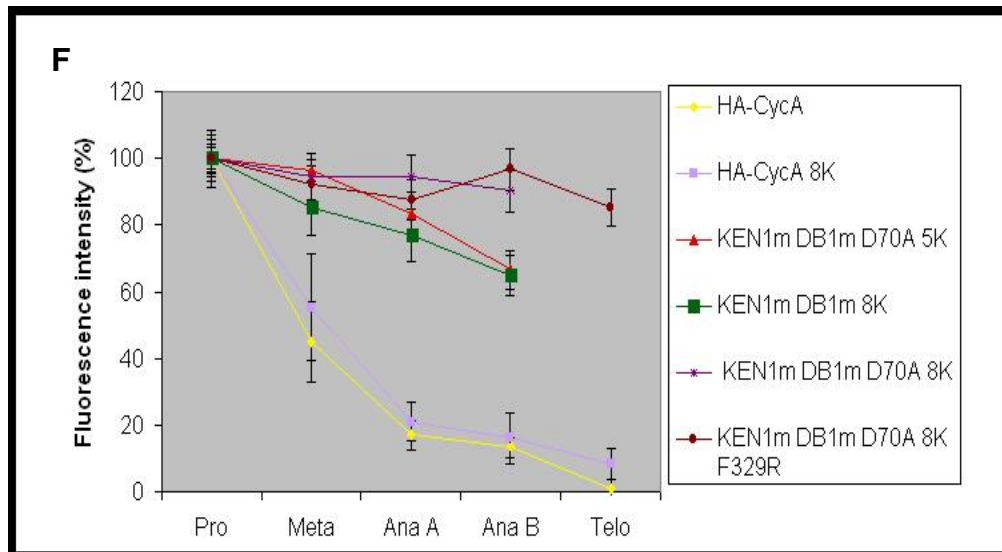
Figure: 24(F) Quantification of HA fluorescence from embryos injected with the constructs in (A) – (E). Embryonic regions expressing the degradation-compromised constructs have cells that arrest in anaphase and lack telophase. Proteolysis of the 8K mutant proceeds much like that of wild-type HA-CycA

The 8K mutant also allowed fairly normal mitotic progression, but metaphase duration was prolonged to ~100 seconds. When the destruction-compromised constructs were tested, a further prolongation in metaphase length was observed. Also, the transition from metaphase to anaphase became unclear and poorly defined (Fig: 25). As seen with the fixed samples, anaphases were found to proceed abnormally, with large chunks of chromatin staying at the spindle equator and the remaining chromatin segregating to the poles (Fig: 25). Similar defective anaphase movements have been observed with stable versions of human CycA2 and *Drosophila* CycA (den Elzen and Pines, 2001; Geley et al., 2001; Jacobs et al., 2001).

These results prove that apart from KEN1, DB1 and D70, the N-terminal region of CycA is important for the lysines contained in there. It brings up a scenario wherein the former three function as recognition signals, which targets the destruction machinery to ubiquitin-acceptor lysines in the vicinity for ubiquitination. These lysines might be preferentially employed and lysines elsewhere on the protein may be used when the ones in the vicinity are absent, because the lack of those eight lysines alone does not prevent destruction.

Figure: 25 Stable CycA delays metaphase-anaphase transition and causes anaphase arrest
Time lapse analysis of mitotic progression in GFP-His2AvD embryos injected with the indicated constructs. Single typical cells are shown for each case. The 0 time point refers to anaphase onset. Metaphase length calculated for each case is indicated. The yellow brackets in panels 4-6 show abnormal chromosome segregation when stable CycA constructs are expressed.

3.7 The second KEN box and second D-box are dispensable for CycA proteolysis

The role of KEN1, DB1 and D70 in CycA degradation is clear from the evidence presented so far. But it is also clear that they are not the only recognition signals, since inactivating all three does not stabilize the protein fully. *Drosophila* CycA has a second KEN box (KEN2) and a second D-box (DB2) at the N-terminus. To see whether KEN2 and/or DB2 serve as the elusive signals, mutations/deletions in those elements were combined with mutations in KEN1, DB1 and D70. But, rather surprisingly; this did not stabilize the protein any further than inactivating the latter elements alone (Fig: 26A&B). Furthermore, when the KEN2-DB2 knock-outs were introduced into the 8K mutant, the resulting construct was proteolysed exactly like the 8K mutant (Fig: 26C&D). These results conclusively prove that the second KEN- and D-boxes have no role whatsoever in CycA proteolysis.

HA-CycA KEN1m DB1m D70A KEN2m ΔDB2

D70A

HA-CycA KEN2m ΔDB2 8K

K19R K25R K28R K37R
K40R K64R K85R K86R
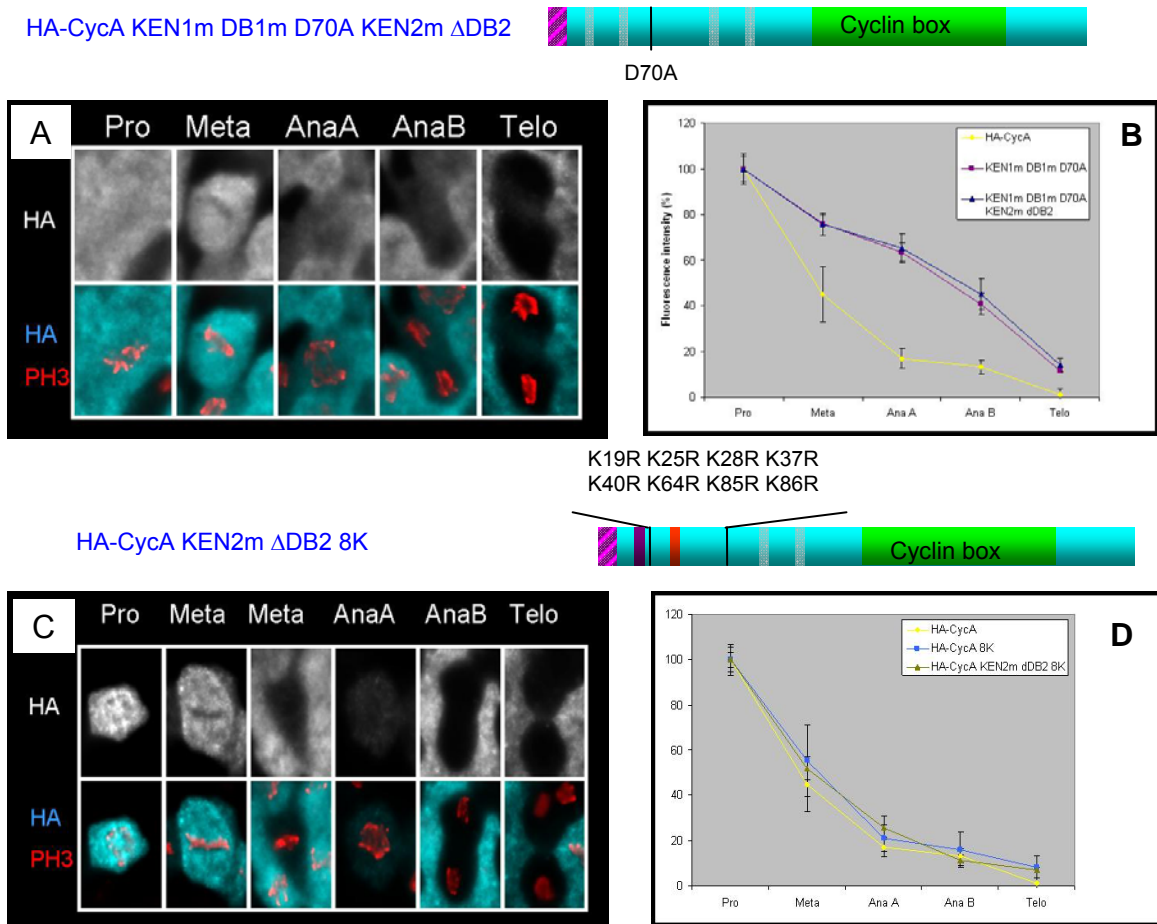
Figure: 26 The second KEN box and second D-box are dispensable for CycA proteolysis
Additionally inactivating KEN2 (K123A) and DB2 (Δ158-170) does not increase the stability of HA-CycA KEN1m DB1m D70A (A&B) or HA-CycA 8K (C&D).

3.8 The CycA C-terminal half can destabilize a heterologous protein under checkpoint conditions

If KEN2 and DB2 do not serve as destruction signals, then which other elements or residues could be involved? It was reasonable to assume that if all the signals are located at the N-terminal half, then the CycA N-terminal half should be degraded like the full length protein. But it was previously shown that HA-CycA 1-170, a truncated version having only the N-terminal 170 amino acids, is degraded with a significant delay in mitosis (Kaspar et al., 2001). The degradation pattern of this truncated version was re-evaluated after re-injecting the construct and

quantifying fluorescence intensities in different mitotic stages (Fig: 27A&B). This showed approximately 80% of the protein remaining in early anaphase and ~40% in anaphase B, which underscores the highly impaired proteolysis of the construct. When the destruction of HA-CycA 1-170 was tested under constant checkpoint conditions in c-metaphase cells, it was found to be fully stable (Fig: 27C&D), which was sort of expected because of the highly inefficient turnover the construct underwent in an unperturbed mitosis. But at the same time, these results were perplexing because HA-CycA 1-170 has all three identified destruction signals and the eight preferentially used lysines, intact. If there are other unknown destruction motifs in this region, then the truncated construct should also possess those motifs. But still its destruction was considerably compromised (Fig: 27). Having said that, this construct is non-functional because it lacks the entire C-terminal portion, which harbors the cyclin box needed for Cdk1 binding and activation. Indeed, when tested in an immunoprecipitation assay with Cdk1, it failed to bind Cdk1 (Fig: 29A). When tested in a kinase assay, it also failed to activate Cdk1 (Fig: 29B). It has been reported that binding to Cdk is essential for the degradation of *Xenopus* cyclin A1 and contributes to the timely destruction of human CycA2 (Geley et al., 2001; Stewart et al., 1994). This raises the possibility that the impaired turnover of HA-CycA 1-170 is due to its inability to interact with Cdk1. In order to validate that possible scenario, HA-CycA 1-170 was fused to the C-terminal half of CycB (residues 243-530). This produces an HA-tagged CycA-CycB chimera. The idea was to restore Cdk1-binding capability to the CycA N-terminal half and see whether that improves its destruction profile. The chimeric protein was functional in kinase assays (Fig: 29). But, as shown in figure 28, it underwent faulty destruction resembling the profile of HA-CycA 1-170.
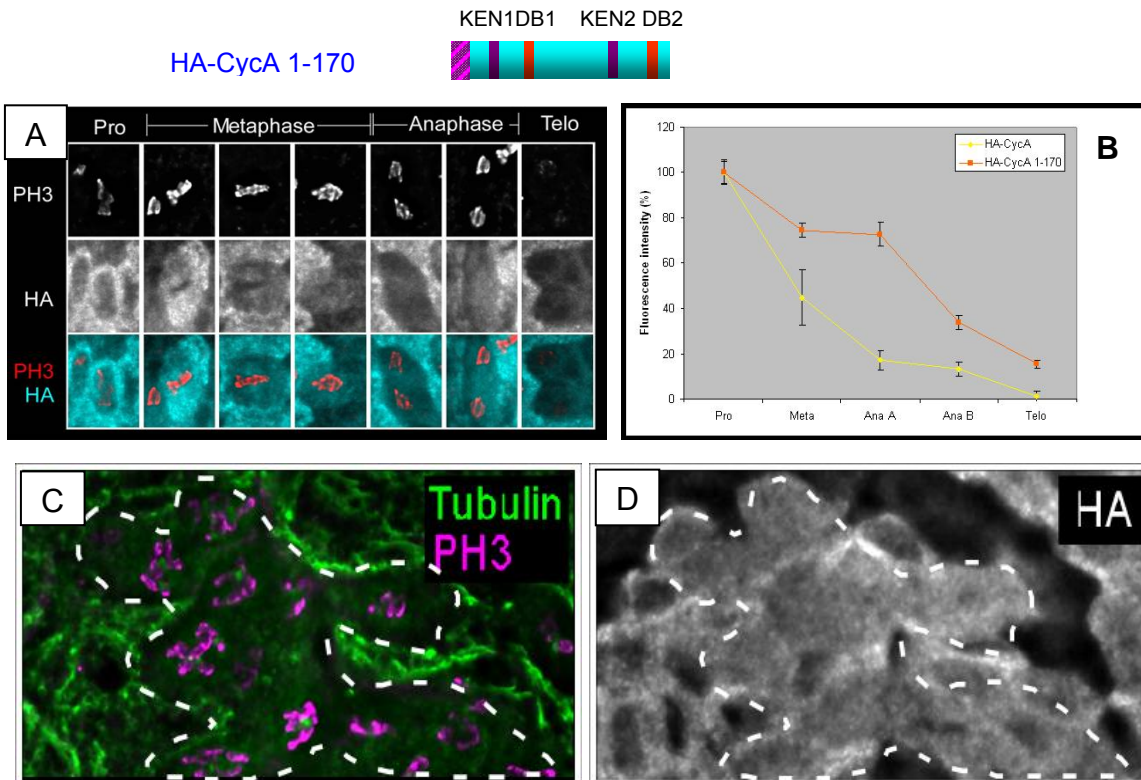
Figure: 27 The CycA N-terminal half undergoes severely compromised turnover
(A) and (B) During an unperturbed mitosis, HA-CycA 1-170 is considerably stable and high HA fluorescence can be detected even in advanced stages such as late anaphase.
(C) and (D) Embryos expressing this construct and treated with colchicine show c-metaphase arrested cells (outlined regions) with condensed chromosomes and deploymerized spindle,but retaining stable levels of HA fluorescence.

This could be because the chimeric protein is not properly folded for it to be efficiently recognized by the destruction machinery. However, it was capable of activating Cdk1 (Fig: 29B). Therefore, any radical alterations in the structure seem unlikely. In short, these results suggest that Cdk1 binding alone may not ensure proper CycA destruction. In this context it was interesting to see how the reciprocal fusion behaves and therefore the reciprocal construct was made. The N-terminal half of CycB (residues 1-242) was fused to the C-terminal cyclin box-containing half of CycA (residues 171-491) to produce the CycB-CycA chimera. Kinase assay showed that this hybrid protein is functional and can activate Cdk1 (Fig: 29B). Interestingly, when the checkpoint destruction of this construct was tested, it was found to be partly destabilized (Fig: 28B).
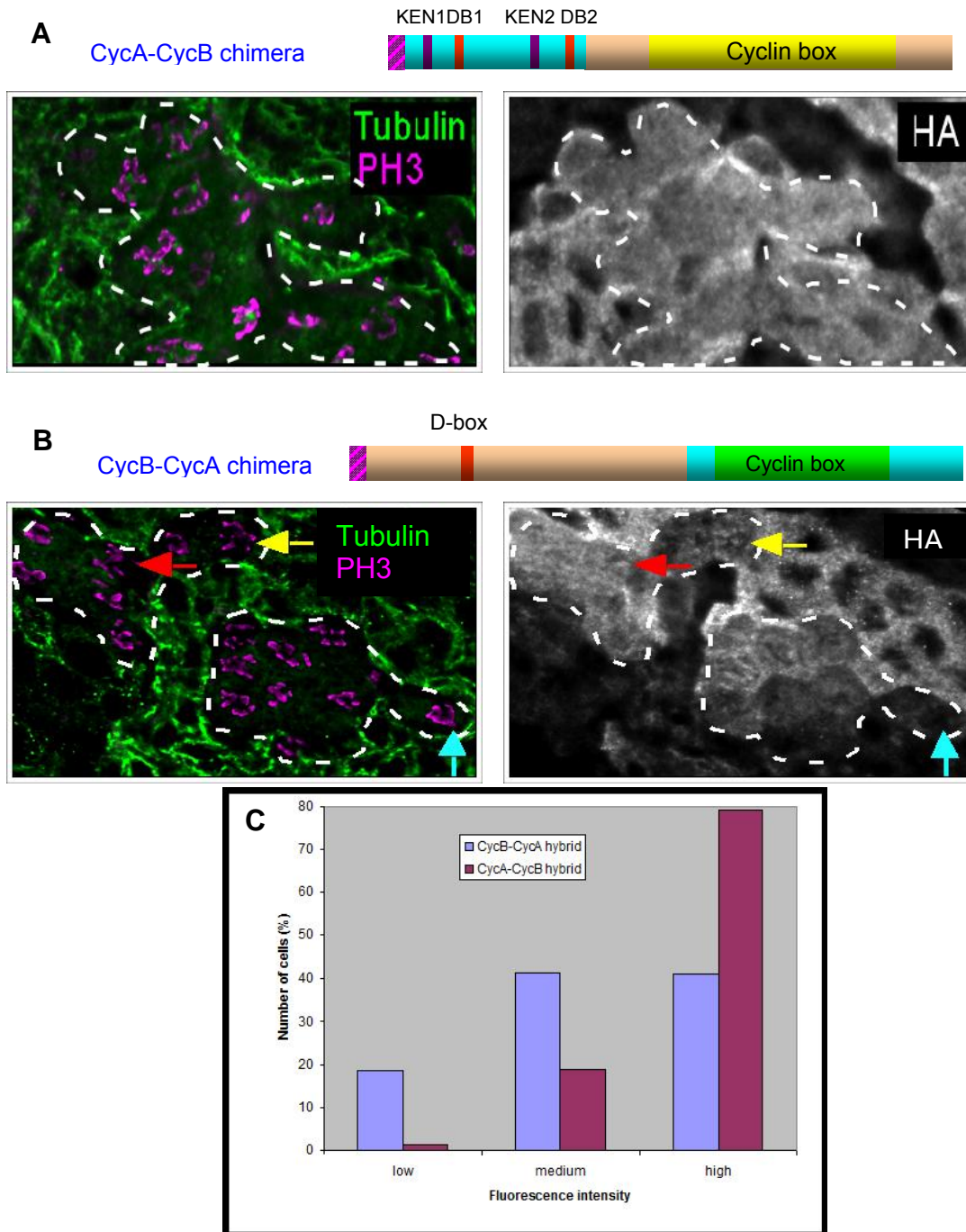
Figure: 28 The CycA C-terminus imparts instability to the CycB N-terminus under checkpoint conditions
(A) The CycA-CycB hybrid protein with the CycB cyclin box, is stable in c-metaphase cells arrested by colchicine (outlined regions). (B) The CycB-CycA hybrid protein with the CycA cyclin box is partially unstable in c-metaphase arrested cells. Cells typically show high (red arrows), medium (yellow arrows) or low (blue arrows) levels of the protein. (C) Quantification of data from embryos expressing these constructs show that levels of the CycB-CycA hybrid construct is reduced to low or medium in more number of cells, than is the case for the CycA-CycB hybrid construct.

This was unexpected because CycB or its N-terminal portion is normally stable under such conditions. Therefore, the CycA C-terminus seems to be capable of bypassing the checkpoint control and facilitate recognition. For both chimeric constructs, the C-terminal residues used for fusion were chosen to ensure that the respective cyclin boxes remain functional.

3.9 The elusive destruction signal lies in the CycA cyclin box

As discussed above, a functional CycB cyclin box does not rectify the impaired turnover of the CycA N-terminal half. To further analyse whether the cyclin box is required for providing Cdk1 binding, the CycA cyclin box had to be altered in such a way that it can bind but cannot activate Cdk1. The cyclin box is a big motif and is extremely sensitive to alterations. Even conservative point mutations can disrupt its function. Therefore, combing the cyclin box for elements contributing to proteolysis is difficult. Nevertheless, one point mutation which replaced phenylalanine at position 329 to arginine (F329R) was identified, which did not dramatically disrupt cyclin box function. F329 aligns with F304 of human CycA2, the substitution of which was reported to cause poor activation of Cdk2 (Geley et al., 2001). F304 is part of a hydrophobic region on CycA2 that strongly interacts with the PSTAIRE helix of Cdk2 (Jeffrey et al., 1995). In *Drosophila* CycA, the F329R substitution did not prevent Cdk1 binding *in vitro*, but prevented Cdk1 activity (Fig: 29). CycA F329R could be be readily precipitated with HA-Cdk1 (Fig: 29A), but nonetheless, kinase assays performed with it turned up negative indicating that somehow, the complex it forms with HA-Cdk1 cannot phosphorylate substrates (Fig: 29B). This mutant was a perfect construct to test whether Cdk1 binding alone is what the cyclin box provides for degradation. HA-CycA F329R should be destroyed like the wild-type protein if Cdk1 binding is the sole contribution of the cyclin box. But figure 30 shows that its mitotic destruction was significantly impaired.
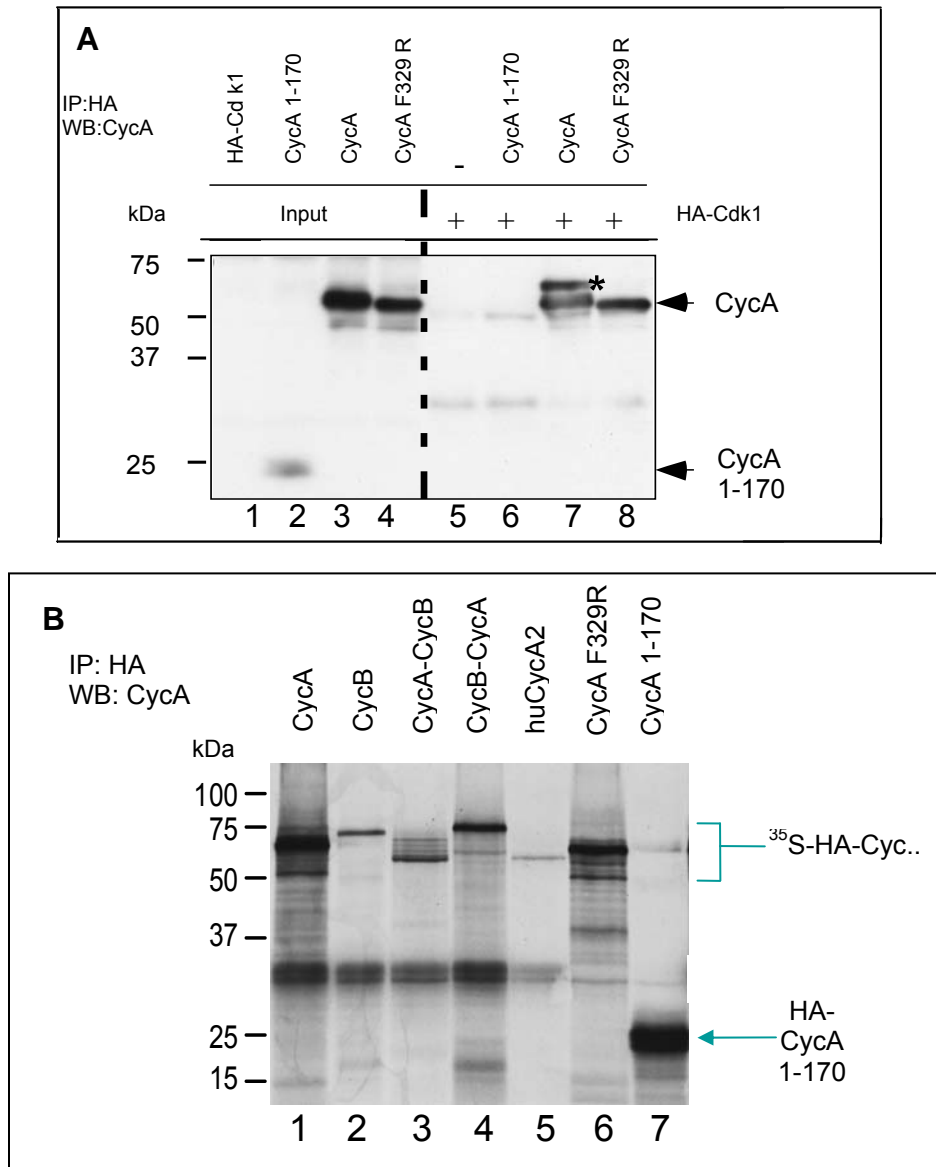
Figure: 29 CycA F329R can bind, but cannot activate Cdk1
(A) Pull down of the indicated CycA constructs with HA-Cdk1 *in vitro* using anti-HA antibody. CycA F329R (panel 8) and WT CycA (panel 7; asterisk indicates phosphorylated forms) co-precipitate with HA-Cdk1, whereas CycA 1-170 which lacks the cyclin box, does not (panel 6). (B) Kinase assay. Cdk1 was pulled down with the indicated HA-tagged ^{35}S-labeled cyclin constructs and the resulting complexes were tested in *in vitro* kinase assays for their ability to phosphorylate Histone H1. All constructs except HA-CycA 1-170 (panel 7) and HA-CycA F329R (panel 6) managed to phosphorylate Histone H1.
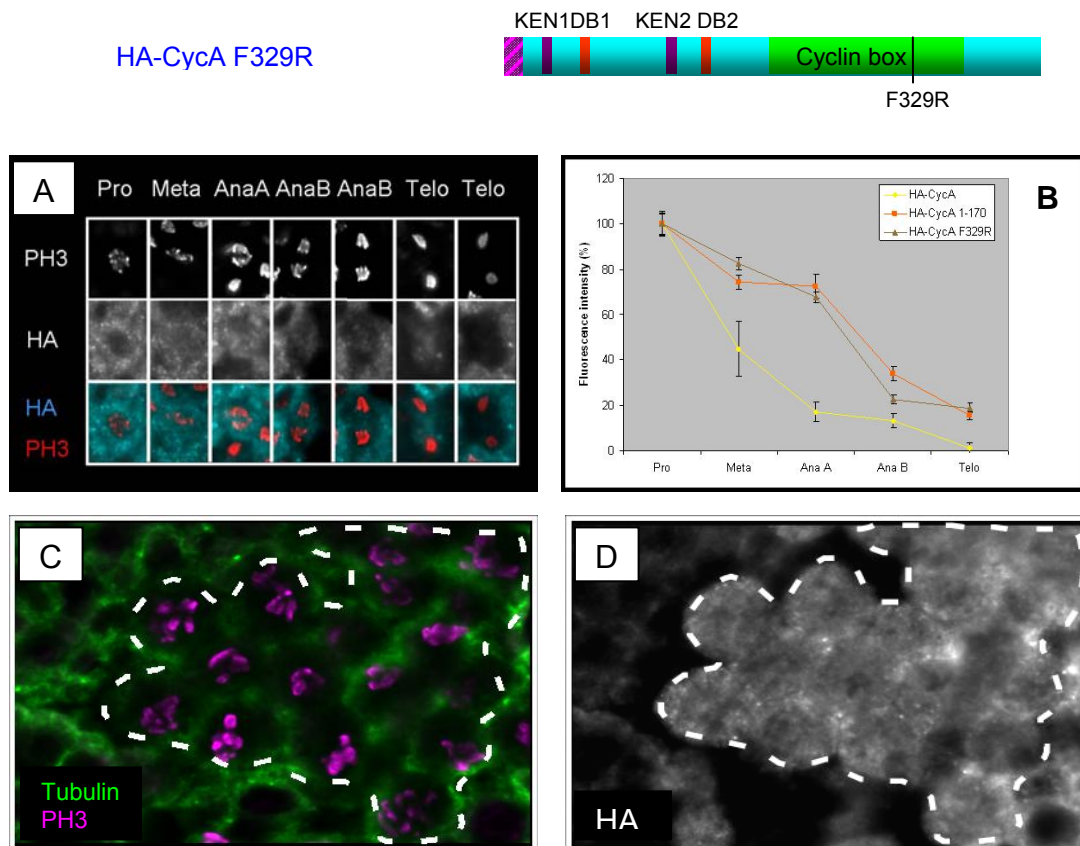
Figure: 30 The cyclin box point mutation F329R is as potent as the cyclin box deletion in severely delaying proteolysis.
(A) In an unperturbed mitosis, HA-CycA F329R is found in high levels until late anaphase and disappears only by telophase. (B) Quantification of data shows that the F329R point mutation delays destruction to the extent obtained with an entire deletion of the C-terminal half. (C) and (D) When embryos expressing this construct are treated with colchicine, c-metaphase cells (outlined regions) retain high levels of the protein, indicating that checkpoint destruction is compromised.

The protein persisted well into late anaphase and levels fell only by telophase (Fig: 30A&B). This delay was comparable to that observed with HA-CycA 1-170, in which the entire C-terminal region including the whole cyclin box is deleted. Furthermore, under constant checkpoint conditions, HA-CycA F329R was totally stable in c-metaphase arrested cells (Fig: 30C&D), much like HA-CycA lacking the entire C-terminus. Since the F329R mutation did not prevent Cdk1 binding, these results suggest that the ability to bind Cdk1 does not guarantee timely destruction. Strikingly, when the F329R substitution was combined with the knock-outs of the N-terminal signals (KEN1, DB1 and D70), HA-CycA was completely stabilized in mitosis (Fig: 31). Injection of this construct gave cells

with constant protein levels in all mitotic stages from prophase till telophase. However, it did not prevent mitotic exit because of the inability to activate Cdk1. These observations show that the residual destruction observed when all three N-terminal signals are lacking, is promoted by the cyclin box or a part of it, the function of which is disrupted by the phenylalanine to arginine substitution at position 329.
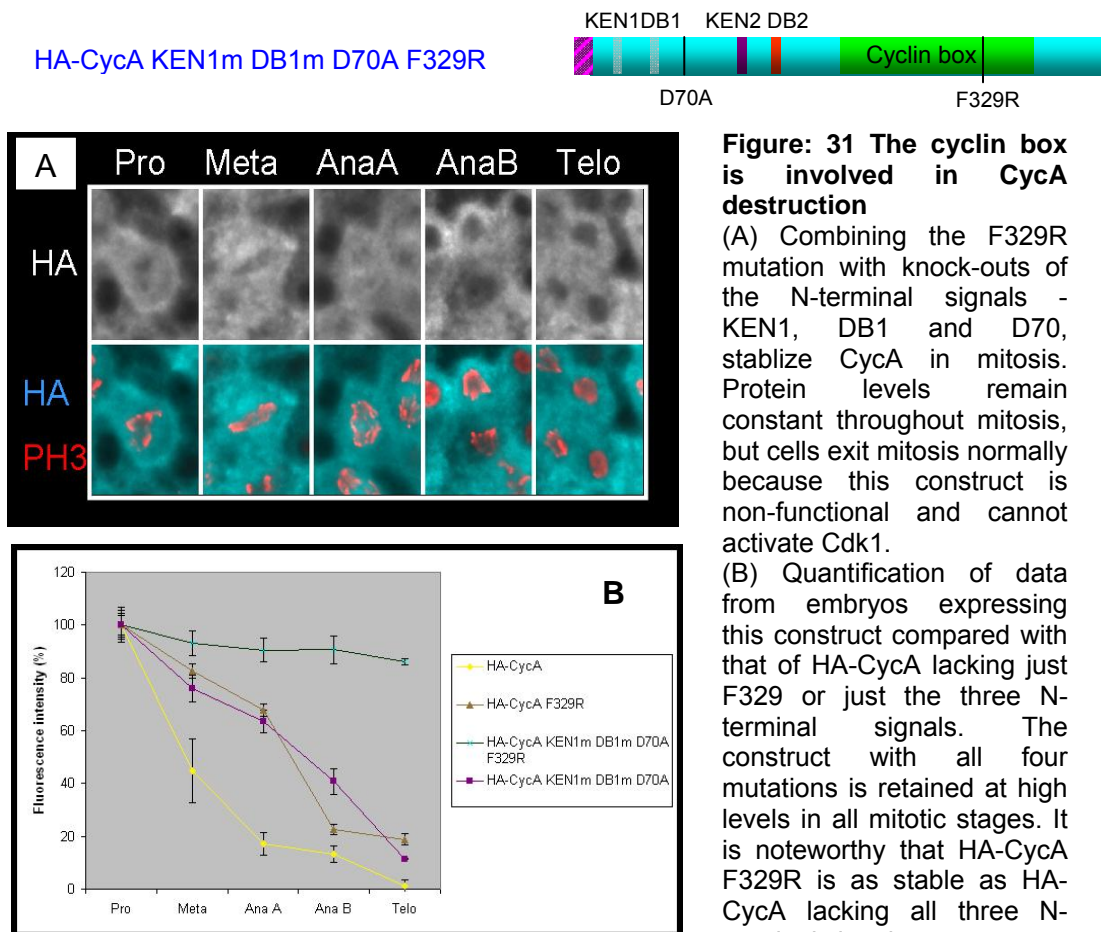
Figure: 31 The cyclin box is involved in CycA destruction

(A) Combining the F329R mutation with knock-outs of the N-terminal signals - KEN1, DB1 and D70, stablize CycA in mitosis. Protein levels remain constant throughout mitosis, but cells exit mitosis normally because this construct is non-functional and cannot activate Cdk1.

(B) Quantification of data from embryos expressing this construct compared with that of HA-CycA lacking just F329 or just the three N-terminal signals. The construct with all four mutations is retained at high levels in all mitotic stages. It is noteworthy that HA-CycA F329R is as stable as HA-CycA lacking all three N-terminal signals.

3.10 Cdk1-mediated CycA phosphorylation is not required for CycA turnover

One reason why the F329R substitution impairs degradation could be because CycA-Cdk1 activity is required for CycA phosphorylation and this activity is prevented by this mutation. Cyclins are generally known to get phosphorylated when they associate with their partner Cdks. There are five potential Cdk1/Cdk2 consensus phosphorylation sites (S/T P) in the *Drosophila* CycA protein sequence. Three of these are located in the N-terminal half: T145, S154 and S180, while two are located in the C-terminal half: T333 and T397. Migration shifts on SDS-PAGE were observed for HA-CycA both *in vitro* and *in vivo* (Fig: 32A, C). These band shifts occur due to phosphorylation, since treating the sample with lambda phosphatase abolishes band shifts (Fig: 32A). Performing a HA-CycA pull down with Cdk1 in the presence of the Cdk1-inhibitor roscovitine abrogates phosphorylation, showing that the band shifts occur due to Cdk1-mediated phosphorylation (Fig: 32B). The HA-CycA F329R mutant, which can bind Cdk1 but cannot activate the bound Cdk1, fails to show migration shifts when expressed *in vivo* in postblastoderm embryos, whereas wild-type HA-CycA readily shows several bands (Fig:32C). Therefore, Cdk1-mediated phosphorylation is the primary modification event happening *in vivo* also. Phosphorylation can occur in two ways – cis and trans. In cis-phosphorylation, Cdk of one complex transfers phosphate groups onto the cyclin from another complex. In trans-phosphorylation, Cdk transfers phosphate groups onto the cyclin subunit in the same complex. To check what mode operates for CycA phosphorylation, HA-tagged CycA F329R-Cdk1 complex was incubated with non-tagged CycA-Cdk1 complex. Since the F329R mutation prevents phosphorylation in cis, the only way HA-CycA F329R can get phosphorylated is in trans, by the wild-type CycA-Cdk1 complex. But even after prolonged incubation, no migration shifts could be observed with the F329R mutant (Fig: 32D). At the same time, HA-CycA-Cdk1 incubated with retic lysate showed migration shifts (Fig: 32D). Therefore, CycA phosphorylation seems to occur in cis. Such cis-phosphorylation also occurs for cyclin B in starfish oocytes (Borgne et al., 1999).
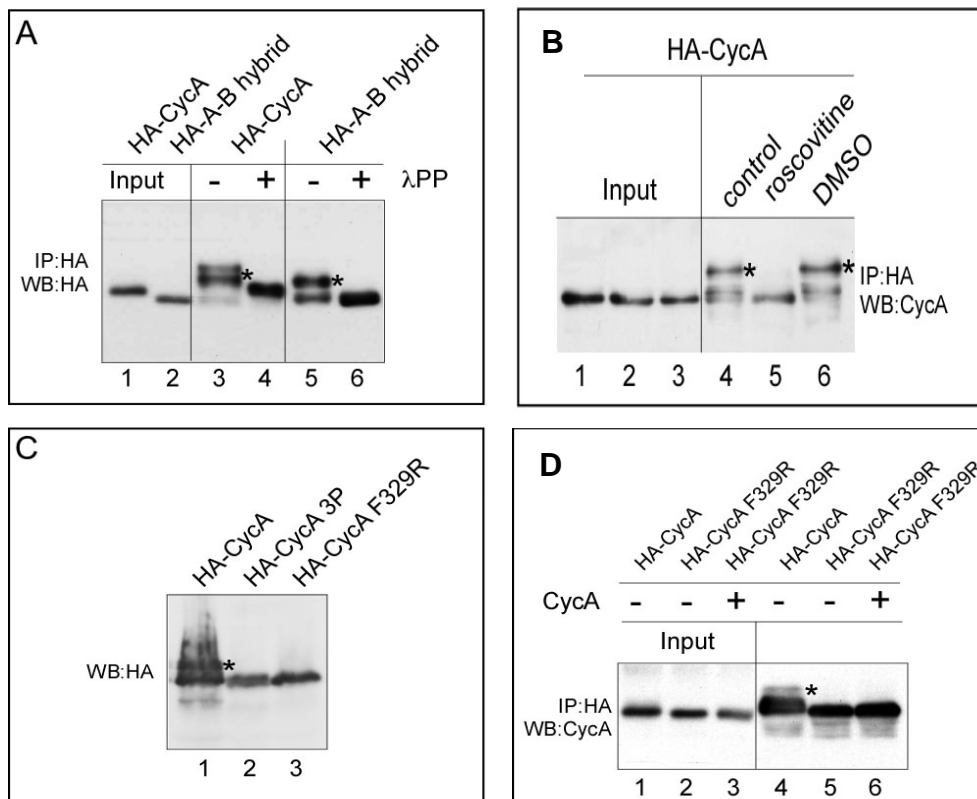
Figure: 32 CycA is cis-phosphorylated on N-terminal phosphorylation sites
(A) *In vitro* phosphorylation of HACycA. HA-CycA and HA-CycA-CycB hybrid show migration shifts when Cdk1 is pulled down with them (asterisk in panels 3 and 5), which diappear on treatment with lambda phosphatise (λPP) (panels 4 and 6).
(B) Cdk1 phosphorylates HA-CycA *in vitro*. HA-CycA was pulled down with Cdk1 in the presence of the Cdk1 inhibitor roscovitine dissolved in DMSO (panel5), just DMSO (panel 6) or water (panel 4). Migration shifts (asterisk) were absent only in the roscovitine-treated sample. (C) *In vivo* phosphorylation of HA-CycA. Stage 5 embryos were injected with RNA encoding the indicated constructs and the protein expressed from it was resolved by Western blotting. Migration shifts were observed for HA-CycA (asterisk, panel 1), but not for HA-CycA lacking the N-terminal P-sites (HA-CycA 3P, panel 2) or the F329R mutant (panel 3). (D) Phosphorylation occurs in cis. HA-CycA F329R-Cdk1 complex was incubated with CycA-Cdk1 complex (panel 6) or retic lysate (panel 5). Migration shifts were not observed in either case. But HA-CycA-Cdk1 complex incubated with retic lysate shows migration shifts (asterisk, panel 4).

The next step was to see whether this self-phosphorylation somehow influences proteolysis. For this, the Cdk1 consensus phosphorylation sites (P-sites) had to be mutated. However, substituting the C-terminal P-sites, T333 and T397 render CycA unable to activate Cdk1 (Dienemann, 2003),probably because those

residues lie within the cyclin box and their replacement tampers with cyclin box function.
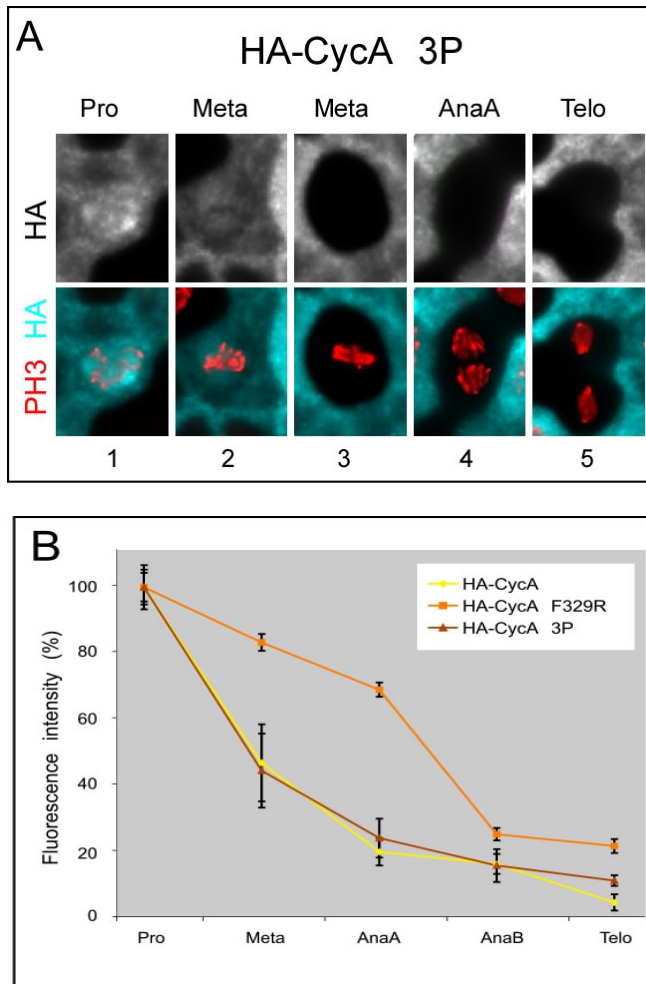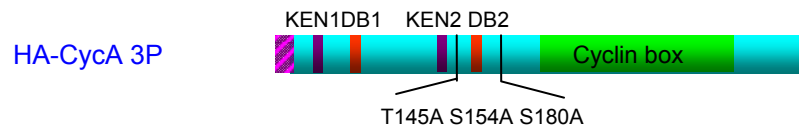
Figure: 33 HA-CycA phosphorylation is not required for turnover
(A) Mitotic cells from an embryo injected with HA-CycA 3P (T145A S154A S180A) are shown. Like for the wild-type, some metaphase cells stain strongly for HA (panel 2), while others totally lack it (panel 3). Anaphase and telophase cells also lack HA staining (panels 4 and 5).
(B) Fluorescence intensities quantified from embryos expressing this construct compared with that of HA-CycA and HA-CycA F329R. The turnover profile of the 3P mutant matches that of wild-type HA-CycA almost exactly.

However, mutating the N-terminal P-sites; either individually or in combination, does not affect functionality (Dienemann, 2003). Therefore it was decided that only the N-terminal P-sites need to be analyzed.

Replacing all three N-terminal sites with alanine (3P mutant) largely abolished HA-CycA phosphorylation *in vivo* (Fig: 32C) indicating that these sites serve as the principal phosphorylation sites on the protein. Next, the destruction of this triple mutant was monitored *in vivo* so as to ascertain how the inability to get

phosphorylated affects degradation. Quite surprisingly, mitotic turnover proceeded normally and the destruction profile looked very similar to that of wild-type HA-CycA (Fig: 33). Thus, phosphorlation does not seem to be necessary for the timely destruction of CycA.

3.11 CycA-Cdk1 activity towards other substrates may be dispensable for proteolysis

Although the above results show that phosphorylation is not a pre-requisite for degradation, it is still possible that CycA-Cdk1 activity is required to phosphorylate other substrates which influence CycA destruction. If this were the case, then a mutant that cannot activate Cdk1 would fail to activate components needed for its turnover. However, with the experimental approach employed in this study, that possibility looks very remote. All constructs used here are expressed in an endogenous CycA-containing background. Embryos undergoing mitosis 14 zygotically express CycA, which can associate with endogenous Cdk1 to phosphorylate and control the function of components that might be needed for CycA destruction. Therefore, even if non-functional mutants are injected, they would encounter components already activated by endogenous CycA-Cdk1 and hence should get degraded normally.

The requirement of CycA-Cdk1 activity for CycA destruction was put to test by co-injecting HA-tagged wild-type CycA with non-tagged CycA F329R. Since CycA F329R is capable of binding Cdk1 but cannot activate the kinase, it might form inactive complexes with Cdk1 *in vivo* and thereby lower the overall CycA-Cdk1 activity in the cell. If CycA F329R critically lowers Cdk1 activity required for proteolysis, the turnover of HA-CycA should be affected.

But, it was observed that HA-CycA turnover proceeds absolutely normally and no delay whatsoever was evident (Fig: 34A). Quantification of data clearly showed that proteolysis of HA-CycA is indistinguishable in the presence or absence of CycA F329R (Fig: 34B). Taken together; these results suggest that mutations or deletions that inactivate the cyclin box (like F329R), do not prevent destruction because of the inability to phosphorylate other substrates or CycA itself.
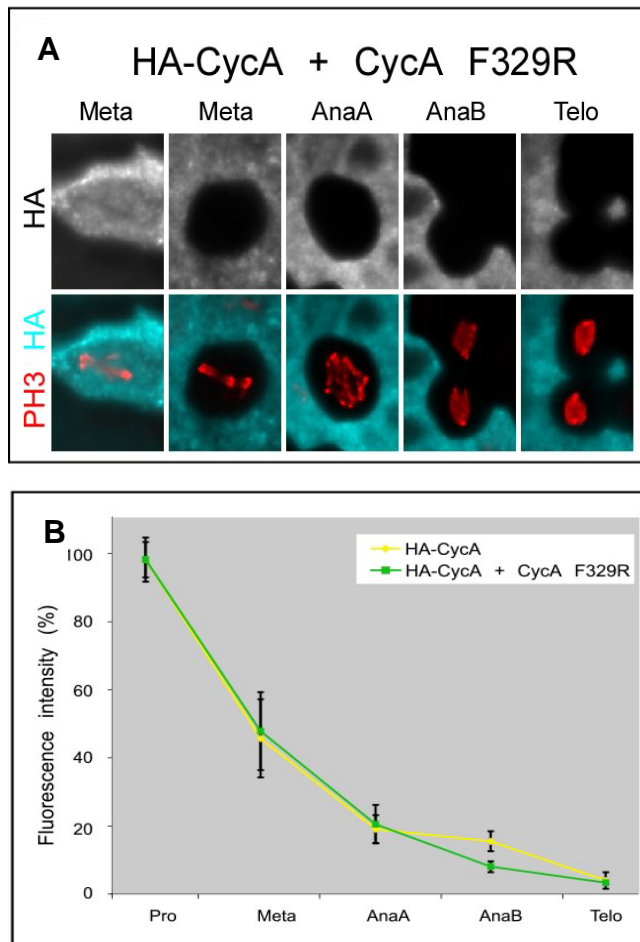
Figure:34 CycA-Cdk1 activity may not be essential for destruction
(A) Mitotic cells from an embryo co-injected with HA-CycA and CycA F329R, and stained with anti-HA antibodies are shown. Some metaphase cells stain brightly for HA while others don't, which resembles the destruction profile of HA-CycA injected alone. Protein signals are completely absent from subsequent stages and HA-CycA shows no hint of undergoing impaired proteolysis.
(B) Fluorescence intensities quantified from embryos co-injected with these constructs show that the destruction profile of HA-CycA in the presence or absence of CycA F329R is virtually indistinguishable.

.

3.12 Human cyclin A2 is improperly degraded in *Drosophila*

Human CycA2 is the best studied form of cyclin A and is homologous to *Drosophila* CycA. Several parallels can be drawn between the two proteins. Like in *Drosophila*, a large N-terminal deletion from residues 40-72 is required to stabilize human CycA2 and mutations in the D-box do not have much effect (den Elzen and Pines, 2001; Geley et al., 2001). Like in *Drosophila* CycA, three lysines close to the D-box of CycA2 are preferentially ubiquitinated (Fung et al., 2005). There are also differences. For instance, human CycA2 lacks KEN boxes. In order to analyze whether conserved mechanisms target the two cyclins for proteolysis, *in vitro* transcribed RNA for human CycA2 was injected into stage 5 *Drosophila* embryos and analyzed in the same way as the *Drosophila* CycA constructs.
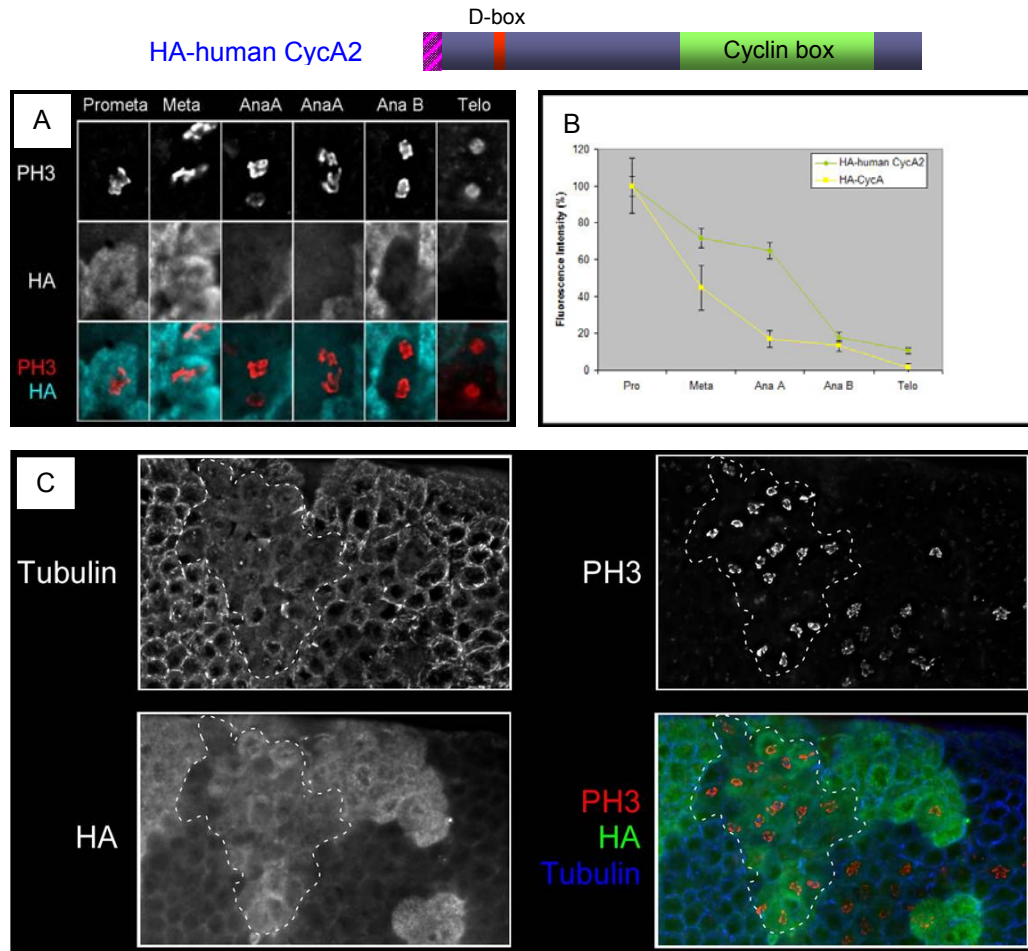
Figure: 35 Destruction of human CycA2 is impaired in *Drosophila*
(A) Mitotic cells from an embryo injected with HA-tagged human CycA2 show high HA signal intensities until anaphase B. (B) Quantification of fluorescence from embryos expressing CycA2 compared with that of CycA shows the increased stability of the former during metaphase and early anaphase. (C) In c-metaphase arrested cells (outlined regions), human CycA2 is more or less stabilized and remains in significantly high levels.

Figure 35A&B show that CycA2 disappears in a delayed fashion during mitosis 14. The protein is stable until early anaphase and gets reduced by late anaphase only which resembles the turn over of several CycA mutants rather than wild-type CycA. The checkpoint destruction of the protein was even more intriguing. As shown in figure 35C, c-metaphase cells accumulated high levels of CycA2, indicating that it was stable. This was much unlike *Drosophila* CycA or even CycA2 in human cells for that matter. These results probably hint at the fact that the destruction machineries targeting both cyclins are different. The manner in which destruction signals are recognized by the APC/C complex could also be

different. Perhaps, the lack of a KEN box in human CycA2 is one reason. Mutating the first KEN box does affect *Drosophila* CycA proteolysis, especially under constant checkpoint conditions. Therefore, the destruction machinery in *Drosophila* might have evolved to recognize KEN boxes for proper ubiquitination and destruction.

4. Discussion

How the differential regulation of cyclin A is achieved and what purpose it serves have been questions of much interest and investigation. This study presents evidence that the cyclin box cooperates with multiple N-terminal signals to bring about the correct spatio-temporal destruction of CycA in *Drosophila*, and that this process selectively employs lysines in the neighborhood of the N-terminal signals.

4.1 The CycA destruction signal consists of two arms

Destruction of CycA during mitosis depends on the presence of two kinds of residues/sequences – those which target the protein to the destruction machinery and those which selectively receive the ubiquitin conjugation. In principle, abrogation of either sequence should impair proteolysis, which is what is observed in this study. By contrast, substrates such as CycB which are also degraded by the ubiquitin-proteasome system possess targeting sequences, but no selectively-used ubiquitin conjugation sites. Instead, random sites spread all over the protein receive the ubiquitin conjugates. Hence, abrogation of the targeting sequences is sufficient to impair proteolysis.

Motifs such as the D-box and KEN box are considered as targeting sequences, while lysine residues function as the sites for ubiquitin attachment. The D-box in cyclin B and securin have been shown to directly interact with the WD40 propeller domain of Cdh1 (Kraft et al., 2005). Peptide competition assays have also demonstrated the KEN box binding to Cdh1 (Burton et al., 2005). Interaction of Cdh1 with these motifs enhances its association with the APC/C in yeast cells, suggesting an ordered assembly of the ternary APC/C-Cdh1-substrate complex. In budding yeast, the anaphase inhibitor Pds1 (securin) binds to Cdc20 via its D-box and this interaction is not abolished even when the spindle checkpoint is turned on, although Pds1 proteolysis is abolished (Hilioti et al., 2001). This might suggest that the spindle checkpoint may not prevent Cdc20-substrate binding,

but rather inactivates the catalytic activity of the APC/C, perhaps by making the substrate inaccessible to the APC/C catalytic core. Meanwhile, two hybrid analysis in yeast provided the first evidence for the direct interaction of a D-box - that of Clb2 (cyclin B) - with the APC/C, specifically the APC/C subunit Cdc23 (Meyn et al., 2002). Further on, coactivator-free APC/C from *Xenopus* egg extracts was found to bind to peptides containing the D-box sequences of cyclin B and mutations in the D-box abolished this interaction (Yamano et al., 2004). Surprisingly, these peptides did not bind Cdc20. The APC/C subunit Doc1/Apc10 has been implicated in mediating direct binding of substrates to the APC/C. APC/C lacking Doc1 is normal with respect to subunit composition, association with E2 enzyme and binding to coactivators, yet it fails to interact with substrates. Doc1 is ideally suited to present substrates for ubiquitination because it directly binds to Apc11, the RING finger subunit that forms the APC/C catalytic center (Zachariae, 2004). Recombinant Apc11 is capable of conjugating multiubiquitin chains to substrates on its own, but not as part of an APC/C complex in the absence of coactivators. This suggests that the coactivators may induce conformational changes in the APC/C to provide access to the catalytic centre and/or the D-box receptor. Cumulatively, these observations show that the optimal interaction of the substrate with the APC/C is dependent on the simultaneous association of the coactivator. Consistent with this, an isotope-trapping approach revealed that both APC/C and Cdc20 are required for productive binding of securin in humans (Eytan et al., 2006).
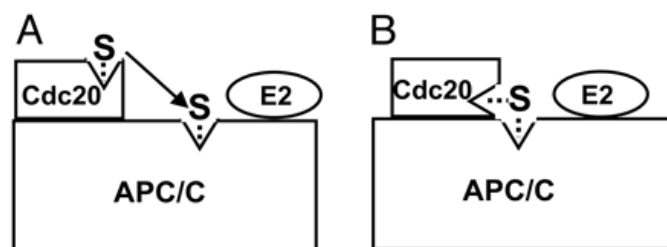
Figure: 36 Two models for synergestic substrate binding by APC/C and coactivator
(A) The coactivator recruits the substrate first via its D-box receptor or other substrate binding sites and then sequentially transfers it onto the substrate binding sites on the APC/C. (B) The substrate binds to a composite substrate binding site formed by APC/C and the coactivator. Adapted from (Eytan et al., 2006).

Either APC/C or Cdc20 could bind securin on its own, albeit at reduced efficiency and relaxed selectivity for the D-box. The multipartite nature of the cyclin A destruction signal can be accounted for with models whereby both core APC/C subunits and coactivators contribute binding sites for substrates (Fig: 36).

4.1.1 The recognition signals in CycA

CycA has two KEN boxes and two D-boxes at its N-terminus, but only KEN1 and DB1 were found to contribute to proteolysis. Both elements act in concert and are incapable of mediating proper destruction in isolation. An alignment of D-boxes from A-type cyclins reveals that CycA DB1 is the least conserved of all; conspicuous by the exchange of leucine for a phenylalanine at position 4 (Fig: 37). The A-type D-box in general diverges from that of the B-type D-box. While the latter conforms to the consensus RxxLxxxxN sequence, the former shows considerable divergence in many species. In *Xenopus*, converting the cyclin B1 and cyclin B2 D-boxes into that of cyclin A1 and cyclin A2 respectively by mutations, abolish destruction, although ubiquitination still occurs (Klotzbucher et al., 1996).

```
Danio rerio (AAK15021)      N R T V L G E L E N S Q . . .
Carassius (AAF82778)        N R T V L G A L E N N Q . . .
Mus musculus (NP_033958)    P R A Q A V L K A G N V . . .
Mesocricetus (P37881)       A R A A L K T G N A . . . . .
Bovine (P30274)             T R A G L A V L R A G N S . .
Human (AAM54042)            T R A A L A V L K S G N P . .
Xenopus (CAA59748)          G R T V L G V L Q E N H . . .
Spisula (CAA38921)          K R S A L G T I T N Q N I . .
Patella (CAA41254)          K R A A L G V I T N Q V N Q Q '
Anopheles (XP_551769)       Q R T M F S V L S N V Q S N V.
Drosophila (BAA01628)       P R A N F A V L N G N N V P
```

Figure: 37 The first D-box of *Drosophila* CycA is divergent from cyclin A D-boxes in other species
Alignment of the cyclin A D-boxes from different species shows that the *Drosophila* CycA DB1 has an F in place of L at position 4.The same can be seen for Anopheles. Therefore insect cyclin A varies from the consensus RxxL D-box sequence. Residues with maximum homology are highlighted in black and those with lesser homology in grey.

Thus, the variations in the A-type D-box may account for it being less efficiently recognized by the destruction machinery. Indeed, while the cyclin B D-box is readily transposable to heterologous proteins such as protein A or even cyclin A, rendering them unstable in mitotis; the cyclin A D-box cannot achieve the same. In this study, fusing the entire N-terminal regulatory region of CycA to the CycB C-terminal half did not allow normal destruction. The CycA KEN1 sequence (KENPGIK) also differs slightly from the reported consensus KEN box sequence KENxxxN/D. In the case of human Cdc20, the KEN box is sufficient for recognition and degradation by APC/C^{Cdh1} and like with the D-box, the KEN box is transposable to protein A, rendering it unstable in mitosis (Pfleger and Kirschner, 2000). By contrast, the variant KEN1 present in CycA is incapable of mediating destruction on its own probably due to the divergence from the consensus sequence.

Apart from KEN1 and DB1, the only other residue found to contribute from the N-terminus was aspartic acid at position 70 (D70) (Matzkies, 2004). Even the conserved aspartic acid at position 77 or the arginine at position 60 was not involved. This suggests that a species-specific mechanism operates for CycA degradation in *Drosophila*. It is possible that D70 is part of a novel destruction motif; but that seems unlikely because mutating surrounding residues have no effect. The role performed by D70 can only be speculated. Like in *Drosophila*, the D-box downstream region of human CycA2 is also crucial for proteolysis, and the D-box plus its downstream sequences are thought to constitute the human CycA2-specific "extended D-box" (Geley et al., 2001). Interestingly, in human CycA2 the D-box is not needed for interaction with Cdc20; instead, the stretch from residues 60-114 (which lies downstream of the D-box), is what is required (Ohtoshi et al., 2000). This makes it plausible that a similar scenario operates in *Drosophila* too. D70 may provide the strongest interaction as part of a docking site downstream of DB1 which mediates Cdc20 binding. Alternatively, D70 may not provide any contacts at all, but might be simply required for stabilizing a α-helix or a β-sheet. However, the N-terminal region of cyclin A is thought to have a floppy structure with no well-defined helices or β-sheets and therefore, structural

alterations may not have as much of an impact there, as in the remainder of the protein.

KEN1, DB1 and D70 act synergistically to effect proteolysis. The more elements that are lacking, the more impaired the destruction is. Mutations in all three signals have no significant effect in isolation. A double knock-out of KEN1 and DB1 delays destruction until the completion of metaphase. A triple knock-out of KEN1,DB1 and D70 cause further delay with significant protein levels detectable even in late anaphase/early telophase, suggesting severely compromised turnover. However, even this triple knock-out cannot cause full stability or produce a mitotic arrest. Hence it was logical to assume that additional elements must be present. The second KEN box and D-box were tested for any contribution to proteolysis, which turned up negative. This was surprising because the DB2 sequence conforms more to the D-box consensus than the DB1 sequence; yet it lacks a role. Human CycA2 also has a second D-box at the N-terminus with the sequence RKPLVPLDY that diverges from the consensus, but conforms to the A-type D-box. However, this second D-box has little or no function in destabilizing the protein (Fung et al., 2005). Perhaps, in cyclin A the additional D- and KEN boxes are not correctly positioned for recognition. This common feature shared by *Drosophila* and human cyclin A suggests that the correct positioning of the D-box is as relevant as its sequence, if it is to be recognized efficiently by the APC/C.

The elusive signal did not seem to be at the N-terminus, because HA-CycA 1-170 underwent impaired proteolysis. Restoring the ability of the CycA N-terminal half to bind Cdk1 via the construction of a CycA-CycB chimeric construct, did not rectify the defective turnover. This is in perfect agreement with observations made using cyclin A-cyclin B fusion constructs in *Xenopus* as well as humans (Fung et al., 2005; Klotzbucher et al., 1996); which reiterates that the cyclin A N-terminal destruction signal is not transferable to another protein, much unlike that of cyclin B. At the same time, the reciprocal CycB-CycA chimeric construct was partially unstable under the spindle checkpoint. This was a very significant observation because it instantly implied that the CycA C-terminal half, most likely the cyclin box, can impart instability to a heterologous protein, when fused with it.

Although similar results have been obtained with human CycA2 (Fung et al., 2005), in this study a much shorter CycA C-terminal region was used, just sufficient to keep the cyclin box functional. Therefore the destabilizing role could be more precisely narrowed down to the cyclin box. In the case of human CycA2, a large C-terminal portion was used which included much of the N-terminal regulatory domain. Hence, the destabilizing effect could not be pinpointed to the cyclin box. These observations present a strong case for the CycA cyclin box to be the mediator of the checkpoint bypass.

In humans and *Xenopus*, association of cyclin A with Cdk was hypothesized to be required for the correct presentation of the destruction signals to the APC/C. However, in this study it was found that a point mutation in the cyclin box (F329R), which did not prevent Cdk1 binding but prevented Cdk1 activity, was sufficient to impair destruction as much as that of CycA lacking the whole cyclin box. Therefore, Cdk1 binding alone does not ensure proper proteolysis. It can still be argued that although HA-CycA F329R can bind Cdk1, the conformation of the complex is different from that involving the wild type, which reduces the efficiency of recognition. But this seems unlikely due to two reasons: (1) the mutant would not have bound Cdk1 if the structure had been dramatically altered and (2) *in vitro* ubiquitination of human CycA2 occurs equally well in the presence or absence of Cdk2 (Rape et al., 2006). Therefore, Cdk binding as such does not seem to make a difference in the way cyclin A is recognized by the destruction machinery.

Experiments further revealed that Cdk1-mediated CycA phosphorylation was not necessary for turnover. Similar observations have been made with human CycA2 as well (Yam et al., 2000). In all probability, CycA-Cdk1 activity towards other substrates is also dispensable for turnover. Thus, the F329R mutation phenotype may not result from the inability to mediate phosphorylation.

Quite significantly, combining the F329R mutation with knock-outs of the N-terminal signals (KEN1, DB1 and D70) completely stabilized CycA in mitosis. Therefore, the cyclin box must possess a destruction signal. It is tempting to speculate that the cyclin box or a part of it disrupted by the F329R substitution, functions as a recognition motif for the destruction machinery. Lending weight to

this hypothesis, mutations in the cyclin box of *Xenopus* cyclin A1 prevent its association with the APC/C (Tim Hunt, personal communication). It is not clear whether F329R knocks-out any special element within the cyclin box. This phenylalanine sits within a conserved hydrophobic region. The corresponding residue in human CycA2, F304, is part of a stretch that establishes extensive contacts with the PSTAIRE helix of Cdk2 (Jeffrey et al., 1995). F304 interacts tightly with isoleucine 52 of the PSTAIRE helix (Fig: 38). It is conceivable that this conserved phenylalanine along with other cyclin box residues establish similar hydrophobic contacts with APC/C subunits or coactivators, thereby contributing to the recognition of cyclin A for degradation.
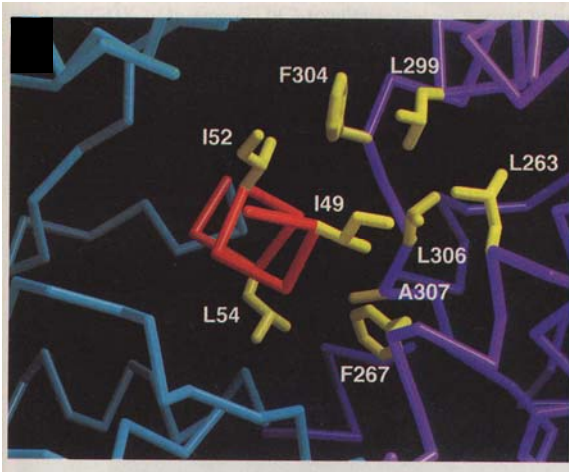
Figure: 38 Part of the human CycA2-Cdk2 interface
Cα view of the extensive hydrophobic interactions between the cyclin box of CycA2 (violet, right) and the PSTAIRE helix of Cdk2 (blue, left) is shown. Hydrophobic side chains are highlighted in yellow. Phenylalanine 304 of CycA2 can be seen interacting with isoleucine 52 of Cdk2. Adapted from (Jeffrey et al., 1995).

4.2 The checkpoint destruction of CycA

Just like CycA, NIMA related kinase 2A (Nek2A), an APC/C substrate , is destroyed in prometaphase in a checkpoint-independent manner (Hames et al., 2001a). Nek2A is a centrosomal kinase that is implicated in spindle-pole separation at the G2-M transition. It was shown recently that Nek2A interacts directly with the APC/C by means of an exposed C-terminal methionine-arginine (MR) dipeptide tail (Hayes et al., 2006). This interaction occurs even in the absence of Cdc20. Thus, Cdc20 is not required for the recruitment of Nek2A and this renders its degradation insensitive to the spindle checkpoint. However, Cdc20 is still required for Nek2A destruction, presumably for activating the

APC/C's ubiquitin ligase function (Hayes et al., 2006). Nek2A's MR tail is similar to the isoleucine-arginine (IR) C-terminal dipeptide tail found in Cdc20, Cdh1 and Doc1/Apc10, which promotes their association with core APC/C subunits (Hayes et al., 2006). By analogy to these subunits, Nek2A is likely to bind to the TPR-containing APC/C core components.

However, CycA lacks C-terminal MR or IR tails and therefore must be employing a different mechanism for circumventing the checkpoint. When the contribution of the four identified destruction signals (KEN1, DB1, D70 and F329) for checkpoint destruction were tested, the F329R substitution was found to have the most drastic effect. Individual knock-outs of the N-terminal signals (KEN1, DB1 and D70) only partially stabilized CycA, whereas the F329 knock-out resulted in complete checkpoint stability. Only double knock-outs of the N-terminal signals produced comparable stabilization. This piece of data makes sense if the cyclin box is indeed the checkpoint-circumventing motif (Fig: 39). In this context, it is relevant to note that mutations in the cyclin box of human CycA2 prevent its interaction with the APC/C (Tim Hunt, personal communication).
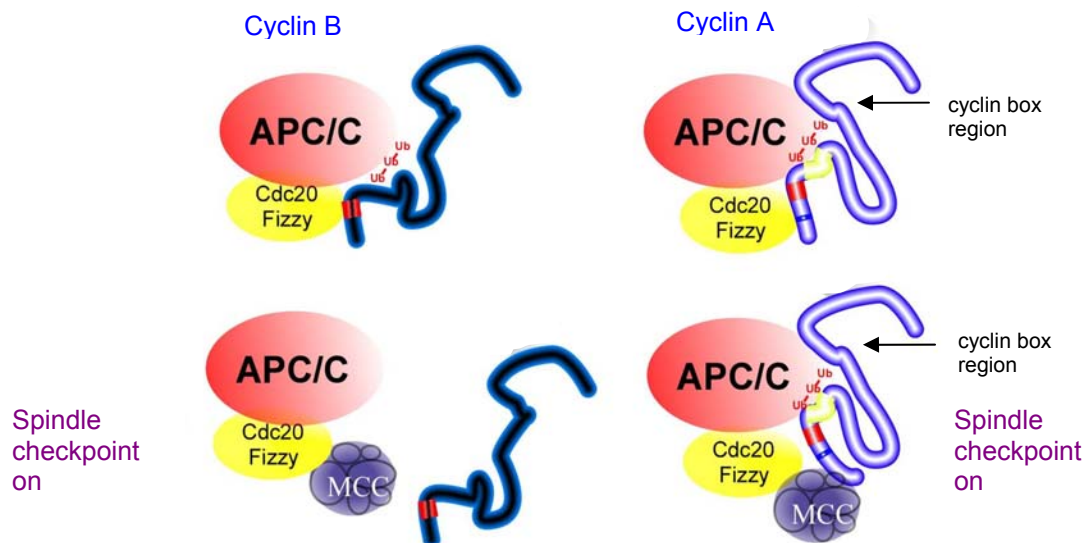
Figure: 39 A model for the checkpoint bypass mediated by the CycA cyclin box
CycB binds with its D-box to the D-box receptor formed by Fzy/Cdc20 and APC/C, and gets ubiquitinated. On activation of the spindle checkpoint, the mitotic checkpoint complex (MCC) associates with Fzy/Cdc20 and disrupts the D-box receptor. This prevents CycB binding thereby stabilizing it. CycA, with its multiple recognition signals, interacts with several regions of the APC/C^{Fzy} complex. Even when the D-box receptor is disrupted by the MCC, the cyclin box and probably some of the N-terminal signals can still interact with the APC/C to mediate CycA ubiquitination.

Therefore, a scenario can be envisaged wherein the cyclin box directly contacts the APC/C in a manner analogous to the MR tail of Nek2A; so that even when the substrate-binding sites on Cdc20 are blocked by spindle checkpoint proteins, cyclin A can still bind and get ubiquitinated.

4.3 CycA has preferentially used lysines flanking the N-terminal destruction signals

Several examples of selectively ubiquitinated proteins are known, such as the yeast Cdk inhibitor (CKI) Sic1, interferon α receptor, Hypoxia Inducible Factor (HIF 1α) and Fanconi anemia protein (Kumar et al., 2004; Paltoglou and Roberts, 2006; Petroski and Deshaies, 2003; Taniguchi et al., 2002). But cyclins were not believed to belong to that category; because it was assumed that specific ubiquitin conjugation on selected lysines does not dictate proteolysis efficiency. Nonetheless, stable CycA constructs described so far all have large N-terminal deletions which remove several lysine residues (den Elzen and Pines, 2001; Geley et al., 2001; Jacobs et al., 2001; Kaspar et al., 2001). In the case of *Drosophila* CycA, the stability of KEN1m Δ40-86 could be essentially mimicked by replacing five lysines between positions 37 and 86, along with mutations in KEN1 and DB1. Smaller deletions such as Δ40-70, which removed fewer lysines, were less stabilizing (Kaspar et al., 2001). The stability observed with previously reported N-terminal truncations, like CycA Δ55 (Jacobs et al., 2001), can also be explained by the elimination of the five lysines in that region along with KEN1 and DB1; although this was not tested. Indeed, a smaller deletion of the region, CycA KEN1m Δ22-55 inactivating KEN1 and DB1, but removing fewer lysines, is degraded more efficiently (Kaspar et al., 2001).

Thus, the lysines flanking the N-terminal signals are preferentially employed for proteolysis. It cannot be ruled out that the lysine mutations affect some other aspect of degradation. But since lysines are primarily ubiquitin acceptor sites, it is more likely that these mutations interfere with selective ubiquitination. In human CycA2, mutating three lysines surrounding the D-box delay proteolysis without preventing ubiquitination (Fung et al., 2005). Therefore, human CycA2 also

possess preferentially used lysines. Based on the observations made with *Drosophila* CycA, it is possible that the "extended D-box" of human CycA2 is nothing but the original nine-residue D-box and the lysines flanking it. The large deletion (Δ40-72) which is thought to remove the "extended D-box", may actually be removing the lysines in that region along with the D-box. However, there could also be other important residues in the extension, similar to D70 in *Drosophila* CycA.

4.4 CycA acts as a negative regulator of chromosome segregation

The destruction-compromised constructs were found to prolong the duration of metaphase. Metaphase lengths were directly proportional to the extent of stability. Long metaphases were followed by missegregation of chromosomes and anaphase arrest. However, over-expression of wild-type HA-CycA in *Drosophila* did not produce a metaphase delay, unlike what has been reported for human CycA2 (den Elzen and Pines, 2001; Geley et al., 2001). The anaphase arrest obtained with the fully stable construct could be revoked by rendering it non-functional with the F329R mutation in the cyclin box. This proves that the mitotic arrest phenotypes are a consequence of stabilized CycA-Cdk1 activity and that the original purpose of CycA destruction might be to facilitate sister chromatid separation. Recent evidence hints at the existence of a proteasome-sensitive component controlling chromosome segregation other than securin and cyclin B in human cells (Holland and Taylor, 2006). It is tempting to speculate that this could be cyclin A. However, the effect of cyclin A on chromosome segregation has been reported to be dose-dependent (den Elzen and Pines, 2001; Jacobs et al., 2001). Expression of non-degradable CycA using *prd-GAL4* in mutant embryos which do not express protein from the endogenous *CycA* gene, produced no observable mitotic delay (Jacobs et al., 2001). On the other hand, expression of stable CycB in a *CycB*-deficient background caused a detectable enrichment of anaphase figures by ~2 fold (Jacobs et al., 2001).
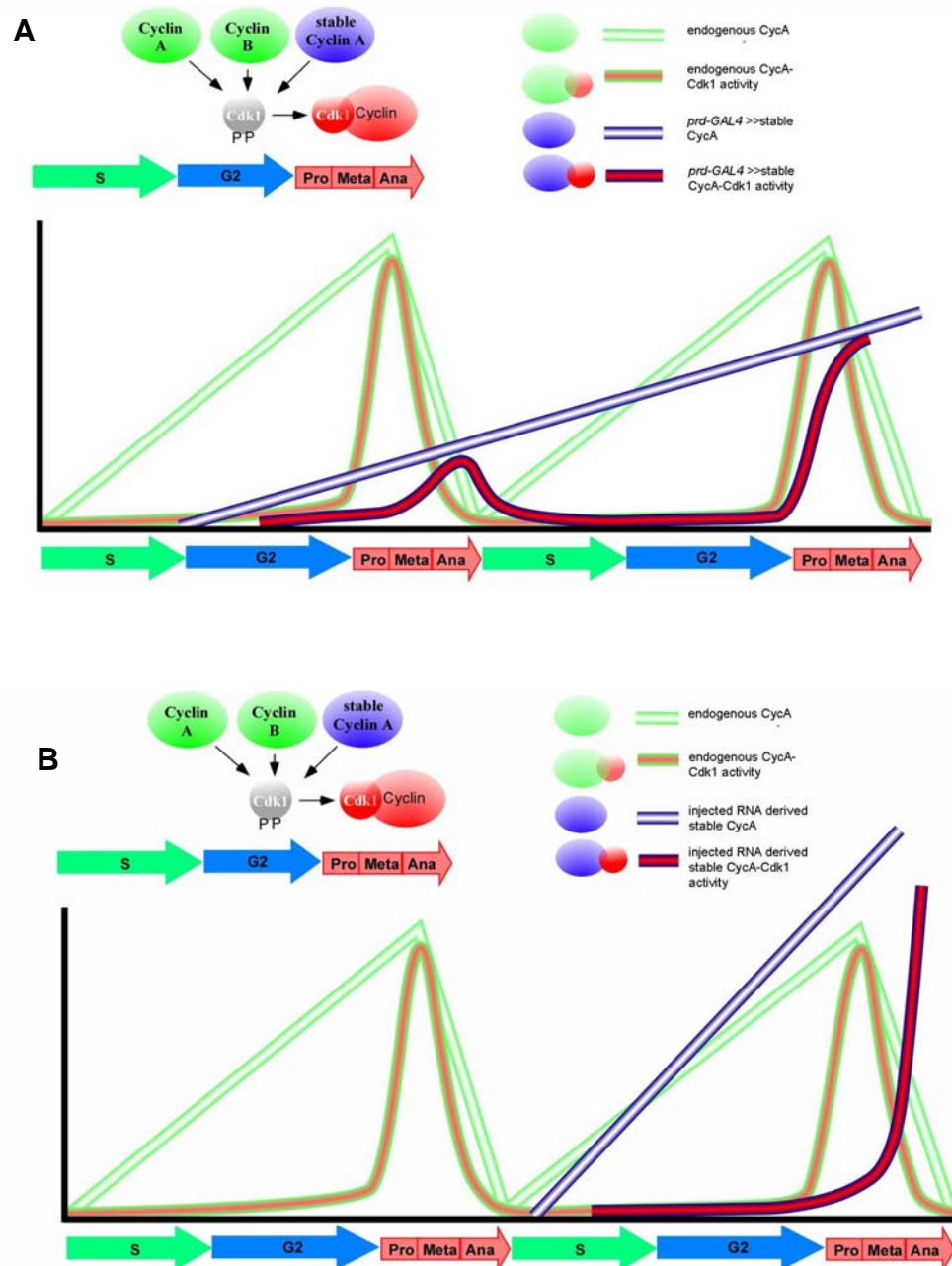
Figure: 40 Differences in stable CycA phenotypes as a consequence of expression timing and concentration

(A) Endogenous CycA levels rise in early S-phase and fall during early mitosis. CycA-Cdk1 activity peaks at the G2-M transition and fall as CycA gets degraded. *prd-GAL4* driven stable CycA expression rise only late in S-phase and the associated Cdk1 acivity remains low during mitosis, owing to the low CycA levels. However, by the next mitosis, stable CycA concentration rises to a level high enough for eliciting a metaphase arrest phenotype.

(B) Injected RNA-derived stable CycA expression starts in S-phase. Although levels are high, Cdk1 is limiting. Hence, stable CycA-Cdk1 activity is not high enough to cause metaphase 14 arrest. Once Cdk1 is freed up by mid-mitosis, high levels of stable CycA associate with it to produce an anaphase arrest.

81

However, this discrepancy can be accounted for if the timing of expression and concentration obtained from a *prd-GAL4* promoter are analyzed. As illustrated in figure 40, endogenous CycA levels normally rise at the onset of S-phase 14 and attain peak levels by early mitosis. In contrast, *prd-GAL4* driven expression initiates later during S-phase so that when cells enter mitosis 14, levels obtained from the transgene are fairly low. Stable CycA expressed in this manner will have to compete with endogenous cyclins for Cdk1. Although Cdk1 would be freed up after endogenous cyclins are proteolysed by mid-mitosis, little stable CycA-Cdk1 activity is expected to be present. These low levels would be too weak to elicit an anaphase phenotype. Stable CycB, being a much more potent inhibitor of chromosome segregation, may elicit a phenotype even at low concentrations. At the same time, stable CycA concentration would rise to significant levels by the next mitosis (mitosis 15), producing an arrest in the metaphase of mitosis 15.

When stable CycA is expressed by RNA injection, expression starts during S-phase and levels comparable to that of endogenous cyclins would be present by the time cells enter mitosis 14. But, the fairly late S-phase expression (RNA is injected when cells are already in S-phase and the protein has to be translated) reduces association with Cdk1, whose levels are limiting. Therefore instead of a strong metaphase 14 arrest, only a delay is obtained. After Cdk1 is freed up following endogenous cyclin destruction, stable CycA can associate with it and the high CycA-Cdk1 activity produces an anaphase 14 arrest.

The bottom line of all this is that CycA may not be a very potent inhibitor of anaphase like securin or CycB, but nevertheless, may still be performing the function as part of a redundant mechanism to prevent premature chromosome segregation in early mitosis. CycA-driven phosphorylation regulating either one or all of Pimples (the securin-like *Drosophila* protein), Three Rows and Sse (the *Drosophila* separase homologue) (Leismann et al., 2000) which orchestrate sister chromatid separation, is a likely scenario.

4.5 CycA evades substrate ordering based on processivity during mitosis

The ordered sequential destruction of APC/C substrates during G1 and mitosis is achieved through the processivity of ubiquitination by the APC/C (Rape et al., 2006). An early substrate gets ubiquitinated in a processive manner; that is, binding of the substrate to the APC/C once or a few times would result in a polyubiquitin chain which is sufficient for proteasomal recognition. In contrast, a late substrate would be modified in distributive fashion; that is, it would rapidly shuttle on and off the APC/C before a recognizable polyubiquitin chain has been assembled (Rape et al., 2006). Therefore, distributive substrates would be susceptible to low APC/C concentrations, competition from processive substrates and deubiquitination by deubiquitinating enzymes (DUBs) (Fig: 41). Consequently, processive substrates would be preferentially polyubiquitinated and degraded earlier than distributive substrates. The differences in processivity are not influenced by the type of coactivator - Cdc20 or Cdh1; instead, it is determined by the recognition signals on the substrate, such as the D-box, KEN box etc (Buschhorn and Peters, 2006). A D-box mutation in securin decreases its processivity. Hence, substrate ordering is established by a mechanism intrinsic to the APC/C and the substrate, similar to kinetic proofreading.

Processivity differences allow APC/C to generate substrate ordering without prior substrate modifications. So geminin is degraded ahead of UbcH10 and cyclin A in G1. Cdc20, Plk1 and Aurora A are turned over in that order during late mitosis (Rape et al., 2006). Cyclin A is a distributive APC/C substrate and therefore gets stabilized throughout most of G1, when the APC/C is occupied by more processive substrates. However, in early mitosis, cyclin A is degraded in an APC/C^{Cdc20}-dependent manner, ahead of more processive substrates such as cyclin B and securin (Buschhorn and Peters, 2006; Rape et al., 2006). Hence, substrate ordering by the APC/C does not apply for mitotic cyclin A degradation. This paradoxical phenomenon probably occurs because of interference from the spindle checkpoint, which prevents APC/C-dependent ubiquitination of more processive substrates, but not that of cyclin A.

In the absence of the checkpoint, processive substrates like cyclin B are degraded prematurely, as early as cyclin A (Rape et al., 2006). Thus, cyclin A escapes substrate ordering based on processivity by circumventing inhibition by the spindle checkpoint.

This scenario supports the existence of a checkpoint-bypassing destruction motif on cyclin A, which could possibly be the cyclin box, from evidence presented in this study. The reason for cyclin A being a distributive APC/C substrate could be the lack of a single strong APC/C interaction motif like the D-box of cyclin B. Therefore, several binding events may be required to provide a long enough dwell time for polyubiquitination. The occurrence of multiple targeting signals on cyclin A is consistent with models wherein both core APC/C subunits and coactivators contribute to substrate recognition (Eytan et al., 2006; Passmore and Barford, 2005).
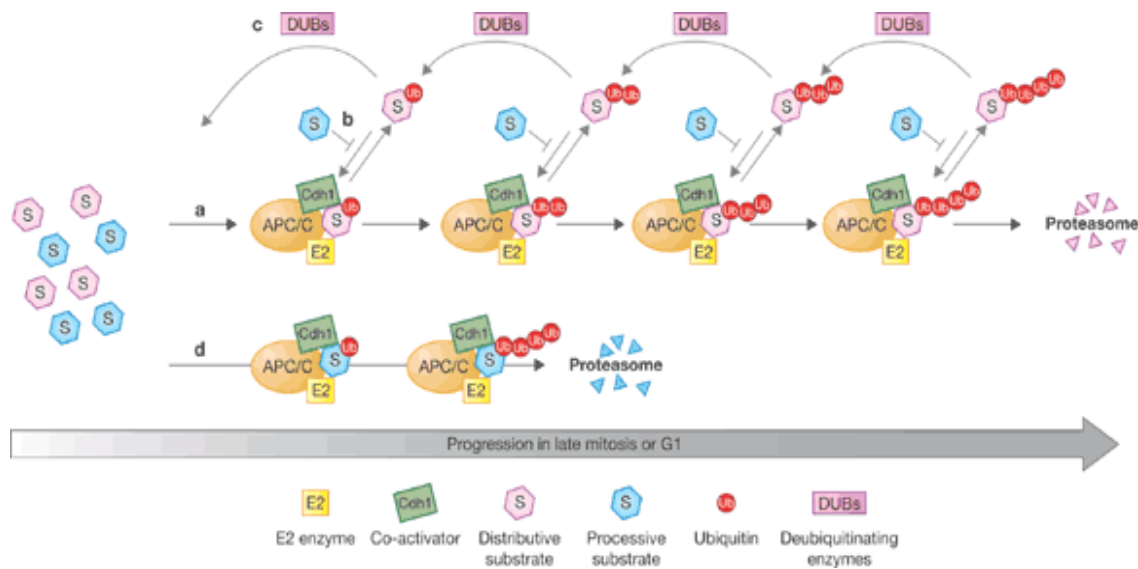
Figure: 41 Processive and distributive ubiquitination of substrates by the APC/C
Each black arrow represents a single ubiquitin binding event.
(a)–(c) Event sequence for a distributive substrate. Polyubiquitin chains are formed on the substrate in several APC/C binding events. At each step, deubiquitinating enzymes (DUBs) can reverse the state and there is also competition from other more processive substrates. (d) Event sequence for a processive substrate. Polyubiquitin chains are formed in one or a few binding events and therefore not subjected to action by deubiquitinating enzymes or competition from other substrates. Adapted from (Buschhorn and Peters, 2006).

4.6 Non-canonical CycA destruction

Apart from its normal mitotic turnover in cellular embryos, CycA is also destroyed in early preblastoderm cell cycles and during meiosis in the germline. These require markedly different components from what is needed during postblastoderm mitosis. Therefore, they can be classified as non-canonical CycA destruction.

4.6.1 CycA destruction in preblastoderm embryos

In this study, CycA destruction was analyzed during mitosis 14 in cellularized embryos. At this stage, CycA is a fairly stable protein during S and G2 phases. But, in the early embryonic cell cycles which rapidly oscillate between S and M phases, CycA has a short half-life even in interphase; while CycB is comparatively stable. Normally, this rapid turnover is compensated by heavy protein synthesis so that the net levels of CycA remain constant. But when protein synthesis is prevented by cycloheximide treatment, CycA levels fall completely in interphase (Edgar et al., 1994). In contrast, CycA levels do not diminish even on cycloheximide treatment during interphase 14 (Edgar et al., 1994). This preblastoderm CycA turnover is under the control of a kinase called Grapes (Grp), which is homologous to Chk1 in vertebrates (Su et al., 1999). In *grp* mutants, the CycA half-life is greatly increased and normal progression through the cell cycle is disturbed (Su et al., 1999). It is likely that this destruction is mediated by the APC/C. Since Cdk1 activity is present at constant levels throughout the preblastoderm cell cycles, the APC/C can be activated even in interphase. However, it is not clear how the APC/C selectively targets CycA, but not CycB, for destruction at this stage. Perhaps, the role of Grp is to phosphorylate and modify CycA so that it is converted into a better APC/C substrate. CycA destruction post the midblastula transition is independent of Grp.

4.6.2 CycA destruction in meiosis

CycA destruction during meiosis requires novel components not involved in mitotic destruction. Cortex (cort), a diverged Fzy homolog that is expressed in the *Drosophila* female germline, associates with the Cdk1-interacting protein, Cks30A to promote destruction of CycA as well as cyclins B and B3 in meiosis (Swan and Schupbach, 2007). Just like Fzy, Cort is an APC/C coactivator which functions in both meiosis I and meiosis II. In meiosis I, Cort and Fzy play largely redundant roles, as only removing both genes produce a significant block in anaphase I. Mutations in either *fzy* or *cort* stabilize cyclins A, B and B3 to a certain extent; but mutations in both genes stabilize them even more. Thus, Fzy and Cort have overlapping roles in promoting anaphase I. But in meiosis II, both genes are essential since mutations in any one of them cause a meiotic arrest and stabilize the cyclins completely. Interestingly, *cort* mutants arrest in metaphase II, while *fzy* mutants arrest in anaphase II (Swan and Schupbach, 2007). This suggests the presence of two APC/C complexes - APC/C^{Cort}, which functions to promote metaphase II and APC/C^{Fzy}, which functions to promote anaphase II. Indeed, *cort* and *fzy* mutations result in different patterns of CycB stabilization on arrested spindles.

Multiple APC/C forms have also been proposed to mediate CycB degradation during mitosis in the cellular embryo (Huang and Raff, 2002). This is based on localization studies of GFP-tagged Cdc27 and Cdc16 subunits. The former localizes to the mitotic chromatin and is believed to be required for CycB turnover at the spindle, while the latter remains in the cytoplasm. Cks30A is a Cdk1-interacting protein which is required for the function of both APC/C^{Fzy} and APC/C^{Cort} in the degradation of CycA and CycB3; but not CycB (Swan et al., 2005; Swan and Schupbach, 2007). Its vertebrate homolog Cks2 is necessary for the activation of APC^{Cdc20} by associating with Cdk1 and promoting its phosphorylation of the APC/C subunits Cdc27 and Cdc16 (Patra and Dunphy, 1998; Spruck et al., 2003).

4.6.3 CycA gets stabilized in response to DNA damage

It is known that DNA damage leads to a delay in entry into mitosis in diverse species such as yeast, mammals and cells of the *Drosophila* gastrula. This is accomplished by inhibiting Cdk1. However in yeast and *Drosophila*, an additional delay occurs at the metaphase-anaphase transition. This is promoted by the stabilization of Pds1 in yeast (Cohen-Fix and Koshland, 1997; Tinker-Kulberg and Morgan, 1999) and CycA in *Drosophila* (Su and Jaklevic, 2001). *CycA* mutants fail to delay metaphase. CycB also gets stabilized under these conditions. Therefore, the DNA damage checkpoint appears to act via APC/C^{Fzy} in order to cause the metaphase delay. However since both CycB and CycA are stabilized, the mode of APC/C inhibition must be different from that of the spindle checkpoint.

4.7 Outlook

The two major discoveries of this study are the use of select lysines in CycA destruction and the identification of a destruction signal within the cyclin box. Nevertheless, both aspects need to be characterized in more detail. The preferentially used lysines have to be analyzed further using *in vitro* ubiquitination assays in order to see how inefficient the ubiquitination reaction is when these lysines are lacking. Human CycA2 also possess selectively used lysines and ubiquitination proceeds quite normally even in the absence of those residues, although proteolysis is compromised. This indicates that certain lysines have to be specifically targeted for proper spatio-temporal destruction. Whether the same is true for *Drosophila* CycA needs to be verified. The lack of an *in vitro* ubiquitination assay using *Drosophila* APC/C and associated components is the major limiting factor in this regard. A quantitative ubiquitination assay would also help ascertain how knock-outs of the recognition signals impair turnover. Several methods have been described for APC/C purification from HeLa cells, budding yeast, frogs, sea urchins and even cow brains (Hershko, 2005; Herzog and Peters, 2005; Passmore et al., 2005a). Most of these employ antibodies against

conserved stretches on APC/C subunits. The unavailability of such antibodies for *Drosophila* APC/C subunits precludes the same techniques being employed for APC/C purification from flies. An attempt was made to immunoprecipitate APC/C from postblastoderm embryo extracts with anti-GFP antibodies targeted against GFP-tagged Cdc16 and Cdc27 subunits (data not shown). However, this yielded little success. Attempting pull-downs of mitotically active APC/C from Schneider S2 cells is also challenging, because only few cells are in mitosis in a given S2 cell population under normal culture conditions. Mitotic populations are not enriched even after treatment with microtubule depolymerizing drugs such as colchicine, nocodazole or taxol, which cause metaphase arrest in other commonly cultured cell types belonging to other species.

Another important issue that needs to be tackled is how CycA negatively controls sister chromatid separation. *In vitro* kinase assays would be an apt approach for checking whether CycA-Cdk1 can phosphorylate Pimples, Three Rows or Sse; the *Drosophila* equivalents of securin and separase. If that turns out to be positive, then the phosphorylated sites can be mapped by mass spectrometry. The identified phosphorylation sites can be mutated to ascertain the role of CycA-driven phosphorylation in chromosome separation.

Interactions of CycA with various APC/C subunits and coactivators need to be established. Human CycA2 has been reported to bind to Cdc20, an interaction that does not need the D-box, but needs the D-box downstream region (Ohtoshi et al., 2000). Human CycA2 is also found to directly contact the APC/C and an intact cyclin box is required for this interaction (Tim Hunt, personal communication). If similar observations can be made with *Drosophila* CycA, that would help in assigning roles to the recognition signals described in this study; namely the aspartate at position 70 and the phenyalanine at position 329.

Finally, as outlined above, CycA proteolysis is promoted in different ways, presumably by different APC/C complexes, in various stages of *Drosophila* development. It remains to be seen whether the same elements promoting mitotic destruction in cellular embryos, mediate the non-canonical proteolysis too. If special elements are employed for the non-canocial turnover, then they need to be identified.

5. Materials and Methods

5.1 Materials

5.1.1 Computers, Software and Equipment

This thesis was prepared using IBM-compatible PCs and Apple Macintosh computers. The softwares used were Adobe Photoshop (Adobe Systems), Axiovision Rel. 4.6 (Zeiss), Canvas (Deneba Systems), EndNote (Thomson ResearchSoft), ImageJ (NIH), Microsoft Word, Excel and Powerpoint (Microsoft Corporation).

Immunofluorescence pictures were acquired on a Zeiss Axioplan Imaging2 microscope with a CCD camera (AxioCamMRm). For high-maginification pictures, z-stacks were taken and then deconvoluted with the Huygens program (SVI). Real time analyses were performed using a Leica SP2 confocal system with a 40X water-cement lens.

Electroporations were carried out using a Gene Pulser (Bio-Rad) and gel photographs were acquired using the Gel Documentation System (Bio-Rad).

Western blotting was performed using Hybond ECL (Amersham Biosciences) nitrocellulose membranes on a Trans-Blot SD (Bio-Rad) machine. Western Blots and autoradiographs were developed using Hyperfilm ECL (Amersham Biosciences) and Biomax MR (Kodak) films respectively, on an Agfa Developer Machine.

PCRs and site directed mutagenesis reactions were carried out on Personal Cycler and TGradient (Biometra) thermocyclers.

Microinjections were performed using a Zeiss Axiolab micromanipulator microscope.

5.1.2 Chemicals

Standard chemicals were purchased from the following companies and concerns: Aldrich, Amersham Biosciences, Applichem, Biomol, Biozym, Carl Roth, Fluka, GIBCO, Merck, Pharmacia, Roche and Sigma.

5.1.3 Special chemicals and kits

^{32}P-ATP	Amersham Biosciences
^{35}S-Methionine	Amersham Biosciences
Altered Sites 2 in vitro mutagenesis system	Promega
Antarctic Phosphatase	New England Biolabs
Apyrase	New England Biolabs
Big Dye Terminator V3.1	Applied Biosystems
Calf Intestinal Phosphatase (CIP)	New England Biolabs
Cellfectin Reagent	Invitrogen
Colchicine	Sigma
Dc Protein assay kit	Bio-Rad
DNA molecular weight marker	Invitrogen
DNase I	New England Biolabs
Easy Pure DNA Purification Kit	Biozym
ECL Western Blotting Detection Reagents	GE healthcare
Expand High Fidelity PCR System	Roche
Glutathione Sepharose 4B	Amersham Biosciences
GST-CIV1	gift from Carl Mann, France (Thuret et al., 1996)
Histone H1	Boehringer Mannheim
Hoechst 33342	Sigma
Illustra GFX PCR DNA and gel band purification kit	GE healthcare
Klenow Enzyme	Boehringer Mannheim
Lambda Phosphatase	New England Biolabs
MEGAscript SP6	Ambion
Normal Goat Serum (NGS)	Dianova
Nucleobond AX-100	Machery & Nagel
Precision Plus protein MW marker	Bio-Rad
Protease Inhibitor Cocktail	Sigma
Protein G Sepharose 4 Fast Flow	Amersham Biosciences
REDTaq DNA polymerase	Sigma

Restriction endonucleases	New England Biolabs, Boehringer Mannheim
Roscovitine	Calbiochem
Schneider's Drosophila Medium	GIBCO
T4 DNA Ligase	New England Biolabs
TNT SP6 Quick Coupled Transcription/Translation System	Promega
Vectashield mounting medium	Vector laboratories

5.1.4 Media, Buffers and Solutions

1Kb ladder	325µl H_2O 125µl 4X gel loading buffer 50µl 1kb ladder (Invitrogen)
Ammonium persulfate (APS)	10% (w/v) in H_2O (store at 4°C)
Ampicillin	50mg/ml in H_2O (stock) 50µg/ml (final concentration) (store at -20°C)
Colchicine	100mM in H_2O (stock) 50µM in Schneider's Medium (final concentration)
Coomassie destaining solution	50% methanol 10% acetic acid
Coomassie staining solution	0.25% Coomassie blue, R250 50% methanol 10% acetic acid
DNA gel loading buffer	0.25% bromophenol blue 0.25% xylene cyanol FF 30% glycerol in H_2O (store at 4°C)
Embryo fixative solution	Heptane 6% formaldehyde in PBT (1:1 ratio)
Embryo fixative solution for tubulin staining	Heptane 37% formaldehyde (1:1 ratio)

Glutathione elution buffer	75mM HEPES (pH 7.4) 150mM NaCl 10mM reduced glutathione 5mM DTT
Heptane glue	Fill a 50 ml falcon tube with brown Tesa tape with the sticky surface on the outside. Cover it with heptane and leave it on a roller shaker overnight. The next day, separate the heptane from the tape and spin it two times at 15,000 rpm for 1h at 4°C. Aliquot the resulting supernatant and store at 4°C.
Hoechst 33342	0.5mg/ml in H_2O
Immunoprecipitation buffer	10mM Tris (pH 7.5) 80mM K-β-glycerophosphate 20mM EGTA 15mM $MgCl_2$ 10% glycerol 0.2% NP40 0.5M DTT 2mM Na_3VO_4
Kinase buffer	25mM HEPES (pH 7.4) 10mM $MgCl_2$ 125µM ATP 0.3mCi/ml γ^{32}P-ATP 250µg/ml Histone H1
Laemmli Buffer (4X)	200mM Tris·Cl (pH 6.8) 400mM DTT 8% SDS 0.4% bromophenol blue 40% glycerol
LB agar (1liter)	10g bacto-tryptone 5g bacto-yeast extract 10g NaCl adjust pH to 7.0 with 5N NaOH 15g bacto-agar

LB Medium (1liter)

10g bacto-tryptone
5g bacto-yeast extract
10g NaCl
adjust pH to 7.0 with 5N NaOH

Lysozyme

50mg/ml in H_2O

PBS

130mM NaCl
2.7mM KCl
7mM Na_2HPO_4
3mM KH_2PO_4
pH 7.4

PBT

0.2% Tween-20 in 1X PBS
(Tween-20 stock solution is
made in 50% ethanol)

Phage precipitation solution

3.75M ammonium acetate (pH 7.5)
20% polyethylene glycol (MW 8,000)

Plasmid prep lysis buffer

200mM NaOH
1% SDS

Plasmid prep neutralization
Buffer

3M Potassium acetate (pH 5.5)

Ponceau S (10X, 100ml)

2g Ponceau S
30g Trichloroacetic acid
30g Sulfosalicylic acid

Pre-kinase wash buffer

25mM HEPES (pH 7.4)
10mM $MgCl_2$
1mM DTT
25µM ATP

Resolving gel buffer (4X, 1liter)

181.7g Tris base
4ml 10% SDS
(adjust pH to 8.8 with HCl)

Resolving gels for SDS-PAGE
(for two mini gels)

	8%	10%	12%	15%
H_2O (ml)	4.7	4.1	3.4	2.4
30% acrylamide (ml)	2.7	3.3	4.0	5.0
4X Resolving gel buffer (ml)	2.5	2.5	2.5	2.5
APS (µl)	100	100	100	100
TEMED (µl)	6	6	6	6

RNase

10mg/ml RNase A in
10mM Tris.Cl (pH 7.5),15 mM NaCl
heat to 100°C for 15 min
cool to RT and store at -20°C

SDS-PAGE running buffer

25mM Tris base
250mM glycine
0.1% SDS

Stacking gel buffer (4X, 500 ml)

30.3g Tris base
20ml 10% SDS
(adjust pH to 6.8 with HCl)

Stacking gels for SDS-PAGE (5%)

	5 ml	10 ml
H_2O	3.45	6.9
30% acrylamide (ml)	0.83	1.7
4X Stacking gel buffer (ml)	0.63	1.25
APS (µl)	50	100
TEMED (µl)	5	8

STE

0.1M NaCl
10mM Tris.Cl (pH 8.0)
1mM EDTA (pH 8.0)

Synthesis buffer(10X)

100mM Tris.Cl (pH 7.5)
5mM dNTPs
10mM ATP
20mM DTT

TE

10mM Tris.Cl (pH 8.0)
1mM EDTA (pH 8.0)

TE-saturated Phenol : chloroform : isoamyl alcohol (25:24:1)	Mix equal parts of TE buffer and phenol. Allow the phases to separate. Mix one part of the lower phenol phase with one part of chloroform : isoamylalcohol (24:1).
Terrific Broth (1liter)	12g bacto-tryptone 24g bacto-yeast extract 4ml glycerol
Tetracycline	5mg/ml in 50% ethanol (stock) 10µg/ml (final concentration)
TFB1	30mM potassium acetate 10mM $CaCl_2$ 50mM $MnCl_2$ 100mM RbCl 15% glycerol (adjust pH to 5.8 with 1M acetic acid)
TFB2	100mM MOPS (pH 6.5) 75mM $CaCl_2$ 10mM RbCl 15% glycerol (adjust pH to 6.5 with 1M KOH)
Transfer Buffer for Western blots	48mM Tris base 39mM glycine 0.037% SDS 20% methanol
Tris-acetate (TAE) (50X, 1 liter)	242g Tris base 57.1ml glacial acetic acid 100ml 0.5M EDTA (pH 8.0)
Tris-borate (TBE) (5X, 1liter)	54g Tris base 27.5g boric acid 20ml 0.5M EDTA (pH 8.0)

5.1.5 Fly stocks

Wild-type *Drosophila melanogaster* (OregonR) or the w[1118] strain were used for most RNA injections and analyses. His2AvDGFP flies were used for real time analysis and live imaging (Clarkson and Saint, 1999).

5.1.6 Bacterial Strains

1. DH5α (for general cloning)

supE44 ΔlacU169 (φ80lacZΔM15) hsdR17 recA1 endA1 gyrA96 thi-1 relA1

Chemically competent DH5α cells purchased from Invitrogen were used for general cloning purposes.

2. ES1301 *mut*S   (for site-directed mutagenesis)

*lac*Z53 *mut*S201::Tn5 *thy*A36 *rha*-5 *met*B1 *deo*C IN(*rrn*D-*rrn*E)

3. JM109   (for propagation of plasmids with mutations)

*end*A1 *rec*A1 *gyr*A96 *thi hsd*R17 ($r_K^-m_K^+$) *rel*A1 *sup*E44 λ-Δ (*lac-pro*AB) [F´ *tra*D36*pro*A+B+ *lac*I$_q$ZΔM15

4. C43 (for expression and purification of recombinant proteins)

F$^-$*ompT gal hsdS$_B$* ($r_B^-m_B^-$) *dcm lon* λDE3

5.1.7 Antibodies

Table: 1 Primary antibodies

No:	Antigen	Source	Embryos	Western blot	Distributor
280	HA	Rabbit	1:200	-	Santa Cruz Biotechnology
282	HA	Rat	1:100	1:3000	Roche
287	HA	Mouse	-	1:250(for IP)	Roche
284	cyclin A	Rabbit	1:250	1:3000	Frank Sprenger
138	PSTAIRE	Mouse	1:2500	1:50000	Sigma
041	Tubulin	Mouse	1:200	1:10000	Amersham
293	p-Histone 3	Rabbit	1:1000	-	Upstate Cell Signaling
343	p-Histone 3	Mouse	1:2500	-	Cell Signaling Technology
294	GFP	Rabbit	1:500	1:1000	Torrey Pines Biolabs

Table: 2 Secondary antibodies for immunohistology

No:	Anti	Source	Fluorochrome	Dilution	Distributor
184	Rat	Goat	Alexa-488	1:500	MoBiTec
198	Rat	Goat	Alexa-568	1:500	MoBiTec
169	Rat	Goat	Cy5	1:500	MoBiTec
290	Rat	Goat	Alexa-647	1:500	Molecular Probes
286	Mouse	Goat	Alexa-488	1:500	Molecular Probes
298	Mouse	Goat	Rhodamine Red-X	1:500	Dianova
227	Mouse	Goat	Alexa-568	1:500	Molecular Probes
297	Mouse	Goat	Alexa-647	1:500	MoBiTec
267	Rabbit	Goat	Alexa-488	1:500	MoBiTec
301	Rabbit	Goat	Alexa-568	1:500	Molecular Probes
182	Rabbit	Goat	Cy5	1:500	Dianova

Table: 3 Secondary antibodies for Western blotting

No:	Anti	Fluorochrome	Dilution
36	Rabbit	HRP	1:3000
38	Rat	HRP	1:3000
39	Mouse	HRP	1:3000

5.1.8 Oligonucleotides

Table: 4

Name	Sequence (5' - 3')	Purpose
AmpR	GTTGCCATTGCTGCAGGCATCGTGGTG	pAlter mutagenesis
TetKO	GCCGGGCCTCTTGCGGGCGTCCATTCC	pAlter mutagenesis
AmpKO	GTTGCCATTGCGGCATCGTGG TGTCAC	pAlter mutagenesis
TetR	GCCGGGCCTCTTGCGGGATATCGTCCA	pAlter mutagenesis
CO-265	GGATAACAATTTCACACAG	Sequencing from SP6 promoter
CO-337	ATTTCTCGAGGCCAATGACAAGGAAACC	CycA,CycB chimera
CO-338	ATATCTCGAGCTCCTTGACTCTTCCAGT	CycA,CycB chimera
CO-339	ATTTCTCGAGCCGCGCAACGATCGCCAG	CycA,CycB chimera
CO-340	TAGTTCTAGATTAAAACTTATAAAACAAATTCACG	CycA cloning
CO-341	TTATTGGATCCTTGGGCAACTCTGCGC	human CycA2 cloning
CO-342	AATATCTAGAGTTACAGATTTAGTGTCTC	human CycA2 cloning
CO-343	CCGGGGGCCAATGGCGCCGTGGGCAATGGCAACAAC	CycA mutagenesis
CO-348	CCGGGATCTCGACGCTCTCCC	CycA cloning
CO-349	ATATCATATGCCCGGGCCCCTGGAACAGAACTTCC	CycA cloning
CO-382	GTTGCGCGGCGGAAGAAGCTTGACTCTTCC	CycA cloning
CO-383	GACAGCGGCTCAAAAAAGCTTAAACTTATAAAAC	CycA cloning
CO-390	TAGTATAGGGGACATATGCCCGGGCCCCTGGAACAG	CycA cloning
CO-391	GACAGCGGCTCAAAACCCGGGAAACTTATAAAAC	CycA cloning
CO-396	ATAAATGAATTCATCTTCTAATACAATTGACATGTC	human CycA2 cloning
CO-397	ATATATCCCGGGCACATTGTTG	CycA cloning

CO-398	TGACCCCGGGGCCATTGAGCACGG--CGAAATTGGCCCGCGGCGCAAG	CycA mutagenesis
CO-401	GTAATACGACTCACTATAGGGCG	Sequencing from T7 promoter
CO-402	CAATTAACCCTCACTAAAGGG	Sequencing from T3 promoter
CO-405	GAAGATTCTCTCCCGCGATCTGTGCACACC	CycA mutagenesis
CO-409	GCGTCCGGCCGGGAGAGTTCAGGTCTTCCG	CycA mutagenesis
CO-410	GAGTACGGCGCCAGGAGATCGAATGTGGTG	CycA mutagenesis
CO-411	TTGACCCCGGGGCCATTGAGCACGGCGAAA	CycA deletion construct
CO-437	CATGGAGCAGAAGCTGATCAGCGAGGAGGATCTGG	CycA deletion construct
CO-438	GATCCAGATCCTCCTCGCTGATCAGCTTCTGCTC	Myc tagged CycA
CO-471	GTAATTGGGGGAAGAGCGGAGAGAAATGCGCTTGC	CycA mutagenesis
CO-472	GTAATTGGGGGAAGAGCGGAGAAAAATGCGCTTGC	CycA mutagenesis
CO-521	CCGGGCATTAGGATTCCGGCC	CycA mutagenesis
CO-522	CGGCCGGAGTGAGGAACACCAGGCAGCCGCTGGC	CycA mutagenesis
CO-534	TATATATGTCGACGCAGAGAACCATGACGTG	CycA mutagenesis

5.1.9 Plasmids

Table: 5

Name	Insert	Vector	Purpose
pVR001	CycA-HA	pUASP	transgenic flies
pVR003	GST-HA-CycA 1-170	pGEX-6P-2	protein expression
pVR004	GST-HA-CycA	pGEX-6P-2	protein expression
pVR005	HA-CycA K13A R46G	pSP64	intermediate construct
pVR006	HA-CycA K13A R46G D70A	pSP64	intermediate construct
pVR009	human CycA2	pSP64	RNA injection
pVR010	CycA C-terminal half: 171-491	pSP64	intermediate construct
pVR011	HA-CycB N-terminal half:1-242	pSP64	intermediate construct
pVR012	HA-CycA R46G L52G	pSP64	intermediate construct
pVR013	HA-CycA R46G L52G D70A	pSP64	RNA injection
pVR014	HA-CycA-CycB chimera	pSP64	RNA injection
pVR015	HA-CycB-CycA chimera	pSP64	RNA injection
pVR022	HA-CycA K13A Δ55-86	pSP64	RNA injection
pVR026	HA-CycA F329R	pSP64	RNA injection
pVR036	HA-CycA 5K	pSP64	RNA injection
pVR039	HA-CycA 8K	pSP64	RNA injection
pVR040	HA-CycA K13A R46G 5K	pAlter	intermediate construct
pVR041	HA-CycA K13A R46G 8K	pAlter	intermediate construct
pVR042	HA-CycA K13A R46G 8K D70A	pAlter	intermediate construct
pVR043	HA-CycA K13A R46G 5K	pSP64	RNA injection
pVR044	HA-CycA K13A R46G 8K	pSP64	RNA injection
pVR045	HA-CycA K13A R46G 8K D70A	pSP64	RNA injection
pVR047	HA-CycA K13A R46G 8K D70A F329R	pSP64	RNA injection
pVR048	HA-CycA K13A R46G D70A F329R	pSP64	RNA injection
pVR050	HA-CycA K13A R46G D70A K123A Δ158-170	pSP64	RNA injection
pVR051	HA-CycA K123A Δ158-170 8K	pSP64	RNA injection
pMM02	HA-CycA K13A R46G	pAlter	intermediate construct
pMMS2	HA-CycA K13A R46G	pAlter	RNA injection
pMMS3	HA-CycA K13A R46G R60A	pSP64	RNA injection
pMMS13	HA-CycA K13A R46G D70A	pSP64	RNA injection
pMMS20	HA-CycA K13A R46G D77A	pSP64	RNA injection
pMK034	HA-CycA Δ40-86	pSP64	RNA injection
pMK037	HA-CycA K13A Δ40-86	pSP64	RNA injection
pTS001	HA-CycA	pSP64	RNA injection, *in vitro* assays
pTS002	HA-CycA	pSP64	RNA injection, *in vitro* assays
pHT-029	HA-CycA	S2 cell	transfection
pAD197	HA-CycA Δ122	pSP64	intermediate construct
pAD207	HA-CycB	pSP64	RNA injection, *in vitro* assays
pAD375	HA-CycA T145A S154A S180A	pSP64	RNA injection, phosphorylation assay

5.2 Methods

5.2.1 DNA Methods and Molecular Cloning

5.2.1.1 DNA restriction digestion

Digestion of plasmid and PCR-amplified DNA with restriction endonucleases were performed in buffers provided by enzyme manufacturers, at recommended temperatures. Plasmid DNA was cut for a minimum of 1.5h and a maximum of 12h. PCR-amplified DNA was usually cut overnight.

5.2.1.2 Dephosphorylation of DNA ends

Dephosphorylation of cut vector DNA ends was performed to minimize intra-vector ligation, especially when the ends were compatible. For dephosphorylation of cut plasmids prior to purification 1µl Calf Intestinal Phosphatase (CIP) was added to the restriction digestion mix and incubated at 37°C for 1h. This was followed by purification of the plasmid. For dephosphorylation of cut plasmids that have already been purified, 1µl Antarctic phosphatase was added to the DNA along with the supplied buffer and incubated at 37°C for 1h. The enzyme was then heat inactivated at 65°C for 5 min, following which the vector was directly used for ligation reactions.

5.2.1.3 Klenow fill-in of DNA ends

DNA 5' overhangs were filled with 1U Klenow enzyme/µg DNA and 40µM of dNTPs; both added directly to the restriction mix and incubated at 25°C for 15 min. The reaction was stopped by the addition of 10 mM EDTA followed by heat inactivation at 75°C for 10 min.

5.2.1.4 DNA electrophoresis

DNA fragments were separated by agarose gel electrophoresis as described (Sambrook et al., 1989) on 1% TAE-agarose gels containing 6µl of 10mg/ml Ethidium Bromide.

5.2.1.5 DNA band purification

DNA fragments separated by agarose gel electrophoresis were visualized on a UV lamp and excised with a sterile scalpel. DNA within the agarose pieces were recovered using the Easy Pure DNA Purification Kit or the Illustra GFX kit.

5.2.1.6 Ligation of DNA fragments

Ligation between purified DNA fragments were set up at an approximate insert: vector molar ratio of 3:1 for sticky-end ligations and 5:1 for blunt end ligations. 4U of T4 DNA ligase enzyme and 1X T4 DNA ligase buffer were mixed with the DNA fragments in a total volume of 20µl. Reactions were either performed overnight at 18°C or for 1h at 25°C.

5.2.1.7 Preparation of JM109 chemically competent cells

2.5ml LB medium was inoculated with a single colony from an LB plate and shook overnight at 37°C. The overnight culture was subcultured by inoculating 2.5ml into 250ml of LB supplemented with 20mM $MgSO_4$ and grown until an OD_{600} of 0.4-0.6 was obtained. Then the cells were recovered by spinning at 4,500 x *g* at 4°C for 5 min. The resulting cell pellet was resuspended in 100ml of TFB1 and kept on ice for 5 min in the cold room. Cells were again pelleted at 4,500 x *g* at 4°C for 5 min and then resuspended in 1/25 original volume of ice-cold TFB2, followed by incubation on ice for 1h. The cell suspension was then aliquoted 50µl/sterile eppendorf tube and stored at -80°C.

5.2.1.8 Preparation of ES1301 *mut*S and DH5α electrocompetent cells

1liter of LB medium was incoluated with 10ml of an overnight culture and grown at 37°C until an OD_{600} of 0.5-0.7 was obtained. The culture was kept on ice for 30 min followed by centrifugation at 4,000 x *g* for 15 min. The resulting cell pellet was resuspended in 1 liter ice-cold 10% glycerol and then spun down as before. The pellet was again resuspended in 20ml ice-cold 10% glycerol and spun down once more. Finally, the pellet was resuspended in 2-3 ml of ice-cold 10% glycerol and aliquoted 50µl/sterile eppendorf tube before storing at -80°C.

5.2.1.9 Transformation of chemically competent cells

1-5µl plasmid DNA was tap-mixed with a thawed 50µl aliquot of chemically competent cells, and kept on ice for 30 min. Cells were subjected to a heat shock for 20 sec at 37°C and transferred immediately onto ice. After a recovery of 2 min on ice, sterile LB medium was added to a total volume of 1ml. Cells were shaken for 1h at 37°C and 100-200µl were plated on LB-agar plates containing the appropriate antibiotic for selecting transformants. Plates were incubated overnight at 37°C.

5.2.1.10 Transformation of electrocompetent cells

Not more than 1µl of plasmid DNA was tap-mixed with a thawed 50µl aliquot of electrocompetent cells. Cells were then pre-incubated with the DNA for 1 min at RT prior to electroporation. Using a Bio-Rad Gene Pulser, cells were subjected to electroporation in a 0.2 cm cuvette (Peqlab), with the following parameters: voltage 2.5kV, capacitance 25µF, resistance 200 ohms and time constant 4.0-4.5 msec. Afterwards, sterile LB medium was added to a final volume of 1ml and cells were allowed to recover at 37°C for 30 min to 1h. 100-200µl was plated on LB-agar plates containing the appropriate antibiotic for selecting transformants. Plates were incubated overnight at 37°C.

5.2.1.11 Preparation of Plasmid DNA

For sequencing purposes, the following protocol was used:

1.5ml of overnight culture containing the plasmid of interest was spun down at 5,000 rpm for 5 min at 4°C. The pellet was resuspended in 250µl TE + RNase. Next, 250µl lysis buffer was added, invert mixed 6-8 times, and incubated at RT for 3-5 min. 250µl neutralization buffer was added, invert mixed 6-8 times and incubated on ice for 10 min. The mix was centrifuged at 14,000 rpm at RT for 10 min. The resulting supernatant was carefully transferred to a fresh eppendorf tube and mixed with 0.8 Vol. isopropanol and centrifuged again as above. The pellet obtained was washed with 500µl 70% ethanol, dried and resuspended in 50µl deionized water. This plasmid was used for test restriction digestions. Positive samples were further mixed with 10µl 5M Lithium Chloride and 3 Vol. 100% ethanol, and then kept on ice for 20 min. It was then centrifuged at 14,000 rpm at 4°C for 10 min. The pellet was washed once with 70% ethanol, dried, resuspended in 20-40µl deionized water and used for setting up the sequencing reaction.

The following protocol was used to prepare plasmid DNA for all other puroposes:

1.5ml of an overnight culture was centrifuged at 5,000 rpm for 5 min at RT. The cell pellet was resuspended in 100 µl TE + RNase, mixed with 100µl lysis buffer and incubated at RT for 3-5 min. 100µl of neutralization buffer was added, mixed and the whole thing was spun at 14,000 rpm at RT for 10 min. The resulting supernatant was transferred to a fresh eppendorf tube and mixed with 500µl 100% ethanol and centrifuged as above. The resulting pellet was washed with 200µl 70% ethanol. The pellet was dried and resuspended in 20µl deionized water.

For obtaining larger amounts of plasmid DNA, a midi-prep was performed with the Nucleobond AX-100 kit according to the manufacturer's instructions.

5.2.1.12 Precipitation of DNA

The DNA to be precipitated was mixed with 1/10 Vol. ammonium acetate, 3 Vol. 96% ethanol and 0.5µl glycogen. The mix was incubated at -80°C for 20 min and then centrifuged at 14,000 rpm for 15 min at 4°C. After discarding the supernatant, the pellet was washed with 1ml of 70% ethanol, dried thoroughly and resuspended in deionized water.

5.2.1.13 Single stranded DNA preparation and site directed mutagenesis

Single stranded circular DNA was prepared and used for site directed mutagenesis according to the protocols provided in the Altered Sites II in vitro Mutagenesis System manual from Promega.

5.2.1.14 DNA sequencing

DNA sequencing reactions were setup in the following manner:

Total volume: 10µl

Plasmid DNA	500 ng
Primer (10 pmol/µl)	1µl
Big Dye Terminator V3.1	1µl
Sequencing buffer (5X)	1.5µl

This was used for the BDT reaction.

BDT reaction: 96°C for 5 min (initial denaturation)

96°C for 30 sec (denaturation)

50°C for 15 sec (annealing)   24 cycles

60°C for 4 min (extension)

4°C   pause

After the BDT reaction, 10µl of deionized water was added to the sample, mixed well and analyzed at the DNA sequencing facility, Cologne Center for Genomics, University of Cologne.
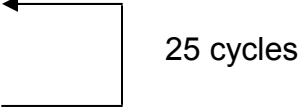
http://www.uni-koeln.de/math-nat fak/genetik/facilities/sequencer/index.html

105

5.2.1.15 DNA amplification by PCR (Polymerase Chain Reaction)

Standard PCR reactions were carried out using either the REDTaq polymerase or the Expand High Fidelity PCR System. The reaction mix was setup according to the manufacturer's instructions in a total volume of 50µl.

The following program was used as a standard:

$95°C$ for 3 min (initial denaturation)

$95°C$ for 30 sec (denaturation)

$56°C$ for 30 sec (annealing)   25 cycles

$72°C$ for 1 min (extension)

$72°C$ for 5min (final extension)

$4°C$ pause

5.2.2 RNA synthesis

10µg of plasmid DNA was linearized using a unique restriction site downstream of the gene of interest. Linearization can be verified on an agarose gel. The linearized DNA was precipitated by adding 4µl 0.5M EDTA, 8µl 3M sodium acetate (pH 5.5) and 300µl 100% ethanol, followed by thorough mixing and incubation at $-20°C$ for a minimum of 1h. The mix was then centrifuged at 14,000 rpm for 15min at $4°C$. The resulting pellet was washed once with 70% ethanol, dried properly and resuspended in 10µl deionized water. This linear template DNA was used to setup the RNA synthesis reaction using the MEGAscript SP-6 kit from Ambion, according to the manufacturer's instructions. The final DNA-free RNA preparation was suspended in 15µl of DEPC-treated water (Invitrogen), concentration adjusted to 3mg/ml and stored at $-80°C$.

5.2.3 Protein Methods

5.2.3.1 SDS-PAGE and Western blotting

Protein samples were resolved on a 1mm thick polyacrylamide gel using the Mini Protean 3 System (Bio-Rad). Samples were mixed with Laemmli buffer (1X final concentration) prior to loading. Beads, cell lysates and embryos were boiled for 10 min before loading. Gels were run at constant current (Amp constant setting) with a starting voltage of 100V that increased to around 200V over the course of the run. Gels were blotted onto Hybond Nitrocellulose membrane using a dry blotting system (Trans-Blot SD). The blotting was done for 30 min at constant current with a starting voltage of 10V. After blotting, the membrane was washed once with 1X PBS and then stained for 5 min with 1X Ponceau S to visualize the bands. Unwanted parts of the membrane were cut off and it was then destained by washing with tap water. Next, the membrane was washed in PBT and then blocked with 10ml of 5% milk in PBT for 1h at RT. Following blocking, the solution was discarded and the membrane was incubated with 4ml of the desired primary antibody (diluted with 5% milk in PBT) and shaken overnight at 4°C. After washing in 5ml PBT for 3 x 10 min, 4ml of an appropriate secondary antibody (diluted with 5% milk in PBT) was added to the membrane and shaken for 1.5h at RT. Finally, the membrane was washed with 5ml PBT for 3 x 10 min and then subjected to ECL for detection of the bands.

5.2.3.2 Coomassie staining of protein gels

Polyacrylamide gels were incubated in approximately 5 Vol. freshly prepared staining solution for a minimum of 30 min. They were then destained by repeated washing with destaining solution until the bands became clearly visible and the background staining got reduced to a minimum. For storage purposes, gels were kept immersed in 20% methanol.

5.2.3.3 Production of GST-fusion proteins

GST-CycA fusion proteins were produced according to the method described (Frangioni and Neel, 1993). A 10ml overnight culture of C43 cells expressing the protein was used to inoculate 500ml of LB-Amp medium. It was shaken at 37°C until an OD_{600} of 0.4-0.5 was reached, following which 0.1mM IPTG was added for inducing protein expression. The culture was grown for a further 3h before the cells were harvested by centrifugation. Pelleted cells were washed with 15ml ice-cold STE buffer, resuspended in 30ml STE containing 100µg/ml lysozyme and kept on ice for 15 min. 5 mM DTT, 30µl protease inhibitor cocktail and 1.5% sarkosyl (N-lauryl sarcosine) were added to the cell suspension and vortexed for 5 sec. Cells were sonicated on ice for 1 min (50% duty cycle, power level 4) using a Branson Sonifier 250 (Heinemann). The lysate was clarified by spinning at 14,000 rpm at 4°C for 10 min. The supernatant was transferred to a fresh falcon tube and 2% Triton X-100 was added to it followed by vortexing for 5 sec. 500ul of a 50% GST sepharose slurry (prepared according to the manufacturer's instructions) was added to the lysate and incubated on a roller mixer at 4°C for 30 min. The beads were then washed 6-8 times with ice-cold PBS and the bound proteins eluted by incubating it with ½ Vol. of ice-cold Glutathione elution buffer on an eppendorf thermoshaker at 4°C for 30 min. The elution step was repeated 2-3 times and the eluates were pooled. Proteins were concentrated using Centricon and Centriprep centrifugal devices (Amicon). Protein concentration was determined using the Bio-Rad *Dc* Protein Assay kit.

5.2.3.4 *In vitro* Translation

In vitro translation was usually performed with the TNT Quick Coupled Transcription/Translation System according to the manufacturer's instructions. Alternatively, it was also performed using Rabbit reticulocyte lysates with the following reaction setup for a total volume of 50ul:

Rabbit reticulocyte lysate	35µl
Amino acids without cysteine (1mM)	0.5µl
Amino acids without leucine (1mM)	0.5µl
RNase inhibitor (RNasin, 40U/ul)	1.0µl
RNA template	2.0µg

The mix was incubated at 30°C for 1.5h.

5.2.3.5 Immunoprecipitation and Kinase assay

Immunoprecipitations were performed using the following protocol:

Cyclin A and Cdk1, either of which was HA-tagged and translated as described above, were mixed together and incubated at 25°C for 30 min along with GST-CIV1, 10 mM $MgCl_2$ and 2 mM ATP. The resulting complex was precipitated onto Protein G-Sepharose beads using mouse HA-antibody (clone 12CA5, Roche) in immunoprecipitation buffer at 25°C for 2h. The beads were recovered by centrifugation at 2,000 rpm for 3 min and then washed 3 x 10 min with 300µl IP buffer. After washing, beads were boiled for 10 min in Laemmli buffer and proteins were resolved by SDS-PAGE and Western blotting.

For kinase assays, cyclin and Cdk1 translations were performed in the presence of 10 mCi/ml of ^{35}S-methionine. Following this, Cdk1 was precipitated with cyclin as described above and the beads were washed with pre-kinase wash buffer. The beads were then incubated in kinase buffer at 25°C for 30 min, followed by boiling, SDS-PAGE and autoradiography.

5.2.3.6 Phosphatase assay

For phosphatase treatment, immunoprecipitations were performed as described above. Washed beads were incubated with 1U lambda phsophatase at 30°C for 1h, followed by boiling, SDS-PAGE and Western blotting.

5.2.3.7 Roscovitine treatment

10 µM Roscovitine was mixed with in *vitro* translated CycA and Cdk1 at the step of complex formation and incubated at 25°C for 30 min, before proceeding as described above.

5.2.3.8 *In vitro* phosphorylation assay

In vitro studies of cyclin phosphorylation were done by co-precipitating them with Cdk1 and then looking for the presence of multiple bands on polyacrylamide gels.

5.2.4 *Drosophila* methods

5.2.4.1 Maintenance of flies

Flies were maintained under standard conditions as described (Ashburner, 1989).

5.2.4.2 Collection of embryos

Embryos were usually collected for 1h from flies kept in egg-laying cages fitted with apple juice agar plates. Collected embryos were dechorionized with water and bleach (1:1) for 1 min, poured through a sieve and washed several times with tap water.

5.2.4.3 RNA injection into embryos

RNA injection was performed according to the method described (Sprenger and Nusslein-Volhard, 1992). Collected embryos were aged until they reached an age of 2.5-3h, when the onset of cellularization in the developing epidermis

becomes evident. Approximately 100 embryos were lined up on a slice of apple juice agar and then stuck onto a coverslip using heptane glue. Embryos were dried in a desiccator for 4 min and covered with 10S Voltalef oil. 0.5µl of RNA (3mg/ml) was placed at one end of an injection needle, which then gets sucked in by capillary action. Using a micromanipulator microscope, RNA was microinjected with the injection needle close to the periphery of the embryos to allow uptake into the newly forming cells. Following injection, embryos were covered with 3S Voltalef oil and incubated in a 25°C incubator for 2h in a moist environment to allow translation of the injected RNA.

Protein injections were performed in the same manner. Concentration of the protein sample was adjusted to 0.5mg/ml prior to injection.

5.2.4.4 Pulling injection needles

1mm borosilicate glass capillaries having an inner filament (0.133mm) were used for constructing injection needles. These capillaries were pulled in a microfilament puller with the following parameters: heat 497, pull 30, velocity 80, time 100.

5.2.4.5 Colchicine treatment

Injected embryos were first incubated at 25°C for 1h to allow translation of the RNA and then immersed in Schneider's medium containing 50µM colchicine. This was followed by further incubation for 60-90 min to allow proper penetration of the drug into the embryos.

5.2.4.6 Embryo fixation

Non-injected embryos were fixed after dechorionization in a 2ml sample tube containing a 1:1 mixture of heptane and methanol (750µl each) with mild shaking. Fixed and devitellinized embryos fall to the bottom, while damaged embryos float at the interface. Injected embryos were fixed in a 1:1 mixture of heptane and 6%

formaldehyde in PBT (750µl each) by rotating on a 3D-shaker for 20 min. Prior to fixation, the oil and heptane glue were washed off from the coverslips with heptane, and the detached embryos were collected in a sample tube.

Embryos subjected to colchicine treatment were fixed in the same manner except that a 1:1 mixture of heptane and 37% formaldehyde was used to facilitate proper tubulin staining.

5.2.4.7 Devitellination of injected embryos

After fixation, embryos were washed with 1ml heptane, 1ml 1X PBS and dried with tissue. They were then transferred onto one sticky surface of a double-sided tape, following which the tape was stuck onto a petri dish by its other sticky surface. The immobilized embryos were covered with 1X PBS and manually devitellinized with a syringe needle (27G, 0.4x20 mm) under a pair of binoculars. Devitellinized embryos were pipetted out with 200µl cut-tips into a 2ml eppendorf tube. The cut-tips were pre-washed with 20% Tween-20 to prevent embryos from sticking onto its sides.

5.2.4.8 Antibody staining and mounting of fixed embryos

Devitellinized embryos were blocked with 500µl of 4% NGS in PBT, rotating for 1h at RT. Then the embryos were shaken overnight at 4°C with the desired primary antibodies diluted with 4% NGS in PBT to a total volume of 300µl. The next day, embryos were washed 3 x 10 min with 500µl PBT. After washing, appropriate secondary antibodies diluted with 4% NGS in PBT were added and the embryos were shaken for 1.5h at RT. This was followed by a 3 x 10 min wash with 500µl PBT. For *Hoechst 33342* staining, 0.2µg/µl RNase was added along with the secondary antibody. After wash, 0.5µl of *Hoechst 33342* (10mg/ml) was added to the embryos and shaken for 5 min at RT. Finally, a 2 x 5 minute wash with 500µl PBT was performed before the embryos were mounted onto a slide with Vectashield mounting medium.

5.2.4.9 Real time analysis of mitosis in living embryos

Embryos from flies expressing GFP-tagged Histone (His2AvD) were injected with the relevant constructs as described above. The RNA was deposited at the anterior part of the embryos, followed by a 30 min incubation period at 25°C. Mitotic progression of cells in the anterior region were followed on a Leica SP2 confocal system using a 40X water-cement lens. Images were recorded every 10 sec. Onset of anaphase in individual cells was set as the zero time-point and metaphase lengths were calculated as the time for which chromosomes showed maximum compaction.

5.2.4.10 Quantification of fluorescence intensities

HA fluorescence intensities of individual cells expressing the protein were determined as the densitometric mean. Background fluorescence from regions of the embryo not expressing the protein was subtracted. The average prophase intensity was set to 100% and the average intensities from succeeding mitotic stages were plotted as a percentage of the prophase value. A total of 169+/-24 cells from 10-12 embryos were analyzed for each construct whose degradation during an unperturbed mitosis was followed.

In experiments using colchicine, HA fluorescence intensities of individual cells from a mitotic domain affected by the drug were determined. The highest value obtained was set to 100%. Based on the levels found in the other cells, they were grouped into three classes: high (having 100-70% intensity of the maximum value), medium (70-40%) and low (below 40%). A total of 103+/-13 c-metaphase arrested cells from 9-10 embryos were analyzed for each construct whose checkpoint destruction was followed.

5.2.4.11 *In vivo* phosphorylation assay

Stage 5 embryos were injected with RNA as described above. After 30 min incubation time at 25°C, embryos were boiled, subjected to SDS-PAGE and Western blotting with anti-HA antibody.

5.2.5 Cell culture methods

5.2.5.1 Culturing of S2 cells

S2 cells were grown in 50ml tissue culture flasks using Schneider's medium supplemented with 5% FBS in a 27°C incubator. Every alternate day the medium was exchanged with fresh medium at a 1:1 ratio.

5.2.5.2 Transfection of S2 cells

10^6 cells were used for transfection. Contents of two flasks were emptied into a 50ml falcon tube and the cells were spun down at 1,100 x *g* for 5 min at 20°C. Pelleted cells were resuspended in 10ml of fresh Schneider's medium with 5% FBS. 3ml of the cell suspension was transferred into one well of a 6-well plate, having a poly-L-lysine coated coverslip in it. Coverslips were coated with poly-L-lysine according to the method described (Russel et al., 2006). The 6-well plate was incubated overnight at 27°C. The next day, a transfection mix was prepared having 100µl Schneider's medium + 10µl Cellfectin + 1.5-2µg plasmid DNA, for each well. The mix was incubated at RT for 15 min. The media in the 6-well plate was replaced with 2ml of fresh medium (without FBS) in each well. Meanwhile, after incubation, fresh media was added to each transfection mix to get a total volume of 1ml. This was then transferred to each well in the 6-well plate. Cells were incubated at 27°C for 5-6h and then 50µl of 5%FBS was added directly to each well. The next day, the media in each well was replaced with 3ml of Schneider's medium + 5% FBS + 0.01M $CuSO_4$. Cells were further incubated for 24h before fixing and staining.

5.2.5.3 Fixing and antibody staining of S2 cells

From each well in the six-well plate, media and unsedimented cells were aspirated out. The cells adhering onto the coated coverslips were washed with

114

1X PBS and then fixed with 4% formaldehyde for 10 min at RT on a rocking platform. Next, the fixative was removed and cells were permeablized with 1ml of 0.5% Triton X-100 in PBS for exactly 30 sec. Cells were washed 2 x 5 min with 1ml PBT and then blocked with PBT having 1% BSA for 30 min at RT. After this, primary antibody diluted to a total of 1ml with PBS was added to each well, and kept on a rocking platform for 1h at RT. Next, cells were washed 4 x 5 min with 1 ml PBT and then covered with secondary antibody diluted in PBS. After 1h incubation at RT, cells were further washed 4 x 5 min with PBT. *Hoechst 33342* staining was performed (diluted 1:10,000 in PBS) for 5 min at RT. After a brief 2 x 5 min wash, the coverslips were mounted on a slide with the cells facing downward, using Vectashield mounting medium and then immobilized with nail polish.

References

Abraham, R. T. (2001). Cell cycle checkpoint signaling through the ATM and ATR kinases. Genes Dev *15*, 2177-2196.

Alberts, B., Bray, D., Hopkin, K., Johnson, A., Lewis, J., Raff, M., Roberts, K., and Walter, P. (2004). Essential Cell Biology, 2 edn: Garland Science).

Alberts, B., Johnson, A., Lewis, J., Raff, M., Roberts, K., and Walter, P. (2002). Molecular Biology of The Cell, 4 edn: Garland Science).

Amundson, R. (2007). Cell Structure/Function,
http://www.kensbiorefs.com/NewCellStr.html

Andreu, J. M., and Timasheff, S. N. (1982). Tubulin bound to colchicine forms polymers different from microtubules. Proc Natl Acad Sci U S A *79*, 6753-6756.

Araki, M., Yu, H., and Asano, M. (2005). A novel motif governs APC-dependent degradation of Drosophila ORC1 in vivo. Genes Dev *19*, 2458-2465.

Ashburner, M. (1989). Drosophila - A laboratory handbook.

Basu, J., Bousbaa, H., Logarinho, E., Li, Z., Williams, B. C., Lopes, C., Sunkel, C. E., and Goldberg, M. L. (1999). Mutations in the essential spindle checkpoint gene bub1 cause chromosome missegregation and fail to block apoptosis in Drosophila. J Cell Biol *146*, 13-28.

Borgne, A., Ostvold, A. C., Flament, S., and Meijer, L. (1999). Intra-M phase-promoting factor phosphorylation of cyclin B at the prophase/metaphase transition. J Biol Chem *274*, 11977-11986.

Brodsky, M. H., Sekelsky, J. J., Tsang, G., Hawley, R. S., and Rubin, G. M. (2000). mus304 encodes a novel DNA damage checkpoint protein required during Drosophila development. Genes Dev *14*, 666-678.

Brown, N. R., Noble, M. E., Endicott, J. A., Garman, E. F., Wakatsuki, S., Mitchell, E., Rasmussen, B., Hunt, T., and Johnson, L. N. (1995). The crystal structure of cyclin A. Structure *3*, 1235-1247.

Buffin, E., Emre, D., and Karess, R. E. (2007). Flies without a spindle checkpoint. Nat Cell Biol.

Burton, J. L., Tsakraklides, V., and Solomon, M. J. (2005). Assembly of an APC-Cdh1-substrate complex is stimulated by engagement of a destruction box. Mol Cell *18*, 533-542.

Buschhorn, B. A., and Peters, J. M. (2006). How APC/C orders destruction. Nat Cell Biol *8*, 209-211.

Chen, R. H. (2007). Dual inhibition of Cdc20 by the spindle checkpoint. J Biomed Sci.

Clarkson, M., and Saint, R. (1999). A His2AvDGFP fusion gene complements a lethal His2AvD mutant allele and provides an in vivo marker for Drosophila chromosome behavior. DNA Cell Biol *18*, 457-462.

Cohen-Fix, O., and Koshland, D. (1997). The anaphase inhibitor of Saccharomyces cerevisiae Pds1p is a target of the DNA damage checkpoint pathway. Proc Natl Acad Sci U S A *94*, 14361-14366.

Dawson, I. A., Roth, S., and Artavanis-Tsakonas, S. (1995). The Drosophila cell cycle gene fizzy is required for normal degradation of cyclins A and B during mitosis and has homology to the CDC20 gene of Saccharomyces cerevisiae. J Cell Biol *129*, 725-737.

De Antoni, A., Pearson, C. G., Cimini, D., Canman, J. C., Sala, V., Nezi, L., Mapelli, M., Sironi, L., Faretta, M., Salmon, E. D., and Musacchio, A. (2005). The Mad1/Mad2 complex as a template for Mad2 activation in the spindle assembly checkpoint. Curr Biol *15*, 214-225.

de Nooij, J. C., Letendre, M. A., and Hariharan, I. K. (1996). A cyclin-dependent kinase inhibitor, Dacapo, is necessary for timely exit from the cell cycle during Drosophila embryogenesis. Cell *87*, 1237-1247.

den Elzen, N., and Pines, J. (2001). Cyclin A is destroyed in prometaphase and can delay chromosome alignment and anaphase. Journal of Cell Biology *153*, 121-136.

Dienemann, A. (2003) Die Bedeutung der subzellulaeren Lokalisierung von Cyclin A in *Drosophila melanogaster*, University of Cologne, Cologne.

Dienemann, A., and Sprenger, F. (2004). Requirements of cyclin a for mitosis are independent of its subcellular localization. Curr Biol *14*, 1117-1123.

Dube, P., Herzog, F., Gieffers, C., Sander, B., Riedel, D., Muller, S. A., Engel, A., Peters, J. M., and Stark, H. (2005). Localization of the coactivator Cdh1 and the

cullin subunit Apc2 in a cryo-electron microscopy model of vertebrate APC/C. Mol Cell *20*, 867-879.

Edgar, B. A., and Datar, S. A. (1996). Zygotic degradation of two maternal Cdc25 mRNAs terminates Drosophila's early cell cycle program. Genes Dev *10*, 1966-1977.

Edgar, B. A., and Lehner, C. F. (1996). Developmental control of cell cycle regulators: a fly's perspective. Science *274*, 1646-1652.

Edgar, B. A., and O'Farrell, P. H. (1989). Genetic control of cell division patterns in the Drosophila embryo. Cell *57*, 177-187.

Edgar, B. A., and O'Farrell, P. H. (1990). The three postblastoderm cell cycles of Drosophila embryogenesis are regulated in G2 by string. Cell *62*, 469-480.

Edgar, B. A., and Orr-Weaver, T. L. (2001). Endoreplication cell cycles: more for less. Cell *105*, 297-306.

Edgar, B. A., Sprenger, F., Duronio, R. J., Leopold, P., and O'Farrell, P. H. (1994). Distinct molecular mechanism regulate cell cycle timing at successive stages of Drosophila embryogenesis. Genes Dev *8*, 440-452.

Eytan, E., Moshe, Y., Braunstein, I., and Hershko, A. (2006). Roles of the anaphase-promoting complex/cyclosome and of its activator Cdc20 in functional substrate binding. Proc Natl Acad Sci U S A *103*, 2081-2086.

Fisher, R. P., and Morgan, D. O. (1994). A novel cyclin associates with MO15/CDK7 to form the CDK-activating kinase. Cell *78*, 713-724.

Foe, V. E. (1989). Mitotic domains reveal early commitment of cells in Drosophila embryos. Development *107*, 1-22.

Frangioni, J. V., and Neel, B. G. (1993). Solubilization and purification of enzymatically active glutathione S-transferase (pGEX) fusion proteins. Anal Biochem *210*, 179-187.

Fung, T. K., Yam, C. H., and Poon, R. Y. (2005). The N-terminal Regulatory Domain of Cyclin A Contains Redundant Ubiquitination Targeting Sequences and Acceptor Sites. Cell Cycle *4*.

Gabellini, D., Colaluca, I. N., Vodermaier, H. C., Biamonti, G., Giacca, M., Falaschi, A., Riva, S., and Peverali, F. A. (2003). Early mitotic degradation of the homeoprotein HOXC10 is potentially linked to cell cycle progression. Embo J *22*, 3715-3724.

Geley, S., Kramer, E., Gieffers, C., Gannon, J., Peters, J. M., and Hunt, T. (2001). Anaphase-promoting complex/cyclosome-dependent proteolysis of human cyclin A starts at the beginning of mitosis and is not subject to the spindle assembly checkpoint. Journal of Cell Biology *153*, 137-148.

Gieffers, C., Dube, P., Harris, J. R., Stark, H., and Peters, J. M. (2001). Three-dimensional structure of the anaphase-promoting complex. Mol Cell *7*, 907-913.

Glickman, M. H., and Ciechanover, A. (2002). The ubiquitin-proteasome proteolytic pathway: destruction for the sake of construction. Physiol Rev *82*, 373-428.

Glotzer, M., Murray, A. W., and Kirschner, M. W. (1991). Cyclin is degraded by the ubiquitin pathway. Nature *349*, 132-138.

Gordon, C. (2004). The ubiquitin Pathway in Fission Yeast, http://www.hgu.mrc.ac.uk/Research/Gordon/

Gould, K. L., and Nurse, P. (1989). Tyrosine phosphorylation of the fission yeast cdc2+ protein kinase regulates entry into mitosis. Nature *342*, 39-45.

Gribskov, M. (2007). A Short Guide to the Proteolytic Pathway, http://plantsubq.genomics.purdue.edu/html/guide.html

Hagan, R. S., and Sorger, P. K. (2005). Cell biology: the more MAD, the merrier. Nature *434*, 575-577.

Hames, R. S., Wattam, S. L., Yamano, H., Bacchieri, R., and Fry, A. M. (2001a). APC/C-mediated destruction of the centrosomal kinase Nek2A occurs in early mitosis and depends upon a cyclin A-type D-box. Embo J *20*, 7117-7127.

Hames, R. S., Wattam, S. L., Yamano, H., Bacchieri, R., and Fry, A. M. (2001b). APC/C-mediated destruction of the centrosomal kinase Nek2A occurs in early mitosis and depends upon a cyclin A-type D-box. EMBO J *20*, 7117-7127.

Hayes, M. J., Kimata, Y., Wattam, S. L., Lindon, C., Mao, G., Yamano, H., and Fry, A. M. (2006). Early mitotic degradation of Nek2A depends on Cdc20-independent interaction with the APC/C. Nat Cell Biol *8*, 607-614.

Hershko, A. (2005). Affinity purification of mitotic anaphase-promoting complex/cyclosome on p13Suc1. Methods Enzymol *398*, 170-175.

Herzog, F., and Peters, J. M. (2005). Large-scale purification of the vertebrate anaphase-promoting complex/cyclosome. Methods Enzymol *398*, 175-195.

Hilioti, Z., Chung, Y. S., Mochizuki, Y., Hardy, C. F., and Cohen-Fix, O. (2001). The anaphase inhibitor Pds1 binds to the APC/C-associated protein Cdc20 in a destruction box-dependent manner. Curr Biol *11*, 1347-1352.

Holland, A. J., and Taylor, S. S. (2006). Cyclin-B1-mediated inhibition of excess separase is required for timely chromosome disjunction. J Cell Sci *119*, 3325-3336.

Huang, J. Y., and Raff, J. W. (2002). The dynamic localisation of the Drosophila APC/C: evidence for the existence of multiple complexes that perform distinct functions and are differentially localised. J Cell Sci *115*, 2847-2856.

Hwang, L. H., Lau, L. F., Smith, D. L., Mistrot, C. A., Hardwick, K. G., Hwang, E. S., Amon, A., and Murray, A. W. (1998). Budding yeast Cdc20: a target of the spindle checkpoint. Science *279*, 1041-1044.

Jacobs, H., Richter, D., Venkatesh, T., and Lehner, C. (2002). Completion of mitosis requires neither fzr/rap nor fzr2, a male germline-specific Drosophila Cdh1 homolog. Curr Biol *12*, 1435-1441.

Jacobs, H. W., Keidel, E., and Lehner, C. F. (2001). A complex degradation signal in Cyclin A required for G1 arrest, and a C-terminal region for mitosis. Embo J *20*, 2376-2386.

Jeffrey, P. D., Russo, A. A., Polyak, K., Gibbs, E., Hurwitz, J., Massague, J., and Pavletich, N. P. (1995). Mechanism of CDK activation revealed by the structure of a cyclinA-CDK2 complex. Nature *376*, 313-320.

Karess, R. (2005). Rod-Zw10-Zwilch: a key player in the spindle checkpoint. Trends Cell Biol *15*, 386-392.

Kaspar, M., Dienemann, A., Schulze, C., and Sprenger, F. (2001). Mitotic degradation of cyclin A is mediated by multiple and novel destruction signals. Curr Biol *11*, 685-690.

King, R. W., Glotzer, M., and Kirschner, M. W. (1996). Mutagenic analysis of the destruction signal of mitotic cyclins and structural characterization of ubiquitinated intermediates. Mol Biol Cell *7*, 1343-1357.

Klotzbucher, A., Stewart, E., Harrison, D., and Hunt, T. (1996). The 'destruction box' of cyclin A allows B-type cyclins to be ubiquitinated, but not efficiently destroyed. Embo J *15*, 3053-3064.

Kraft, C., Vodermaier, H. C., Maurer-Stroh, S., Eisenhaber, F., and Peters, J. M. (2005). The WD40 propeller domain of Cdh1 functions as a destruction box receptor for APC/C substrates. Mol Cell *18*, 543-553.

Kumar, K. G., Krolewski, J. J., and Fuchs, S. Y. (2004). Phosphorylation and specific ubiquitin acceptor sites are required for ubiquitination and degradation of the IFNAR1 subunit of type I interferon receptor. J Biol Chem *279*, 46614-46620.

Lane, M. E., Sauer, K., Wallace, K., Jan, Y. N., Lehner, C. F., and Vaessin, H. (1996). Dacapo, a cyclin-dependent kinase inhibitor, stops cell proliferation during Drosophila development. Cell *87*, 1225-1235.

Larochelle, S., Pandur, J., Fisher, R. P., Salz, H. K., and Suter, B. (1998). Cdk7 is essential for mitosis and for in vivo Cdk-activating kinase activity. Genes Dev *12*, 370-381.

Lee, L. A., and Orr-Weaver, T. L. (2003). Regulation of cell cycles in Drosophila development: intrinsic and extrinsic cues. Annu Rev Genet *37*, 545-578.

Lehner, C. F., and O'Farrell, P. H. (1989). Expression and function of Drosophila cyclin A during embryonic cell cycle progression. Cell *56*, 957-968.

Lehner, C. F., and O'Farrell, P. H. (1990). The roles of Drosophila cyclins A and B in mitotic control. Cell *61*, 535-547.

Leismann, O., Herzig, A., Heidmann, S., and Lehner, C. F. (2000). Degradation of Drosophila PIM regulates sister chromatid separation during mitosis. Genes Dev *14*, 2192-2205.

Lilly, M. A., and Duronio, R. J. (2005). New insights into cell cycle control from the Drosophila endocycle. Oncogene *24*, 2765-2775.

Littlepage, L. E., and Ruderman, J. V. (2002). Identification of a new APC/C recognition domain, the A box, which is required for the Cdh1-dependent destruction of the kinase Aurora-A during mitotic exit. Genes Dev *16*, 2274-2285.

Lohka, M. J., Hayes, M. K., and Maller, J. L. (1988). Purification of maturation-promoting factor, an intracellular regulator of early mitotic events. Proc Natl Acad Sci U S A *85*, 3009-3013.

Mainprize, T. G., Taylor, M. D., Rutka, J. T., and Dirks, P. B. (2001). Cip/Kip cell-cycle inhibitors: a neuro-oncological perspective. J Neurooncol *51*, 205-218.

Mao, Y., Abrieu, A., and Cleveland, D. W. (2003). Activating and silencing the mitotic checkpoint through CENP-E-dependent activation/inactivation of BubR1. Cell *114*, 87-98.

Matzkies, M. (2004) Identifizierung von Abbausequenzen in Cyclin A aus *Drosophila melanogaster*, University of Cologne, Cologne.

May, K. M., and Hardwick, K. G. (2006). The spindle checkpoint. J Cell Sci *119*, 4139-4142.

Merrill, P. T., Sweeton, D., and Wieschaus, E. (1988). Requirements for autosomal gene activity during precellular stages of Drosophila melanogaster. Development *104*, 495-509.

Meyn, M. A., 3rd, Melloy, P. G., Li, J., and Holloway, S. L. (2002). The destruction box of the cyclin Clb2 binds the anaphase-promoting complex/cyclosome subunit Cdc23. Arch Biochem Biophys *407*, 189-195.

Morgan, D. O. (1995). Principles of CDK regulation. Nature *374*, 131-134.

Morgan, D. O. (1997). Cyclin-dependent kinases: engines, clocks, and microprocessors. Annu Rev Cell Dev Biol *13*, 261-291.

Musacchio, A., and Salmon, E. D. (2007). The spindle-assembly checkpoint in space and time. Nat Rev Mol Cell Biol *8*, 379-393.

Nakayama, K. I., and Nakayama, K. (2006). ubiquitin ligases: cell-cycle control and cancer. Nat Rev Cancer *6*, 369-381.

Nurse, P. (1990). Universal control mechanism regulating onset of M-phase. Nature *344*, 503-508.

O'Connell, M. J., Walworth, N. C., and Carr, A. M. (2000). The G2-phase DNA-damage checkpoint. Trends Cell Biol *10*, 296-303.

Ohtoshi, A., Maeda, T., Higashi, H., Ashizawa, S., and Hatakeyama, M. (2000). Human p55(CDC)/Cdc20 associates with cyclin A and is phosphorylated by the cyclin A-Cdk2 complex. Biochem Biophys Res Commun *268*, 530-534.

Orr, B., Bousbaa, H., and Sunkel, C. E. (2007). Mad2-independent Spindle Assembly Checkpoint Activation and Controlled Metaphase-Anaphase Transition in Drosophila S2 Cells. Mol Biol Cell *18*, 850-863.

Paltoglou, S., and Roberts, B. J. (2006). HIF-1alpha and EPAS ubiquitination mediated by the VHL tumour suppressor involves flexibility in the ubiquitination mechanism, similar to other RING E3 ligases. Oncogene.

Pan, J., and Chen, R. H. (2004). Spindle checkpoint regulates Cdc20p stability in Saccharomyces cerevisiae. Genes Dev *18*, 1439-1451.

Parry, D. H., and O'Farrell, P. H. (2001). The schedule of destruction of three mitotic cyclins can dictate the timing of events during exit from mitosis. Current Biology *11*, 671-683.

Passmore, L. A., and Barford, D. (2004). Getting into position: the catalytic mechanisms of protein ubiquitylation. Biochem J *379*, 513-525.

Passmore, L. A., and Barford, D. (2005). Coactivator functions in a stoichiometric complex with anaphase-promoting complex/cyclosome to mediate substrate recognition. EMBO Rep *6*, 873-878.

Passmore, L. A., Barford, D., and Harper, J. W. (2005a). Purification and assay of the budding yeast anaphase-promoting complex. Methods Enzymol *398*, 195-219.

Passmore, L. A., Booth, C. R., Venien-Bryan, C., Ludtke, S. J., Fioretto, C., Johnson, L. N., Chiu, W., and Barford, D. (2005b). Structural analysis of the anaphase-promoting complex reveals multiple active sites and insights into polyubiquitylation. Mol Cell *20*, 855-866.

Patra, D., and Dunphy, W. G. (1998). Xe-p9, a Xenopus Suc1/Cks protein, is essential for the Cdc2-dependent phosphorylation of the anaphase- promoting complex at mitosis. Genes Dev *12*, 2549-2559.

Peng, C. Y., Graves, P. R., Thoma, R. S., Wu, Z., Shaw, A. S., and Piwnica-Worms, H. (1997). Mitotic and G2 checkpoint control: regulation of 14-3-3 protein binding by phosphorylation of Cdc25C on serine-216. Science *277*, 1501-1505.

Peters, J. M. (2006). The anaphase promoting complex/cyclosome: a machine designed to destroy. Nat Rev Mol Cell Biol *7*, 644-656.

Petroski, M. D., and Deshaies, R. J. (2003). Context of multiubiquitin chain attachment influences the rate of Sic1 degradation. Mol Cell *11*, 1435-1444.

Pfleger, C. M., and Kirschner, M. W. (2000). The KEN box: an APC recognition signal distinct from the D box targeted by cdh1. Genes Dev *14*, 655-665.

Rape, M., Reddy, S. K., and Kirschner, M. W. (2006). The processivity of multiubiquitination by the APC determines the order of substrate degradation. Cell *124*, 89-103.

Reber, A., Lehner, C. F., and Jacobs, H. W. (2006). Terminal mitoses require negative regulation of Fzr/Cdh1 by Cyclin A, preventing premature degradation of mitotic cyclins and String/Cdc25. Development *133*, 3201-3211.

Reis, A., Levasseur, M., Chang, H. Y., Elliott, D. J., and Jones, K. T. (2006). The CRY box: a second APC(cdh1)-dependent degron in mammalian cdc20. EMBO Rep *7*, 1040-1045.

Russel, T. J., Dye, L., and Schram, V. (2006). Coating coverslips with Poly-L-Ornithine or Poly-L-Lysine, http://mic.nichd.nih.gov/coat_cov_poly.htm

Russell, P., and Nurse, P. (1987). Negative regulation of mitosis by wee1+, a gene encoding a protein kinase homolog. Cell *49*, 559-567.

Russo, A. A., Jeffrey, P. D., Patten, A. K., Massague, J., and Pavletich, N. P. (1996a). Crystal structure of the p27Kip1 cyclin-dependent-kinase inhibitor bound to the cyclin A-Cdk2 complex. Nature *382*, 325-331.

Russo, A. A., Jeffrey, P. D., and Pavletich, N. P. (1996b). Structural basis of cyclin-dependent kinase activation by phosphorylation. Nat Struct Biol *3*, 696-700.

Sambrook, J., Fritsch, E. F., and Maniatis, T. (1989). Molecular cloning: a laboratory manual: Cold Spring Harbor Laboratory Press).

Sibon, O. C., Laurencon, A., Hawley, R., and Theurkauf, W. E. (1999). The Drosophila ATM homologue Mei-41 has an essential checkpoint function at the midblastula transition. Curr Biol *9*, 302-312.

Sibon, O. C., Stevenson, V. A., and Theurkauf, W. E. (1997). DNA-replication checkpoint control at the Drosophila midblastula transition. Nature *388*, 93-97.

Sigrist, S., Jacobs, H., Stratmann, R., and Lehner, C. F. (1995). Exit from mitosis is regulated by Drosophila fizzy and the sequential destruction of cyclins A, B and B3. EMBO J *14*, 4827-4838.

Sigrist, S. J., and Lehner, C. F. (1997). Drosophila fizzy-related down-regulates mitotic cyclins and is required for cell proliferation arrest and entry into endocycles. Cell *90*, 671-681.

Simmons, K. (2006). The Life Cycle of Cells
http://kentsimmons.uwinnipeg.ca/cm1504/lifecyclecells.htm

Smith, A. V., and Orr-Weaver, T. L. (1991). The regulation of the cell cycle during Drosophila embryogenesis: the transition to polyteny. Development *112*, 997-1008.

Sprenger, F., and Nusslein-Volhard, C. (1992). Torso receptor activity is regulated by a diffusible ligand produced at the extracellular terminal regions of the Drosophila egg. Cell *71*, 987-1001.

Spruck, C. H., de Miguel, M. P., Smith, A. P., Ryan, A., Stein, P., Schultz, R. M., Lincoln, A. J., Donovan, P. J., and Reed, S. I. (2003). Requirement of Cks2 for the first metaphase/anaphase transition of mammalian meiosis. Science *300*, 647-650.

Stemmann, O. (2007). Chromosome Segregation in Mitosis and Meiosis
http://www.biochem.mpg.de/en/research/rg/stemmann/

Stewart, E., Kobayashi, H., Harrison, D., and Hunt, T. (1994). Destruction of Xenopus cyclins A and B2, but not B1, requires binding to p34cdc2. Embo J *13*, 584-594.

Su, T. T., Campbell, S. D., and O'Farrell, P. H. (1999). Drosophila grapes/CHK1 mutants are defective in cyclin proteolysis and coordination of mitotic events. Curr Biol *9*, 919-922.

Su, T. T., and Jaklevic, B. (2001). DNA damage leads to a Cyclin A-dependent delay in metaphase-anaphase transition in the Drosophila gastrula. Curr Biol *11*, 8-17.

Sudakin, V., Chan, G. K., and Yen, T. J. (2001). Checkpoint inhibition of the APC/C in HeLa cells is mediated by a complex of BUBR1, BUB3, CDC20, and MAD2. J Cell Biol *154*, 925-936.

Swan, A., Barcelo, G., and Schupbach, T. (2005). Drosophila Cks30A interacts with Cdk1 to target Cyclin A for destruction in the female germline. Development *132*, 3669-3678.

Swan, A., and Schupbach, T. (2007). The Cdc20 (Fzy)/Cdh1-related protein, Cort, cooperates with Fzy in cyclin destruction and anaphase progression in meiosis I and II in Drosophila. Development *134*, 891-899.

Takada, S., Kelkar, A., and Theurkauf, W. E. (2003). Drosophila checkpoint kinase 2 couples centrosome function and spindle assembly to genomic integrity. Cell *113*, 87-99.

Taniguchi, T., Garcia-Higuera, I., Xu, B., Andreassen, P. R., Gregory, R. C., Kim, S. T., Lane, W. S., Kastan, M. B., and D'Andrea, A. D. (2002). Convergence of the fanconi anemia and ataxia telangiectasia signaling pathways. Cell *109*, 459-472.

Taylor, S. S., Scott, M. I., and Holland, A. J. (2004). The spindle checkpoint: a quality control mechanism which ensures accurate chromosome segregation. Chromosome Res *12*, 599-616.

Thornton, B. R., and Toczyski, D. P. (2006). Precise destruction: an emerging picture of the APC. Genes Dev *20*, 3069-3078.

Thuret, J. Y., Valay, J. G., Faye, G., and Mann, C. (1996). Civ1 (CAK in vivo), a novel Cdk-activating kinase. Cell *86*, 565-576.

Tinker-Kulberg, R. L., and Morgan, D. O. (1999). Pds1 and Esp1 control both anaphase and mitotic exit in normal cells and after DNA damage. Genes Dev *13*, 1936-1949.

Vagnarelli, P., and Earnshaw, W. C. (2004). Chromosomal passengers: the four-dimensional regulation of mitotic events. Chromosoma *113*, 211-222.

Whitfield, W. G., Gonzalez, C., Maldonado-Codina, G., and Glover, D. M. (1990). The A- and B-type cyclins of Drosophila are accumulated and destroyed in temporally distinct events that define separable phases of the G2-M transition. Embo J *9*, 2563-2572.

Yam, C. H., Siu, W. Y., Lau, A., and Poon, R. Y. C. (2000). Degradation of Cyclin A Does Not Require Its Phosphorylation by CDC2 and Cyclin-dependent Kinase 2. J Biol Chem *275*, 3158-3167.

Yamano, H., Gannon, J., Mahbubani, H., and Hunt, T. (2004). Cell cycle-regulated recognition of the destruction box of cyclin B by the APC/C in Xenopus egg extracts. Mol Cell *13*, 137-147.

Yang, R., Morosetti, R., and Koeffler, H. P. (1997). Characterization of a second human cyclin A that is highly expressed in testis and in several leukemic cell lines. Cancer Res *57*, 913-920.

Yu, H. (2006). Structural activation of Mad2 in the mitotic spindle checkpoint: the two-state Mad2 model versus the Mad2 template model. J Cell Biol *173*, 153-157.

Zachariae, W. (2004). Destruction with a box: substrate recognition by the anaphase-promoting complex. Mol Cell *13*, 2-3.

Zachariae, W., and Nasmyth, K. (1999). Whose end is destruction: cell division and the anaphase-promoting complex. Genes Dev *13*, 2039-2058.

Zielke, N. (2006) Functional analysis of the cell cycle regulator Rca1in *Drosophila melanogaster*, University of Cologne, Cologne.

Zielke, N., Querings, S., Grosskortenhaus, R., Reis, T., and Sprenger, F. (2006). Molecular dissection of the APC/C inhibitor Rca1 shows a novel F-box-dependent function. EMBO Rep *7*, 1266-1272.

8. Abbreviations

3D	Three dimensional
AnaA	Anaphase A
AnaB	Anaphase B
APC/C	Anaphase Promoting Complex/Cyclosome
APS	Ammonium Persulfate
ATP	Adenosine Triphosphate
BDT	Big Dye Terminator
BSA	Bovine Serum Albumin
CAK	Cdk activating kinase
Cdk	Cyclin dependent kinase
CKI	Cdk inhibitor
Cort	Cortex
Cyc	*Drosophila* cyclin
CycA2	human cyclin A2
DB/D-box	Destruction box
DDR	Destruction box1 downstream region
DMSO	Dimethyl Sulfoxide
DNA	Deoxyribonucleic acid
ECL	Enhanced chemiluminescence
EDTA	Ethylene Diamine Tetra Acetic acid
EM	Electron Microscopy
Fzr	Fizzy-realted
Fzy	Fizzy
g	gram
g	gravity units
GFP	Green Fluorescent Protein
Grp	Grapes
GST	Glutathione-S-Transferase
h	hour(s)
HA	Hemagglutinin
kDa / MDa	kilo Dalton / Mega Dalton

128

μ	micro
M	Molar
M14	Mitosis 14
MBT	Midblastula transition
MCC	Mitotic Checkpoint Complex
Meta	Metaphase
mg / ml / mM	milligram / milliliter / millimolar
min	minute(s)
mRNA	messenger RNA
NGS	Normal Goat Serum
P-sites	Cdk1/Cdk2 consensus phosphorylation sites
PAGE	Polyacrylamide Gel Electrophoresis
PBS	Phosphate Buffered Saline
PCR	Polymerase Chain Reaction
PH3	Phosphorylated Histone 3
Pro	Prophase
Prometa	Prometaphase
Rca1	Regulator of cyclin A 1
RNA	Ribonucleic acid
rpm	revolutions per minute
RT	room temperature
SDS	Sodium Dodecyl Sulfate
sec	second(s)
Telo	Telophase
U	Unit(s)

9. Single and three letter code for amino acids

A	Ala	Alanine
C	Cys	Cysteine
D	Asp	Aspartate (Aspartic acid)
E	Glu	Glutamate (Glutamic acid)
F	Phe	Phenylalanine
G	Gly	Glycine
H	His	Histidine
I	Ile	Isoleucine
K	Lys	Lysine
L	Leu	Leucine
M	Met	Methionine
N	Asn	Asparagine
P	Pro	Proline
Q	Gln	Glutamine
R	Arg	Arginine
S	Ser	Serine
T	Thr	Threonine
V	Val	Valine
W	Trp	Tryptophan
Y	Tyr	Tyrosine

7. Zusammenfassung

Der Abbau von cyclin A ist seit der Entdeckung dieses mitotischen Cyclins rätselhaft geblieben. Obwohl es ein Substrat des Anaphase Promoting Complex/Cyclosome (APC/C) ist, der den Abbau der mitotischen cycline initiiert, wird cyclin A vor allen anderen Substrate abgebaut. Weiterhin wird der Abbau nicht durch Aktivierung des mitotischen Spindelcheckpoints blockiert, der den Eintritt in die Anaphase verhindert indem der Abbau der anderen APC/C-Substraten verhindert wird. Die Entzifferung des Abbausignals in cyclin A ist dabei das vorrangige Ziel, um dieses Verhalten von cyclin A zu verstehen. Allerdings zeigte sich, dass cyclin A keine einfache Abbausequenz, wie sie zum Beispiel bei cyclin B vorzufinden ist, besitzt. In cyclin A aus *Drosophila* (CycA) wurden verschiedene Elemente identifiziert, so eine D-Box und eine KEN-Box, die Inaktivierung beider Elemente führte jedoch zu keiner Stabilisierung. In der vorliegenden Arbeit wurde die Suche nach den Abbausequenzen extensiv erweitert. Dabei zeigte sich dass sowohl N- als auch C-terminale Regionen des Proteins beteiligt sind. Neben der KEN- und D-box spielt dabei auch ein Aspartat an der Position 70 eine Rolle und alle Elemente haben einen additiven Einfluss auf den Abbau. Im C-terminalen Teil konnte die cyclinbox als wichtiges Element identifiziert werden. Punktmutationen in den drei N-terminalen, sowie eine Punktmutation in der cyclinbox führten zur Stabilität in der Mitose. Von entscheidender Bedeutung ist die cyclinbox auch für den Abbau von cyclin A unter Bedingungen in denen der Spindelcheckpoint aktiv ist. Die Ergebnisse zeigen auch, dass diese Funktion der cyclinbox nicht über die konservierte Funktion der Cdk1 Bindung verläuft; wahrscheinlich ermöglicht die cyclinbox einen direkten Kontakt mit dem APC/C. Neben der Erkennung von cyclin A spielen auch bestimmte Lysinreste, die für die Ubiquitinylierung benutzt werden, eine Rolle beim Abbau von cyclin A. Es konnten acht Lysinreste, die in der Umgebung der N-terminalen Signale liegen, identifiziert werden, die präferentiell für den Abbau benutzt werden. Werden sie mutiert, kann bei der Anwesenheit eines normalen C-terminus, der Abbau jedoch weiterhin erfolgen. Es wird vermutet, dass die N-terminalen Abbausequenzen unter diesen Umständen

einen guten Kontakt zum APC/C ermöglichen, so dass auch nicht präferentielle Lysinreste als Ubiquitinakzeptoren benutzt werden können. Solch ein Wechsel von präferentiellen zu anderen Ubiquitinakzeptorstellen kann anscheinend nur durch die N-terminalen Abbauerkennungssequenzen ermöglicht werden. Zusammenfassend konnte in dieser Arbeit die Abbausignale in CycA identifiziert werden und eine Erklärung gefunden werden, wie der Abbau bei Aktivierung des mitotischen Spindelcheckpoints möglich ist.

10. Erklärung

Ich versichere, dass ich die von mir vorgelegte Dissertation selbständig angefertigt, die benutzten Quellen und Hilfsmittel vollständig angegeben und die Stellen der Arbeit - einschließlich Tabellen, Karten und Abbildungen -, die anderen Werken im Wortlaut oder dem Sinn nach entnommen sind, in jedem Einzelfall als Entlehnung kenntlich gemacht habe;dass diese Dissertation noch keiner anderen Fakultät oder Universität zur Prüfung vorgelegen hat; dass sie - abgesehen von unten angegebenen Teilpublikationen - noch nicht veröffentlichtworden ist, sowie dass ich eine solche Veröffentlichung vor Abschluss des Promotionsverfahrens nicht vornehmen werde. Die Bestimmungen dieser Promotionsordnung sind mir bekannt. Die von mir vorgelegte Dissertation ist von PD Dr. Frank Sprenger betreut worden.

Köln, April 2007   Vimal Ramachandran

Teilpublikationen:

Ramachandran V, Matzkies M, Dienemann A, Sprenger F.
Cyclin A degradation employs preferentially used lysines and a cyclin box function other than Cdk1 binding.
Cell Cycle. 2007 Jan;6(2):171-81. Epub 2007 Jan 15.

11. Lebenslauf

Name:		Ramachandran
Vorname:		Vimal
Adresse		AG Leptin,Institut für Genetik, Zülpicher Str.47, 50674 Köln
Geburtsdatum/-ort:		01.02.1979 in Calicut, Indien
Staatsangehörigkeit:		Indisch
Familienstand:		Verheiratet
Schullaufbahn:	1982-1996	Grund und Hauptschule
Studium und Berufliche Tätigkeit:	1996-1999	Bachelor of Science in Zoology, University of Calicut, Indien
	1999-2001	Master of Science in Biotechnology, Cochin University of Science and Technology, Cochin, Indien
	Okt 2001-Dec 2003	Junior Research Fellow (JRF), Molecular Biophysics Unit, Indian Insititute of Science, Bangalore, Indien
		Project Titel: "Biophysical characterization and stability studies of the proteins CcdB and Gal4"
	Apr 2004-heute	Promotion unter Betreuung von PD Dr.Frank Sprenger am Institut für Genetik der Universität zu Köln mit dem Titel:
		"Defining the residues governing the mitotic destruction of *Drosophila* cyclin A"

12. Acknowledgements

I would like to express my gratitude to my supervisor Dr.Frank Sprenger for providing me the opportunity to do this work. His expertise, understanding and patience added considerably to my PhD experience. I appreciate the support, encouragement and assistance he provided at all levels, throughout the course of my PhD.

I am grateful to Prof. Dr. Maria Leptin for the support she has offered right from the beginning. It was through her kindness that I got this chance. Her leadership and attention to detail have set an example I hope to match some day.

My sincere thanks goes out to Dr.Kevin Johnson for his timely advice at critical junctures and exchange of knowledge. I also acknowledge the valuable insights and comments provided by Dr.Thomas Klein, Prof.Dr.Siegfried Roth, Dr.Veit Riechmann and Dr.Arp Schnittger over the years.

A thesis is never solely the work of the author. Special thanks to Matthias Matzkies, Dr.Axel Dienemann and Dr.Markus Kaspar who established the assays and laid down the foundations on which I could build upon. I also thank all the past and present members of the Sprenger, Leptin and Klein labs for creating the right working atmosphere and lending a helping hand whenever it mattered.

Dr. Brigitte v.Wilcken-Bergmann arranged my accommodation and helped me with all related activities including formalities such as filling up forms and extending visas. Her services and support are gratefully acknowledged. I also thank members of the office staff, Inge Götz-Krichi and Dr.Klaus Reiners for all the instances in which their assistance helped me along the way.

I recognize that this research would not have materialized without financial assistance from SFB 635. Their aid is duly acknowledged.

I thank my parents for instilling in me confidence and a drive for aiming high.

With all my heart I thank the indispensable people in my life - my wife and my son, whose love and affection from afar made this work possible. This work is dedicated to them.